

Stochastic Modeling and Performance Analysis of Intelligent Reflecting Surface assisted Wireless Communication Systems

Thesis

Submitted in partial fulfillment of the requirements for the degree of

DOCTOR OF PHILOSOPHY

by

DHRUVAKUMAR T

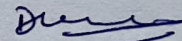


**DEPARTMENT OF ELECTRONICS & COMMUNICATION ENGINEERING
NATIONAL INSTITUTE OF TECHNOLOGY KARNATAKA
SURATHKAL, MANGALORE - 575025, INDIA**

October 2022

DECLARATION

I hereby *declare* that the Research Thesis entitled **STOCHASTIC MODELING AND PERFORMANCE ANALYSIS OF INTELLIGENT REFLECTING SURFACE ASSISTED WIRELESS COMMUNICATION SYSTEMS** which is being submitted to the National Institute of Technology Karnataka, Surathkal in partial fulfillment of the requirements for the award of the Degree of **Doctor of Philosophy** in **Department of Electronics and Communication** is a *bonafide report of the research work carried out by me*. The material contained in this thesis has not been submitted to any University or Institution for the award of any degree.



Dhruvakumar T

Register No.: 177107EC003

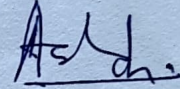
Department of Electronics and Communication Engineering

Place: NITK Surathkal

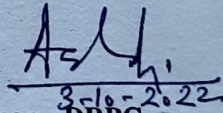
Date: 03/10/2022

CERTIFICATE

This is to *certify* that the Research Thesis entitled **STOCHASTIC MODEL-
ING AND PERFORMANCE ANALYSIS OF INTELLIGENT REFLECTING
SURFACE ASSISTED WIRELESS COMMUNICATION SYSTEMS** submitted by
Dhruvakumar T, (Reg. No.: 177107EC003) as the record of the research work carried
out by him, is *accepted as a Research Thesis submission* in partial fulfillment of the
requirements for the award of the degree of **Doctor of Philosophy**.



Dr. Ashvini Chaturvedi
Research Guide
Professor and Head
Department Electronics and Communication Engg.
NITK Surathkal - 575025



Chairman - DRPC

(Signature with Date and Seal)

प्राध्यापक एवं विभागाध्यक्ष / PROF & HEAD
ई एवं सी विभाग / E & C Department
एन आई टी के, सुरतकल/NITK, Surathkal
मंगलूर / MANGALORE - 575 025

ACKNOWLEDGEMENTS

First and foremost, I take this opportunity to thank the Lord Almighty for enabling me to work persistently in pursuit of this research work, and for empowering me with the strength and perseverance towards the fruitful accomplishment of the task.

I offer my deepest gratitude to my research supervisor, Dr. Ashvini Chaturvedi who has been a constant source of support and encouragement to me. His timely counselling has always guided me technically and morally. His profound knowledge and thorough patience have always been a beacon of light for me throughout my journey. He has been a hands-on advisor who was always ready to help and I have learned a great deal from him.

I owe my sincere thanks to Prof. U. Shripathi Acharya and Prof. T. Laxminidhi, former heads of the Department of Electronics and Communication Engineering, for their valuable advice and administrative support. I would also like to acknowledge the encouragement, guidance and assessments provided by my RPAC members, Dr. Gururaj S Punekar and Dr. U. Shripathi Acharya. I would like to take this opportunity to thank my committee members for taking time to provide useful and insightful feedback to improve my thesis. I take this opportunity to thank all the teaching and non-teaching staff and the lab technicians for offering their valuable expertise at all times which has helped me realize the goals of my work at a faster pace.

I would like to thank the Principal, Director and management of Sree Siddaganga Education Trust, Tumakuru for deputing me to Ph.D at NITK, Surathkal. I particularly thank my fellow scholars who have been a part of my journey and helped me technically and motivated me. Surviving Ph.D. would have been impossible without all my awesome friends. I take this opportunity to genuinely thank all my friends from far and near who have always been with me, never failing to support me and lift me at times of

need. I will forever be indebted to them for their invaluable friendship, care, concern and timely interventions.

Throughout the different phases of my Ph.D., the love and support provided by my family know no bounds, I thank them for always having worked behind the scenes for me. Their silent prayers and gentle chiding have moulded me into the person I am today. A special word of thanks to my mother Daya Thippeswamy, wife Kumuda and daughter Dwani for the sacrifices they have made and for always believing in me.

ABSTRACT

In a wireless terrain, presence of various obstacles leads to compliance of Non-line-of-sight (NLOS) norms between a transmitter (base station, BS) and a receiver (user), which renders severe degradation in the Quality of service (QoS) of the wireless links and thereby limits the anticipated performance. Presence of IRS panels stimulates a supplementary wireless channel that enhances reliable end-to-end connectivity between a transmitter and a receiver, especially when a direct path (line-of-sight, LOS) experiences either severe signal degradation or completely lost in shorter epochs. Using Intelligent Reflecting Surface (IRS), performance of a wireless network can be improved by smartly re-configuring the passive reflecting elements which are embedded on a planar surface.

In this thesis, as geographical terrain experience ubiquitous presence of obstacles, using estimate of performance measures such as Achievable rate, Outage probability, Coverage probability and Ergodic capacity, it is validated that in such scenarios IRS-assisted wireless communication system performance is significantly enhanced with respect to a conventional wireless system. A mathematical framework for Time-invariant (TI) and Time-variant (TV) channel models is proposed. A comprehensive analysis is performed in terms of Achievable rate, Outage probability, Ergodic capacity and Coverage probability estimate. During these performance measures, distance between a BS and a receiver is considered as a primary variable while regulating parameters such as; transmit power, number of Embedded Reflecting Elements (EREs), separation distance between EREs and receiver speed for an Urban Micro-street canyon (UMi-SC) and an Urban Micro-open square (UMi-OS) wireless terrain. In addition, terrain equipped with multiple IRS panels are studied to achieve a better network coverage enhancement.

The thesis investigates the network outage performance of multiple IRS-assisted wireless terrain. Different case studies are presented in which a receiver experiences a

direct (LOS) link and/or IRS reflected links, and all these links are characterized using kappa-mu ($\kappa - \mu$) shadowed fading. Here, an IRS panel resulting in maximum instantaneous signal-to-noise ratio (SNR) is selected to participate in establishing an end-to-end wireless link. An exact analysis comprising $\kappa - \mu$ shadowed fading impact on outage probability and ergodic capacity of a wireless link and subsequently, approximating the $\kappa - \mu$ shadowed fading channel by Nakagami-m fading model is presented. An analytical framework is presented to estimate the outage probability and ergodic capacity of an end-to-end wireless link for different wireless terrain equipped with multiple IRS panels and experiencing different degree of fading along with varying data/vehicular-traffic statistics. While incorporating geographical attributes driven spatial aspects and the distinct vehicular traffic originated in distinct time-intervals exact $\kappa - \mu$ shadowed fading model is considered. For all these scenarios, numerical results demonstrate the precision achieved in approximation accuracy.

Urban terrain that characterizes with high rise buildings and huge size sign boards along the road can be equipped with IRS panels at appropriate locations to enable Virtual Line-Of-Sight (VLOS) links between BSs and users through these IRS panels. Due to surrounding spatial attributes, temporal characteristics of wireless terrain and users' behavioural aspects, a single stochastic model doesn't suffice to approximate the terrain's characteristics and the associated underlying propagation mechanism. In this thesis, to accommodate diversified spatial and temporal characteristics of terrain in a reasonable manner, usage of Poisson Point Process (PPP) and Poisson Cluster Process (PCP) is proposed to model the users' distribution and IRS panels deployment. Coverage probability is estimated to validate the proposed stochastic models, while regulating the cluster size. Furthermore, the efficacy of IRSs equipped wireless terrain is demonstrated in terms of enhanced coverage probability for a broad ranging SINR threshold. An analytical framework is presented to estimate the coverage probability of a wireless link for varying fading conditions in multiuser environment with multiple IRS panels. Mapping of real world vehicular traffic scenarios with PPP and PCP is established and accordingly proposed models of PPP and PCP are considered to address location aspect of IRS panels and BSs.

TABLE OF CONTENTS

ACKNOWLEDGEMENTS	iii
ABSTRACT	v
LIST OF FIGURES	xiii
LIST OF TABLES	xiv
ABBREVIATIONS	xv
MATHEMATICAL NOTATIONS	xvi
1 INTRODUCTION	1
1.1 Introduction to Intelligent Reflecting Surface	3
1.1.1 Architecture of an IRS panel	3
1.1.2 Signal propagation in IRS-assisted wireless Terrain	5
1.1.3 Advantages of IRS	6
1.1.4 Application scenarios of IRS	7
1.2 Motivation	8
1.3 Problem Definition	10
1.4 Research objectives	11
1.5 Methodology	12

1.6	Organization of the Thesis	13
2	IRS-ASSISTED WIRELESS NETWORK SCENARIOS AND PERFORMANCE MEASURES	15
2.1	Comparison of IRS and relay-based wireless transmission links	15
2.2	IRS-aided wireless communication system	19
2.3	Environment scenario specifications	22
2.3.1	Indoor scenarios	24
2.3.2	Outdoor scenarios	25
2.4	Comprehensive performance metrics	27
3	CHANNEL MODELING AND PERFORMANCE ANALYSIS OF IRS-ASSISTED WIRELESS TERRAIN	31
3.1	Introduction	31
3.2	Channel modelling of wireless terrain	33
3.2.1	Time-Invariant (TI) channel model	34
3.2.2	Time-Variant (TV) channel model	36
3.3	IRS panels deployment in wireless terrain	38
3.3.1	Modeling of diverse signal propagation scenarios	38
3.3.2	Achievable rate	40
3.3.3	Coverage enhancement	42
3.4	Simulation results	44
3.4.1	Wireless terrain assisted with a single IRS panel	46
3.4.2	Wireless terrain assisted with a single or multiple IRS panels	48

3.4.3	Single IRS panel assisted wireless terrain with the regulation in number of active EREs:	49
3.4.4	Wireless terrain with a single IRS panel and variations in transmit power level:	50
3.4.5	ERE spacing driven distance centric analysis for single IRS panel assisted wireless terrain:	52
3.4.6	Impact of mobile receiver velocity in a single IRS panel-assisted wireless terrain:	52
3.5	Summary	54
4	OUTAGE PROBABILITY ANALYSIS FOR MULTIPLE IRS-ASSISTED WIRELESS NETWORKS	55
4.1	Introduction	55
4.2	System model	58
4.3	Spatial attributes driven channel model	62
4.3.1	IRS panel selection	63
4.3.2	Outage probability analysis	65
4.3.3	Ergodic capacity analysis	66
4.4	Numerical results	68
4.4.1	Outage probability and Ergodic capacity estimate with regulation in ERE	69
4.4.2	Outage probability and Ergodic capacity dependency on vehicular traffic	72
4.5	Summary	76
5	STOCHASTIC MODELING AND COVERAGE ANALYSIS OF IRS-	

ASSISTED CELLULAR NETWORK WITH INTERFERENCE MITIGATION	77
5.1 Introduction	77
5.2 System model	81
5.2.1 Signal propagation model	84
5.3 Point process functionals	88
5.3.1 Coverage probability analysis	90
5.3.2 Thomas Cluster Process (TCP)	92
5.4 Results and discussion	94
5.4.1 Impact of varying cluster size on Coverage probability	96
5.4.2 Impact of IRS-assistance on Coverage probability	99
5.5 Summary	101
6 CONCLUSION AND FUTURE WORK	103
6.1 Conclusion	103
6.2 Future work	104
REFERENCES	107

LIST OF FIGURES

1.1	Architecture of IRS	4
1.2	Reflecting element schematic embedded on IRS panel (a) Structure of PIN diode, and (b) Structure of Varactor diode	4
1.3	Schematic of (a) obstructed wireless link without IRS, (b) VLOS link enabled through IRS	6
1.4	Diverse applications of IRS	8
2.1	Wireless communication system supported with (a) relays and (b) IRS	16
2.2	A schematic of wireless network using (a) relays, UDN and DAS, and (b) multiple IRSs	18
2.3	System architecture for IRS-assisted communication system	20
2.4	Prototype of IRS-assisted wireless communication system	21
2.5	IRS-assisted wireless communication for outdoor and indoor deployments	23
2.6	A transmission setup for indoor scenario	24
2.7	A transmission setup for outdoor scenario spanning 500 m (a) location of the transmitter and receiver on the map (b) the transmitter unit (c) the site of the receiver; (d) a snap of the receiver while data transmission.	26
3.1	IRS-assisted wireless terrain	39
3.2	Coverage enhancement using IRS panels for (a) UMi-OS and (b) UMi-SC	43

3.3	Achievable rate for a single IRS-assisted scenario (a) UMi-OS and (b) UMi-SC	47
3.4	Achievable rate for single or multiple IRS-assisted scenarios (a) UMi-OS and (b) UMi-SC	48
3.5	Achievable rate for a single IRS-assisted scenario (a) UMi-OS complying LOS, (b) UMi-SC complying LOS, (c) UMi-OS complying NLOS and (d) UMi-SC complying NLOS	50
3.6	Achievable rate for a single IRS-assisted scenario (a) UMi-OS complying LOS, (b) UMi-SC complying LOS, (c) UMi-OS complying NLOS and (d) UMi-SC complying NLOS	51
3.7	Achievable rate for a single IRS-assisted scenario (a) UMi-OS complying LOS, (b) UMi-SC complying LOS, (c) UMi-OS complying NLOS and (d) UMi-SC complying NLOS	53
3.8	Achievable rate for a single IRS-assisted scenario with parametric variation in the receiver speed (a) UMi-OS and (b) UMi-SC	54
4.1	Multiple IRS-assisted wireless communication system.	59
4.2	Schematic diagram comprising IRS locations, Receiver positions and viable links in (a) lightly fading zone, (b) moderately fading zone and (c) severely fading zone	64
4.3	Numerical results demonstrating the impact of EREs for light fading zone on (a) Outage probability and (b) Ergodic capacity	70
4.4	Numerical results demonstrating the impact of EREs for moderate fading zone on (a) Outage probability and (b) Ergodic capacity	71
4.5	Numerical results demonstrating the impact of EREs for severe fading zone on (a) Outage probability and (b) Ergodic capacity	72

4.6	Numerical results demonstrating the impact of vehicular traffic in wireless terrain equipped with IRS panels having 64 EREs for light fading zone on (a) Outage probability and (b) Ergodic capacity	73
4.7	Numerical results demonstrating the impact of vehicular traffic in wireless terrain equipped with IRS panels having 64 EREs for moderate fading zone on (a) Outage probability and (b) Ergodic capacity	74
4.8	Numerical results demonstrating the impact of vehicular traffic in wireless terrain equipped with IRS panels having 64 EREs for severe fading zone on (a) Outage probability and (b) Ergodic capacity	75
5.1	A schematic of IRS-assisted cellular network	81
5.2	Schematics of cellular networks formed by combining PPP and PCP approach for IRS panels and users (a) IRS-PPP, user-PPP (b) IRS-PPP, user-PCP (c) IRS-PCP, user-PPP and (d) IRS-PCP, user-PCP	82
5.3	Illustration of distance characterization and channel models with reference to a user (a) Mode-1 (Direct link) and (b) Mode-2 (IRS-assisted link)	85
5.4	A pictorial representation of varying cluster size (σ) with respect to a serving IRS panel	95
5.5	Coverage probability with cluster size (σ) regulation (a) IRS-PPP, user-PCP (b) IRS-PCP, user-PPP and (c) IRS-PCP, user-PCP	98
5.6	Coverage probability with cluster size (σ) regulation (a) Sparsely distributed users-PPP and (b) closely spaced users-PCP	100

LIST OF TABLES

1.1	A comparison of 5G and 6G key performance indicators	2
2.1	Comparison between IRS and relay mechanism	17
2.2	List of main industry progress, prototypes and projects related to IRS	22
2.3	Channel parameters and specifications in outdoor scenarios	27
2.4	Summary of performance metrics for IRS-assisted wireless networks	29
2.5	Summary of performance metrics for IRS-assisted wireless networks, continue from Table 2.4.	30
3.1	Pathloss model parameters for UMi-SC and UMi-OS	35
3.2	Wireless terrain specification having fixed network parameters	45
3.3	Wireless terrain specification having variable network parameters . .	45
4.1	Geographical segments and wireless channel Parameters.	68

ABBREVIATIONS

BS	base station
CDF	cumulative distribution function
CSI	channel state information
ERE	embedded reflecting elements
FSPL	free space path loss
IRS	intelligent reflecting surface
LOS	line-of-sight
NLOS	non-line-of-sight
PCP	Poisson cluster process
PDF	probability density function
PGFL	probability generating functional
PLE	path loss exponent
PPP	Poisson point process
QoS	quality of service
SCBS	small-cell base station
SNR	signal to noise ratio
SINR	signal to interference noise ratio
TCP	Thomas cluster process
TI	time-invariant
TV	time-varying
UMi-SC	urban micro- street canyon
UMi-OS	urban micro- open square canyon
VLOS	virtual line-of-sight

MATHEMATICAL NOTATIONS

ϕ^t	azimuth angle of departure
ϕ^r	azimuth angle of arrival
θ^t	elevation angle of departure
θ^r	elevation angle of arrival
α	complex path gain
δ	inter-element spacing in an IRS panel
ξ	normalization factor
γ	signal to noise ratio
r_l	total length of the l^{th} propagation path from a transmitter to a receiver
r_s	length of the propagation path from a scattering cluster to a receiver
h_T	transmitter antenna height
h_R	receiver antenna height
(x, y, h)	Cartesian coordinates of network elements (BS, IRS panel and receiver)
$L(d)$	attenuation associated with propagation path having distance d
ν^{RX}	speed of a Receiver
h_d	direct link channel between a BS and a mobile receiver
\mathbf{h}_{bi}	channel between a BS and an IRS panel
\mathbf{h}_{im}	channel between an IRS panel and a mobile receiver
$\mathbf{a}(\phi_l^{IRS}, \theta_l^{IRS})$	IRS array response vector
Θ	IRS Phase shift matrix
S	source
D	destination

R	R^{th} IRS panel
N	number of ERE
P_T	transmit power
$h_{S,D}$	direct link channel between a BS and a mobile receiver
$\alpha_{S,D}$	shape parameter of the direct link
α_r	shape parameter of the r^{th} IRS link
$\beta_{S,D}$	scale parameter of the direct link
β_r	scale parameter of the r^{th} IRS link
κ	ratio of the total power of the dominant component to the total power of the scattered waves
μ	the number of multipath clusters
m	the shadowing parameter
Γ	Gamma function
Z	aggregate channel power due to direct and IRS-assisted links
$h_{r,n}$	channel between a BS and n^{th} element of r^{th} IRS panel
$g_{r,n}$	channel between an n^{th} element of r^{th} IRS panel and a receiver
$L_{h_{S,D}}$	pathloss fading coefficients of a direct link
$L_{h_{r,n}}$	pathloss fading coefficients of a BS-IRS link
$L_{g_{r,n}}$	pathloss fading coefficients of an IRS-user link
Θ_r	phase shift matrix induced by r^{th} IRS
\mathcal{R}	total number of IRS panels
N_0	noise power spectral density
x	distance between a user and nearest BS/IRS
y	distance between a user and interfering BS/IRS
β	free space path loss channel power gain
λ_b	base station density
λ_r	IRS density
Φ_b	PPP for base stations
Φ_r	PPP for IRSs
Φ_u	PPP for users

h_{BU}	direct link channel between a BS and a user
\mathbf{h}_{BR}	channel between a BS and an IRS panel
\mathbf{h}_{RU}	channel between an IRS panel and a user
I_b	aggregate interference due to all base stations
I_r	aggregate interference due to all IRS
Θ_x	phase shift matrix of nearest serving IRS
Θ_i	phase shift matrix of interfering IRS
S_{d_x}	received signal power from a serving BS at a distance x
S_{r_x}	received signal power from a serving IRS at a distance x
τ	instantaneous time

CHAPTER 1

INTRODUCTION

The recent advancements in wireless communication has witnessed the deployment of Fifth-generation (5G) technology standard in a few segments of civilian and military regimes. Precisely, the 5G wireless technology is meant for realizing bandwidth intense network applications with diverse service requirements. It also promises to provide massive connectivity, enhanced mobile broadband and ultra low latency, by exploiting advanced technologies such as massive multiple-input multiple-output (MIMO), millimeter wave (mmWave) communications, ultra-dense network (UDN), and so on. However, these technologies inheritate limitations such as excessive power consumption and usage of expensive hardware. For instance, enhancing number of base stations (BSs) or access points (APs) in a UDN results in scaling total energy consumption of a wireless network in linear proportion. Subsequently, it leads to increased hardware cost and enhanced interference. Further, transceivers architecture at mmWave frequencies involves complex signal processing and it is a challenging task to satisfy QoS requirements especially in a harsh propagation environment. In parallel, with the advancements in multimedia technology and Artificial Intelligence (AI), stringent demands of user community become challenging with unprecedented performance requirements.

In this perspective, wireless industry and academia have put an inimitable effort to develop and standardize the Beyond-5G (B5G) and sixth generation (6G) wireless networks in the present era. The upcoming B5G/6G technology is expected to support usage scenarios including extreme capacity backhaul, enhanced blindspots, short range device-to-device communication, smart rail mobility, multi-sensory extended reality, industrial automation and robotics, autonomous mobility, and connectivity in remote areas and so on. A brief comparison of 5G and 6G technologies in terms of distinguished specifications of Key Performance Indicators (KPI) is given in Table 1.1.

Table 1.1: A comparison of 5G and 6G key performance indicators (Rajatheva et al., 2020)

Key Performance Indicator	5G	6G
Peak data rate	20 Gb/s	1 Tb/s
User experienced data rate	0.1 Gb/s	1 Gb/s
Peak spectral efficiency	30 b/s/Hz	60 b/s/Hz
User experienced spectral efficiency	0.3 b/s/Hz	3 b/s/Hz
Maximum bandwidth	1 GHz	100 GHz
Area traffic capacity	10 Mb/s/m ²	1 Gb/s/m ²
Connection density	10 ⁵ devices/km ²	10 ⁷ devices/km ²
Energy efficiency	not specified	1 Tb/J
Latency	1 ms	100 μs
Reliability	99.999%	99.99999%
Jitter	not specified	1 μs
Mobility	500 km/h	1000 km/h

As per communication engineering fundamentals, it can be easily inferred that the operating carrier frequency should be very high in order to provide larger bandwidth. However, at higher operational frequencies owing to excessive penetration losses, wireless propagation environment experiences exceptionally high attenuation. Thus, a wireless link gets severely degraded during NLOS mode of propagation between transmitter and receiver. One of the prominent technology which can alleviate this limitation exploits reconfigurability of wireless channel and it is enabled by Intelligent Reflecting Surface (IRS) deployment. Advantage of using IRS in a wireless network is that, they are capable of reconfiguring the wireless propagation environment in a smart and adaptive manner. IRS panels deployed in an area have the capabilities to improve the propagation conditions by introducing a virtual Line-of-Sight (VLOS) path to enhance the coverage and capacity of wireless network. Recently, the researchers have developed techniques to model the IRS-assisted channel and studied the performance analysis based on the applications driven QoS requirements. However, still there exists many research gaps and challenges that require sophisticated techniques appropriate for the specific realistic scenarios. Motivation, problem definition, formulation of objectives and organization of the thesis are also discussed in this chapter. In this thesis, the upcoming technology refers to the B5G/6G technology.

1.1 Introduction to Intelligent Reflecting Surface

IRS is considered as the most promising technique which is able to significantly improve the performance of wireless communication networks, by smartly reconfiguring wireless propagation environment in an adaptive manner with usage of massive low-cost passive reflecting elements embedded on a planar surface (Wu and Zhang, 2020). It is worth mentioning that, the literature on the IRS technology makes use of different terminologies, such as Reconfigurable Intelligent Surface (RIS) (Dai et al., 2020), (El-Mossallamy et al., 2020), Large Intelligent Surface (LIS) (Yan et al., 2020), (Yuan et al., 2020), and programmable metasurface (Tang et al., 2019) etc. Though, terminologies are different, basic operating principle and underlying mechanism being passive and tunable reflecting surface remains the same.

1.1.1 Architecture of an IRS panel

The hardware implementation of IRS is based on the concept of “metasurface”, which is made of two-dimensional (2D) metamaterial that is digitally controllable (Cui et al., 2014). Typically, the metasurface consist of a large number of reflecting elements or meta-atoms embedded on a planar array as shown in Figure 1.1. A typical architecture of IRS consists of three layers and a smart controller. In an outer layer, a large number of metallic patches or reflecting elements are printed on a dielectric substrate to directly interact with incident signals. Behind this layer, a copper plate is used to avoid signal energy leakage. Last and the inner most layer is a control circuit board that is responsible for adjusting amplitude coefficient/phase shift of each reflecting element, and for it the desired regulation is triggered by a smart controller attached to an IRS.

Specifically, different elements of an IRS panel can independently reflect incident signal by controlling its amplitude and/or phase and thereby collaboratively achieve fine-grained 3D passive beamforming for direction specific signal enhancement or nulling. Phase shifts introduced by individual IRS elements are controlled by a smart IRS controller, which gets relevant information from a transmitter (base station) over a

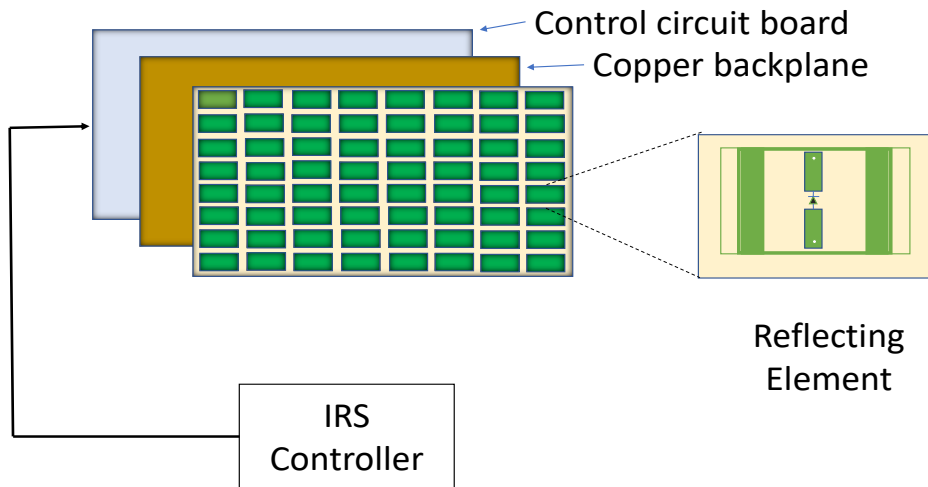


Figure 1.1: Architecture of IRS (Wu and Zhang, 2020).

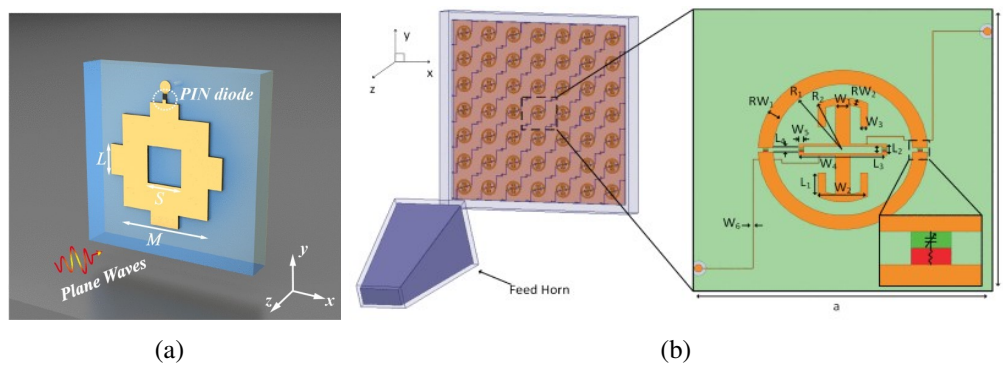


Figure 1.2: Reflecting element schematic embedded on IRS panel (a) Structure of PIN diode (Wang et al., 2020), and (b) Structure of Varactor diode (Trampler et al., 2020)

backhaul link. By properly designing reflecting elements, including geometrical shape, size/dimension, orientation, arrangement, and so on, the salient features of an individual signal response can be modified accordingly. Size of each reflecting element should be smaller than the operating wavelength, so that an arbitrary reflecting element scatters an incoming signal with approximately uniform gain in all the directions (Özdoğan et al., 2019).

In wireless communication applications, reflection coefficients of each element should be tunable to cater to dynamic wireless channels arising by virtue of user mo-

bility, and thus requires reconfigurability in real time. In order to realize IRS, different methods have been proposed to reconfigure reflection coefficients by using electronic devices such as positive-intrinsic-negative (PIN) diodes, varactor diodes, field-effect transistors (FETs), or micro-electromechanical system (MEMS) switches. Structure of a reflecting element implemented using PIN diode and varactor diode is shown in Figure 1.2. PIN diode is used as a controller to turn on/off a specific reflecting element, in order to reverse phase reflection (Wang et al., 2020). Whereas, to achieve continuous phase shift reflection, a varactor diode is used in (Trampller et al., 2020). In practice, field-programmable gate array (FPGA) can be implemented as a controller, which also acts as a gateway to communicate and coordinate with other network elements by means of separate wireless links.

1.1.2 Signal propagation in IRS-assisted wireless Terrain

In wireless communication, blockages caused by miscellaneous geographical objects, such as buildings, foliage, vehicles, etc., are more severe at high carrier frequency transmission, since at these frequencies propagating signals experience exceptionally high penetration losses and thus suffer from massive attenuation. In these geographical terrain, wireless network assisted with IRSs can be used to improve link establishment. With reference to communication setup established in future communication, a comparison of cellular users in absence of IRS, and with IRS is shown in Figure 1.3.

In Figure 1.3a, a communication link is established with only those users, who are in LOS with respect to a base station. Users under the shadow of environmental objects suffer with penetration loss, due to blocked LOS path. This results in a degraded performance for a cellular user under harsh environment scenarios. This shortcoming can be overcome by deploying IRS panels at appropriate locations to improve the link establishment as shown in Figure 1.3b. Here, it can be seen that a user deprived of a direct LOS with a base station, has an alternative VLOS path to establish the communication via IRS. This is possible, when responses of IRS are optimized to reflect the incoming signal in a particular direction. Thus, in a wireless terrain wherein users suf-

fer with severe attenuation due to blockages caused by surrounding objects, presence of IRS panels significantly enhances VLOS link establishment.

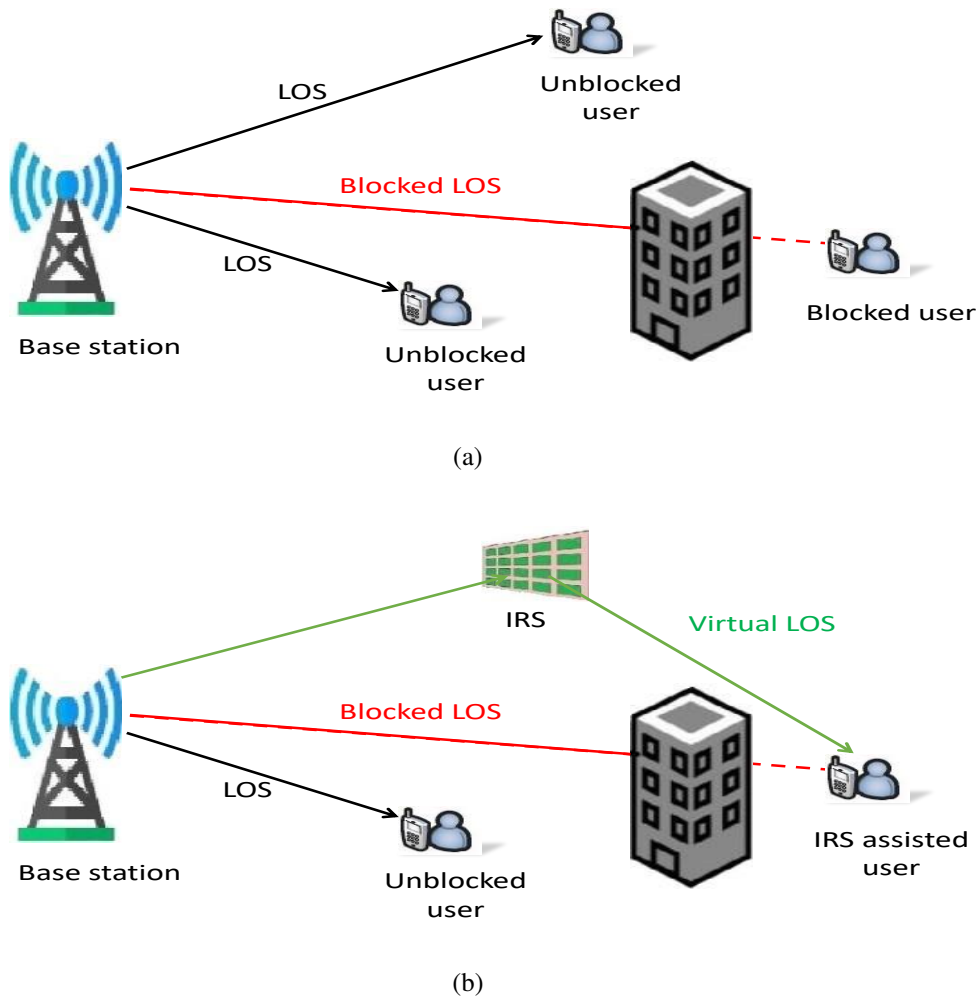


Figure 1.3: Schematic of (a) obstructed wireless link without IRS, (b) VLOS link enabled through IRS

1.1.3 Advantages of IRS

There are several advantages of IRSs, which are listed here.

- **Ease of deployment:** The IRS panels can be mounted easily on the facade of buildings or lamp posts in a given wireless terrain for outdoor scenarios. While, IRSs can also be deployed on walls or ceilings for indoor scenarios. Usually,

purpose of using IRS panels is served when these panels are deployed in a terrain, wherein user experiences severe fading/shadowing due to surrounding obstacles.

- Enhancement in spectral efficiency: IRS panels are capable of reconfiguring a wireless propagation environment by compensating for power loss by forming an alternative VLOS path over long distances.
- Environment friendly: The main advantage of IRS panels is that they are passive reflectors. Amount of power consumed by IRS panels is very minimal as compared to conventional relaying systems, such as, Amplify-and-Forward and Decode-and-Forward system. Thus, deploying IRS panels is more energy efficient and environment friendly than the conventional relaying systems.
- Compatibility: The functionality of IRS, to passively reflect electromagnetic wave make them suitable for full-duplex communication. Also, IRS-assisted wireless networks are compatible with the standards and hardware of existing legacy wireless networks.

1.1.4 Application scenarios of IRS

Several applications of IRS-assisted wireless network for future communication is illustrated in Figure 1.4. Usage of IRSs is not limited to a particular scenario, since it finds applications in indoor scenario, outdoor scenario, for smart city environment, in Internet of Things (IoT) networks and so on. In general, deployment of IRSs is more appropriate at locations experiencing blindspots and/or unwarranted fading, for example at a busy traffic junction or any indoor/outdoor scenarios characterized with a high density of users and obstacles.

In terms of usage of IRSs in wireless networks, these panels help in enhancing coverage area of a cellular network by providing an alternative LOS path. They assist a cell-edge user who suffers from both high signal attenuation from its serving BS and severe co-channel interference from a neighbouring BS. IRSs also acts as a signal reflection hub to support simultaneous low-power Device-to-Device (D2D) transmissions.

IRSs can also be used to transmit secret information to legitimate user securely, while cancelling out the reflected signal for any unintended eavesdropper. IRSs also find applications in enhancing the QoS for a vehicular network. Further, IRSs can be deployed on Unmanned Aerial Vehicle (UAV), where it has added advantage of portability of IRSs. So these movable IRSs can be used in smart city environments for providing QoS connection. Finally, application in smart industry automation and wireless sensor networks assisted by IRS, finds its usefulness in terms of achieved energy efficiency.

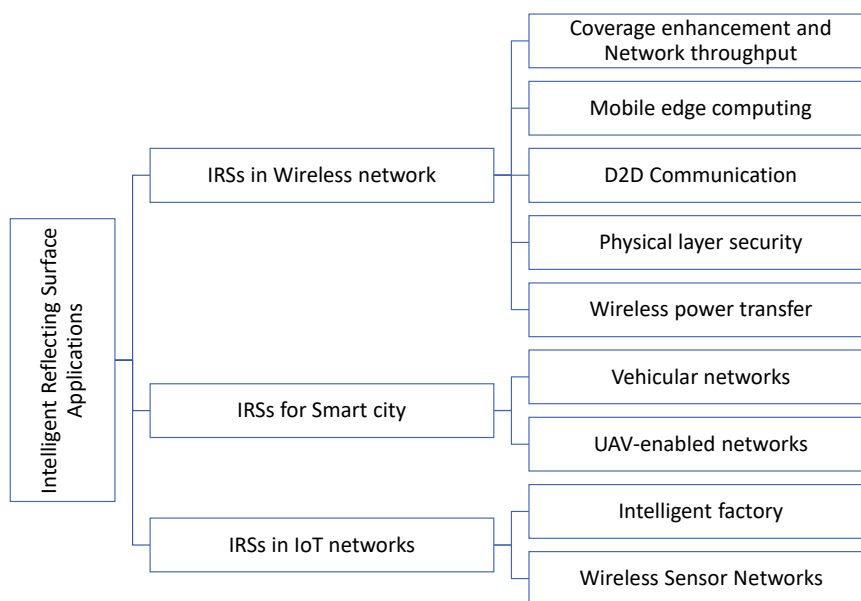


Figure 1.4: Diverse applications of IRS.

1.2 Motivation

An exhaustive set of channel modeling approaches for IRS-assisted wireless terrain is given in section 3.1. However, these methods have inherent limitations in terms of considered channel characteristics. Among these, the primary and prominent limitation is a hypothesis under which a wireless channel under investigation is treated as time-invariant (TI), which is not true in a majority of practical scenarios and use cases, especially in an outdoor wireless environment. Another presumption is a priori knowledge of perfect Channel State Information (CSI), which is difficult to acquire since IRS

doesn't have radio resources that can facilitate a precise estimate of channel state. Using inference from these observations, in this thesis an attempt is made to model wireless channel in terms of impulse response characterization with reasonably good approximation. For two different geographical scenarios belonging to Urban-micro (UMi), i.e., open street (OS) and street canyon (SC), localized geometry features of a segment of wireless terrain as well as in vicinity of a mobile receiver are incorporated during channel modeling. Depending upon the LOS and NLOS compliance, an end-to-end wireless link between a base station (BS) and a mobile receiver through IRS panels are represented as a cascade arrangement of Time-Invariant (TI) and Time-variant (TV) channel models.

Shadowing and multipath propagation affect the performance of a wireless communication system in a considerable manner. Severity of fading in any localized wireless terrain is non-uniform, this attributes to inherent spatial aspects in close vicinity of receiver and time dependent vehicular traffic characteristics along with presence of temporary blockages in short epochs. Work carried out in this thesis aims to provide a comprehensive analysis about the impact of presence of multiple IRS panels in a wireless terrain on shadowed fading. This is one of the early attempts to estimate wireless link's outage probability for multiple IRS-assisted wireless terrain. A outage probability analysis of multiple IRS-assisted cooperative communication system is performed, where different link segments of an end-to-end wireless link are presumed to govern by the $\kappa - \mu$ shadowed fading model.

Stochastic geometry deals with a study of spatial patterns that are random in nature. Recently, stochastic geometry find a significant role in the analysis of heterogeneous network (HetNet) in cellular communication. It helps in providing some key insights for network design using analytical approaches. The basic underlying mechanism is, to model random locations of wireless nodes by a random set of points (often referred to as a point process) and subsequently analyzing performance of a wireless network using the properties of the point process. In this context, performance analysis of IRS-assisted cellular communication using stochastic geometry is a very new approach. For this purpose, tools from stochastic geometry are of particular interest, where a strategy is to

endow appropriate distributions for locations of different network entities and subsequently utilizing properties of these distributions to characterize network performance. Performance analysis of IRS panels assisted cellular communication using stochastic geometry is still in infancy.

1.3 Problem Definition

In wireless communication systems architecture, so far emphasis has been on configuring transceivers as wireless channel behaviour is upto some extent unpredictable and beyond the scope of any regulation. The ubiquitous presence of fixed (geography induced) and movable (owing to surrounding vehicles) obstacles contributes to vulnerable degradation in receiving signal strength during course of signal propagation by virtue of randomness associated with NLOS components. Further, in various use cases of mobile/cellular communication owing to inherent relative motion between transmitter-receiver pair, channel behaviour becomes further complex and it adversely affect signal propagation characteristics. Even if both of these link entities (source and receiver) are static, obstacles and scatterers may introduce relative velocities. These situations give rise to time variations of the wireless channel due to the Doppler effect, which hinders parameters estimation and degrades detection performance. A major regulating factor that impacts the impulse response measurement/characterization is attenuation associated with the propagation paths corresponding to several NLOS components. Thereby it is quite obvious that the performance evolves around propagation dynamics of NLOS components. These observations fuel a need to counter the unwarranted variations in received signal strength mainly due to inevitable NLOS components and subsequently enhancing the performance measures namely, achievable rate, outage probability and coverage probability.

Appropriate positioning of network elements in a cellular communication system using stochastic approach needs precise location and time information. Typically, any geographical terrain in an urban scenario experiences various degree of fading during

different time intervals and at specific locations. Owing to surrounding geospatial aspects, fading zones can be classified as light fading zone, moderate fading zone and severe fading zone. Similarly, due to heterogeneous behaviour of users, data/vehicular traffic patterns can be classified into distinguished time intervals as wee hours, off-peak hours and peak hours, with a unique characteristic; increasing order of users density in short epochs during different time of the day. Usually, users experience localized blindspots, one such occurrences may be, during peak hours of a day and in a geographical terrain characterized by a severe fading zone. There is a need for modeling these kinds of wireless terrain using suitable approximations with an emphasis on outage and coverage analysis.

1.4 Research objectives

In this work, formulated objectives are described as:

- To develop analytical channel models that:
 - (a) Characterizes Time-Invariant and Time-varying channel behaviour for outdoor use cases such as; UMi-open square and UMi- street canyon scenarios
 - (b) Enhance achievable rate and coverage span by deploying appropriate number of IRS panels at suitable locations, with hypothesis based on empirical observations obtained from an unregulated wireless terrain.
- To establish an outage performance evaluation for wireless terrain equipped with multiple IRS panels and comprises different fading zones, while wireless channel is modelled using $\kappa - \mu$ shadow fading.
- To propose and validate stochastic models that characterize location of IRS panels and users by PPP and PCP distribution, and BSs by PPP distribution. Subsequently, performing coverage analysis for these presumed stochastic distribution for wireless terrain experiencing varying degree of fading by virtue of spatial and temporal attributes.

1.5 Methodology

Wireless link established between a base station and a user in a mmWave communication network is highly non-deterministic. The unregulated behaviour of the wireless propagation channel due to NLOS components are countered by deploying IRS panels in between transceivers at appropriate locations in a wireless terrain. Primary theme proposed in this work is ubiquitous presence of obstacles make signal propagation characteristics vulnerable owing to randomness associated with NLOS components. Thereby, presence of IRS panels transforms and decomposes a Time Variant channel between a base station (BS) and a mobile receiver into a Time Invariant model between BS and IRS panels, and TV model between IRS panels and a mobile receiver.

Primarily, this thesis presents an analytical framework in which an end-to-end wireless link between the BS and mobile receiver is characterized as a hybrid of TI and TV channels' impulse response models. To be more precise, the presence of IRS panels decomposes an overall TV channel between the BS and a mobile receiver into a TI channel model between the BS and IRS panels, and a TV channel model between the IRS panels and a mobile receiver. This is one of the unique approaches in which inference of local geographical factors is projected towards impulse response characterization of IRS-assisted outdoor wireless terrain. Further, for short spans of 100 m and 180 m, channel response is estimated much frequently, thus it can be interpreted that strength of the receiving signal at the location of the mobile receiver is estimated at equi-space distant points during shorter periodic epochs.

Analysis of a wireless terrain under various fading zones needs a mathematical modeling for outage validation. Wireless network outage performance of multiple IRS-assisted geographical terrain is investigated, while receiver experiences direct and/or reflected links and are characterized using $\kappa - \mu$ shadowed fading. Here, an IRS panel with maximum instantaneous signal-to-noise ratio (SNR) is selected to participate in

establishing an end-to-end wireless communication link.

In this thesis, to characterize the surrounding dynamics of diverse wireless terrain in a holistic manner, three different fading zones, namely; lightly fading, moderately fading and severely fading zones are considered. Further, for any urban or semi-urban wireless terrain, data traffic pattern varies depending upon the timing of operation. Corresponding to three different vehicular traffic characteristics, performance measures estimated for three distinct observation time-slots viz; peak hours, off-peak hours, and wee hours.

On exploiting stochastic geometry based analytical framework, this is one of the early attempt to use IRSs as network element and model the locations of IRSs and users by unified approach of PPP/PCP, depending upon the spatio-temporal behaviour of wireless terrain considered. In this context, network coverage can be significantly improved in a cellular network assisted by multiple IRSs panels.

1.6 Organization of the Thesis

Aim of the thesis is to develop an analytical channel models for IRS-assisted wireless network and to make analysis of various performance metrics for different outdoor environment scenarios in presence of IRS panels. This thesis is organized into six chapters based on the analyses and performance metrics measured for different objectives. The chapter 1 of the thesis describes the architecture of IRS and its working principle, advantages and applications of IRS-assisted networks. Motivation to carried out performance analysis of wireless terrain, problem definition, research objectives and structure of the thesis is given in this chapter.

In the second chapter, a comprehensive summary of various outdoor and indoor wireless scenario along with relevant specifications is given. A holistic set of performance metrics that is quite often measured is also described in this chapter for different scenarios. Some IRS prototypes designed and developed are also briefly presented in this chapter.

Chapter 3 focuses on the channel modeling and analysis of achievable rate and coverage enhancement in urban wireless terrain assisted with IRS panels. The literature survey section covers the exhaustive coverage of channel modeling schemes so far used for IRS equipped wireless terrain. Mathematical framework for Time-Invariant and Time-Varying channel scenarios is furnished in this chapter. In particular, two outdoor terrain namely UMi-OS and UMi-SC are considered that facilitate IRS-assisted wireless communication. Further, estimate of achievable rate enhancement and more reliable coverage using multiple IRS panels is validated. Chapter concludes with the performance analysis of the proposed mathematical framework in terms of obtained simulation results.

In chapter 4, an analytical framework is presented to estimate outage probability of an end-to-end communication link for wireless terrain equipped with multiple IRS panels. A detailed schematic and characteristics of a wireless terrain is also described in this chapter. Further, channel model for the considered wireless terrain and the analytical framework of the outage probability for multiple IRS-assisted wireless terrain is presented. While uncovering the local surrounding spatial/geographical characteristics and distinct vehicular traffic patterns, a comprehensive outage probability analysis and its inference is presented and concluded in last section.

In chapter 5, a unified analytical framework is proposed to approximate IRS panels and users locations for coverage analysis while imparting due concern to interference mitigation. The literature survey section covers the state-of-the-art schemes exploiting stochastic modeling approaches for approximating the location of network entities. Further, detailed schematics and characteristics of a wireless terrain with stochastic approach is described, followed by mathematical framework for analysing coverage probability. Finally, chapter concludes with the performance analysis of the proposed unified analytical framework in terms of simulation results.

Chapter 6 concludes contributions of the thesis by summarizing different mathematical framework. Future scope to develop efficient techniques that yield improved performances for future wireless communication paradigms is also briefly presented.

CHAPTER 2

IRS-ASSISTED WIRELESS NETWORK SCENARIOS AND PERFORMANCE MEASURES

Introduction

In this chapter, architecture of IRS-assisted wireless network is compared with the traditional relay based wireless network. The key advantages of IRS based network over relay based wireless networks are highlighted. Subsequently, two broad paradigms of deploying IRSs in future wireless network i.e., indoor and outdoor propagation environments are illustrated with a review of analytical models as well as prototype testbeds. Furthermore, a comprehensive summary of performance metrics, which are used to analyse the performance of IRS-assisted wireless terrain are discussed.

2.1 Comparison of IRS and relay-based wireless transmission links

In order to support exceptionally high bandwidth, millimeter wave (mmWave) communication is considered as a potential technique to cater unprecedented data rate for upcoming wireless technology. However, one of the basic challenges of mmWave communication is its vulnerability to blockage effects, which are inevitable in form of buildings, foliage, and vehicles etc. Thus, users (mobile receiver) experience blockage of the direct transmission/LOS path with respect to the base station (BS) due to the presence of obstacles in the surrounding environment. This major limitation of signal propagation can be addressed by adding a supplementary link, that is referred as VLOS and it mitigates blockage effects. This can be achieved by deploying the relays or IRS panels to enhance the quality of received signals as shown in Figure 2.1, which depicts an outdoor terrain equipped with a single relay/IRS. A wireless terrain assisted by a relay unit

and an IRS panel in presence of obstacles is illustrated in Figure 2.1a and Figure 2.1b, respectively, for an outdoor propagation environment. For the case of relay assisted wireless networks, different kinds of relays are used in practice, namely; amplify-and-forward (AF), decode-and-forward (DF) and full-duplex (FD) relays. Though, relays are used to facilitate a reliable connection between BS and user via an alternative path, it has many shortcomings as compared to that of a wireless terrain assisted by an IRS. In Table 2.1, a comparison of IRSs with different kinds of relays for a variety of operational and system parameters is given.

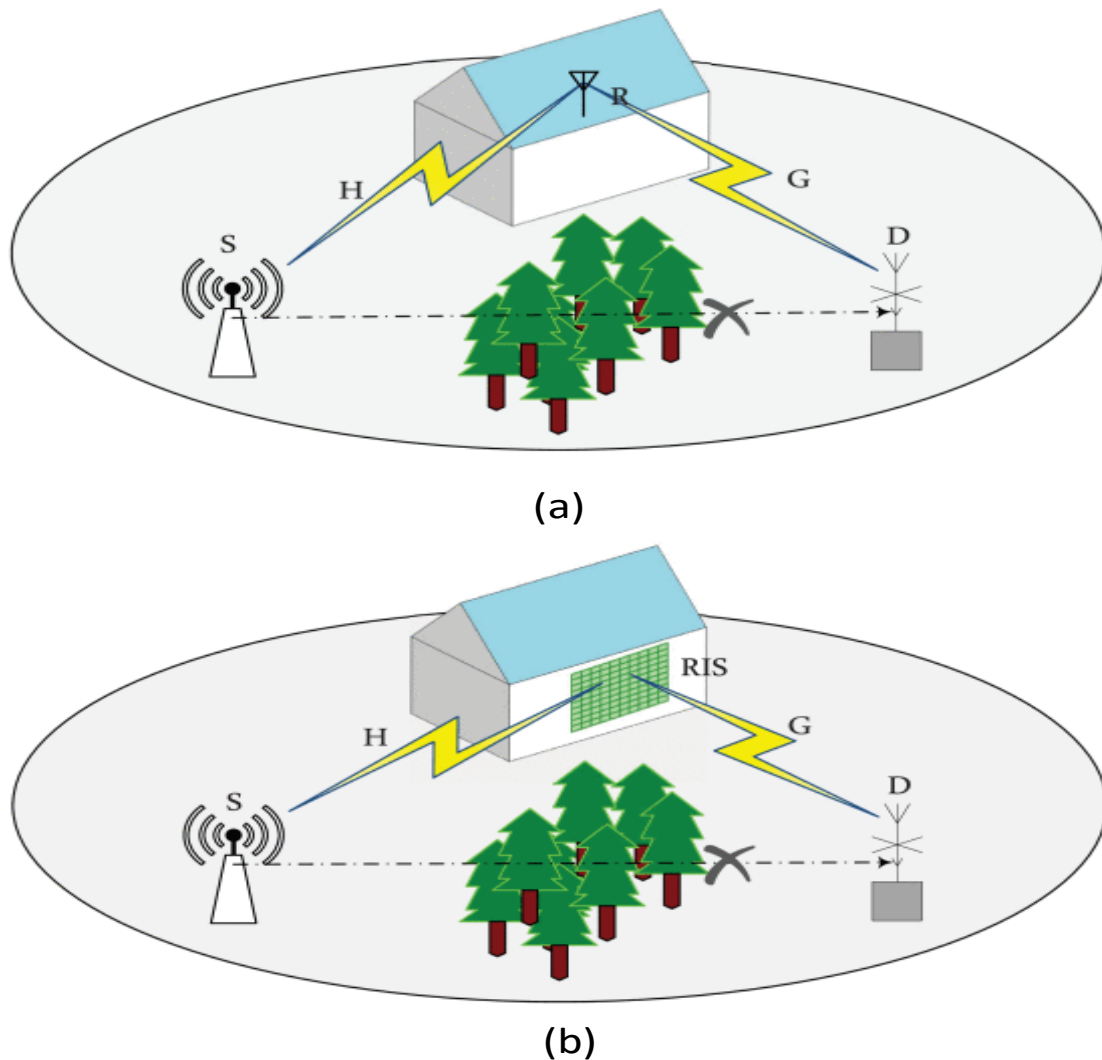


Figure 2.1: Wireless communication system supported with (a) relays and (b) IRS (Du et al., 2021).

Looking into comparative analysis as given in Table 2.1, it can be observed that IRS panels have advantages over relay mechanisms for a variety of practical applica-

Table 2.1: Comparison between IRS and relay mechanism (Pan et al., 2021).

Operational/system parameters	IRS	AF Relay	DF Relay	FD Relay
RF chains	No	Yes	Yes	Yes
Signal Processing	No	No	Yes	Yes
Noise	No	Yes	Yes	Yes
Duplex	Full	Half	Half	Full
Hardware cost	Low	Median	High	Very high
Power consumption	Low	Median	High	Very high

tions. The primary advantage of IRS panels is that, since these are passive reflecting elements, IRS panels deployment doesn't require sophisticated signal processing operations and the associated complex RF transceiver hardware. Hence, IRSs equipped wireless terrain incur less operating cost in terms of hardware and power consumption compared to conventional systems with relays. Further, since IRSs can be fabricated with light weight and limited layer thickness, they can be easily installed on walls, lamppost, ceilings, sign boards along the road and so on. In addition to it, an IRS can be operated in full-duplex mode as it doesn't induce unwarranted phenomena such as self-interference and thermal noise. Thus, IRSs achieve higher spectral efficiency compared to active half-duplex relay mechanism. However, deployment and efficient utilization of IRS panels need some careful investigations as there are some limitations associated with users of IRS panels. As an illustration, by considering an IRS as a totally passive element, the CSI is usually performed at the communication ends, i.e., the transmitter or the receiver. This leads to degradation in the accuracy of channel estimation, and high computation and power requirements when considering large IRSs (Pérez-Adán et al. (2021)). Moreover, in futuristic cellular networks, IRS panels will be deployed as inevitable network elements, and usual mode of communication is full-duplex. In view of this, on various operational issues, such as, hardware complexity

of RF chain, associated complexity of signal processing algorithm, accompanied noise, relatively high cost, and exceptionally high power consumption etc., yield an edge to IRS based network architecture over the relay-based network architecture. In summary, owing to low cost, relatively less complex signal processing, ease of deployment, and spectral efficiency the IRSs emerges as a potential technology for the next generation wireless networks.

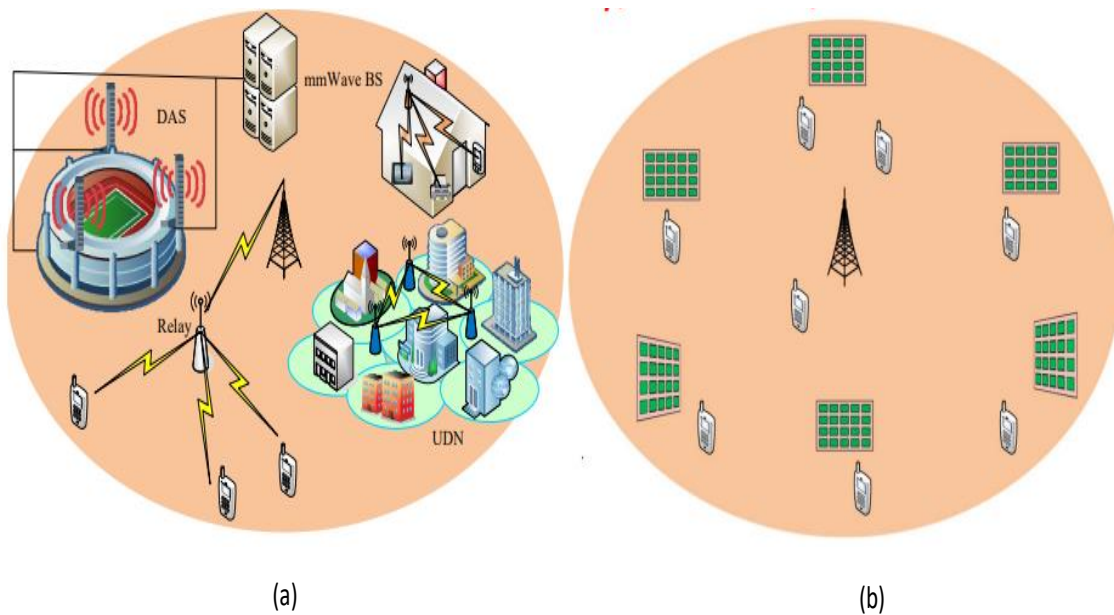


Figure 2.2: A schematic of wireless network using (a) relays, UDN and DAS, and (b) multiple IRSs (Wu and Zhang, 2020).

A comparison of wireless terrain assisted with existing technologies and multiple IRS panels is shown in Figure 2.2. An end-to-end wireless link in the conventional networks involves using active relays, small cell for ultra dense network (UDN) users and distributed antenna system (DAS) as shown in Figure 2.2a. The wireless communication system assisted with a single IRS can be scaled with multiple IRSs as shown in Figure 2.2b for multi-user environment scenarios. The major drawbacks in these conventional wireless networks is that, the network architecture consumes more energy and are costlier due to active components usage. Subsequently, the networks experience complicated interference management and bottleneck in the backhaul link. Whereas, IRS-assisted networks consume a very low energy due to usage of passive components and are cost effective. Further, they are used for local coverage without the need of an

inter-IRS interference management.

Relay terminals and IRS units assisted wireless terrain characteristics and performance is summarized as follows. A Cooperative multiple antenna deployment links was proposed in (Feteiha and Hassanein, 2016), here vehicles act as relaying terminals using Decode-and-Forward relaying for Long Term Evolution-Advanced network. For a full-duplex relay exploiting Amplify and Forward protocol, the effect of distance, path loss exponent, and residual self-interference on the vehicle-to-vehicle communication system is analyzed in (Nguyen et al., 2019). A mechanism for broadcasting warning messages to vehicles complying NLOS conditions at road-intersections in an urban scenario with reduced time delay is proposed in (Alodadi et al., 2017). Using non-orthogonal multiple access (NOMA) scheme, the outage probability and average achievable rate of vehicular communication links at road-intersections in the presence of interference are proposed in (Belmekki et al., 2020). The key differences and similarities between IRSs and relays based wireless network architectures are given in (Di Renzo et al., 2020) along with spectral efficiency analysis.

2.2 IRS-aided wireless communication system

The system architecture and prototype of an IRS-assisted wireless communication system is depicted in Figure 2.3 and 2.4, respectively. The system is composed of Personal Computers, universal software radio peripherals (USRPs), an IRS unit, a FPGA-based master control board. The transmitter section consists of a host computer, a USRP device and an antenna unit designed to transmit at desired operating frequency. IRS unit is placed at an appropriate location between the transmitter and receiver so as to serve as a smart reflector that reflects impinging signal as a beam towards the intended receiver. While operating the system in real-time, there is a need for adaptation of the reflection coefficients, which can be exercised by introducing a feedback link that connects IRS unit and a receiver.

Further, in the outer layer of IRS, a large number of metallic patches are printed on

a dielectric substrate to directly interact with incident signals. Unlike, the active relay assisted wireless system, which performs signal regeneration and retransmission, IRS does not include active transmit module, rather it reflects the incident signal as a passive array. The control circuit board is responsible for adjusting the amplitude and/or phase shift of reflected signal that is enabled by elements of an IRS and is regulated by a smart controller attached to the IRS.

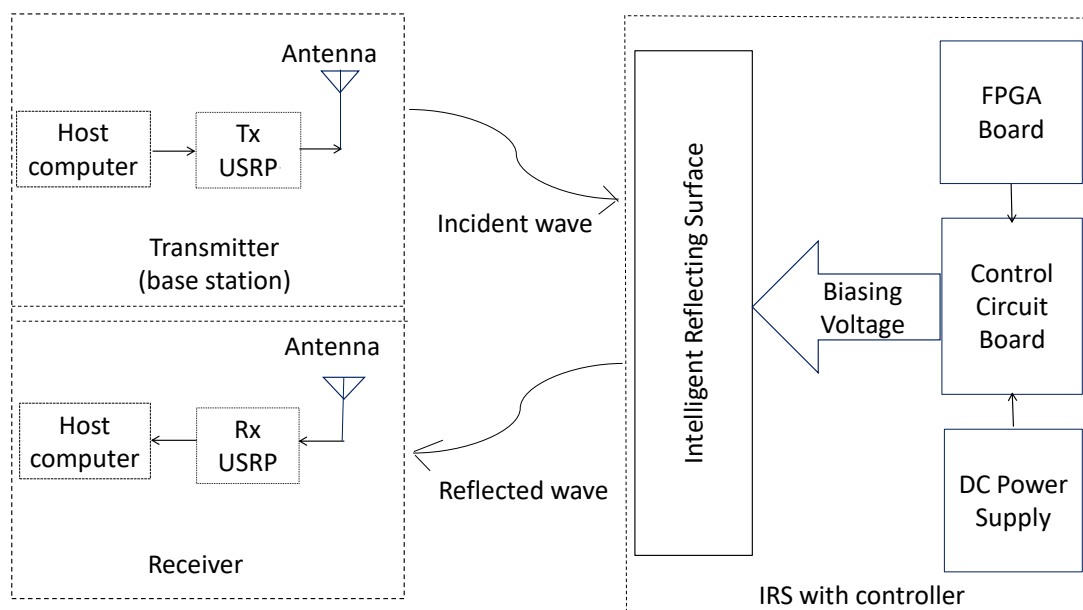


Figure 2.3: System architecture for IRS-assisted communication system (Pei et al., 2021).

The basic operation involved in the design of reflecting surface is based on the generalized Snell's law of reflection (Özdoğan et al., 2019). According to the generalized Snell's law, each reflecting surface can independently tune the angle of reflection and phase of the reflected ray, where it gives an information about ideal phase shift that is required to create a narrow beam oriented towards an intended receiver. The underlying mechanism that facilitates reconfigurable aspects of the wireless environment in a controllable manner is to introduce desired regulation of reflected signal components' amplitude coefficients and phase shifts. In order to generate variable phase shift, PIN diodes can be used which are embedded in each reflecting element. The PIN diode can be controlled by switching to either "ON" or "OFF" state, by applying different biasing voltages via a direct-current feeding line, thus triggering the reflecting elements to

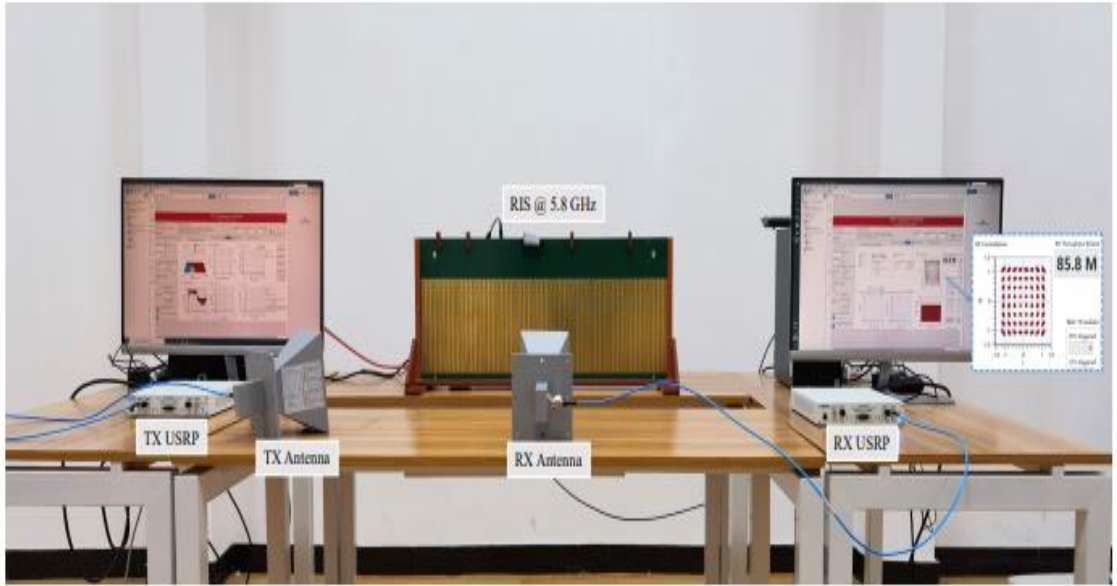


Figure 2.4: Prototype of IRS-assisted wireless communication system (Pei et al., 2021).

result in a phase-shift difference of π in the incident signal.

A prototype IRS unit designed and fabricated (Pei et al., 2021) for wireless communication system is shown in Figure 2.4. The reflecting elements are arranged in the form of a Uniform Planar Array with a 55×20 element grid, constituting 1100 elements in a single IRS panel. The dimension of the fabricated IRS unit during experimentation is $80.08 \text{ cm} \times 31.30 \text{ cm}$, indicating the compactness of the IRS panel for the ease of deployment at appropriate locations. Further, IRS can be configured to operate in any part of the radio frequency spectrum, including frequencies from sub-6 GHz to THz span, thus supports a wide range of operating frequencies.

Recently wireless industry has paved initiatives to implement and commercialize IRS based technologies to create new value chains, and several startups have been launched to advance in this new field of research. The prominent companies and research projects with a brief about primary activity and objectives is given in Table 2.2. As an illustration, the Metawave startup company is working towards automotive radar, 5G wireless and artificial intelligence (AI), active repeaters and passive relays. The Greenerwave is investigating on 4D imaging radar, millimeter wave 5G to broadband satellite communications, Internet of Things (IoT) and RFID. The Pivotal commware is

Table 2.2: List of main industry progress, projects and prototypes related to IRS (Wu et al., 2021a)

Sl. No.	Company	Primary activity and achievement
1	NTT DOCOMO and Metawave (DoCoMo, 2018)	Demonstrated the first meta-structure reflectarray at 28 GHz band for 5G technology
2	Pivotal Commware (pivotalcommware, 2020)	Demonstrated software defined antennas using the holographic beamforming technology
3	NTT DOCOMO and AGC Inc. (Docomo, 2020)	Demonstrated the first prototype dynamic metasurface for 5G technology
4	Greenerwave (greenwave, 2020)	Developed reconfigurable meta surface based on physics and propagation
Sl. No.	Research project	Primary objective
1	VisorSurf (visorsurf, 2020)	Development of a software driven hardware platform for functional metasurface
2	ARIADNE (ariadne, 2020)	Design of a metasurface with the integration of artificial intelligence (AI) and new radio techniques
3	Pathfinder (cordis, 2020)	To develop intelligent metasurface assisted wireless 2.0 networks with theoretical and algorithmic base

researching in the domain of 5G mmWave technologies, systems and applications using holographic beamforming.

2.3 Environment scenario specifications

IRS panels can be deployed for both outdoor and indoor scenario usage as shown in Figure 2.5. Though the radio wave propagation mechanism in an indoor and outdoor environment is regulated by phenomenons such as reflection, scattering and diffraction, the signal propagation conditions in an indoor environment is much dynamic like; door/windows are open or closed, and the mounting place of antenna on desk or ceiling

etc.,. Whereas, the Doppler spread effect due to relative motion between the transmitter and receiver affects the radio propagation mechanism significantly in an outdoor environment. Further, by virtue of parameter namely doppler spread as relative motion is not significant in an indoor environment compared to outdoor environment. The indoor channel characteristics is not as dynamic as the outdoor one. Whereas, characterizing the shadow fading channel in an outdoor terrain is more complex due to dynamic channel variations on account of large moving surrounding obstacles.

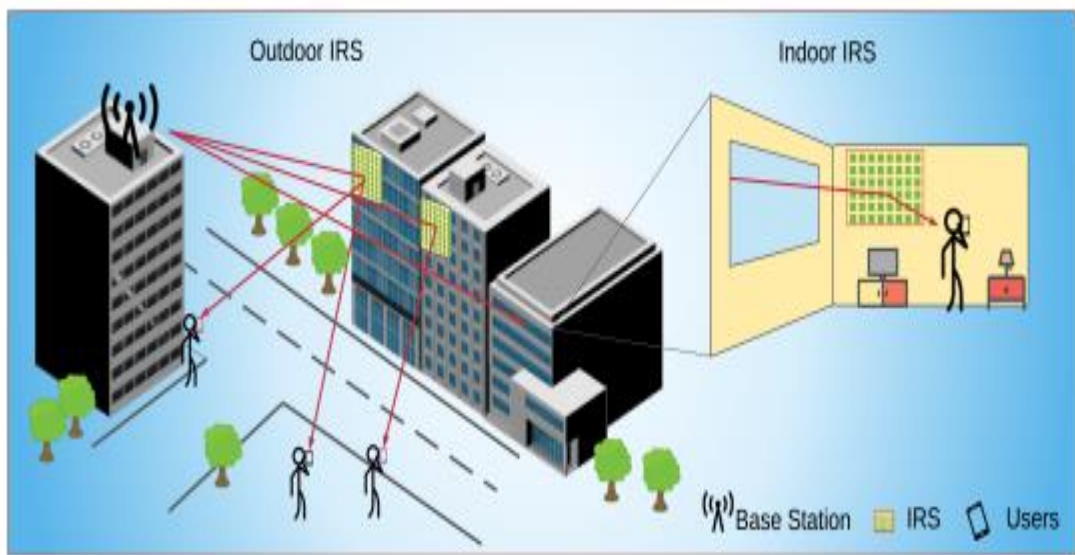


Figure 2.5: IRS-assisted wireless communication for outdoor and indoor deployments (Elbir and Mishra, 2020).

For indoor environment scenarios, it is appropriate to consider the near-field propagation effects, while considering the channel modeling aspects. In this case, the far-field assumption may not hold good, since the IRS is either closer to transmitter or receiver (Dajer et al., 2021). Whereas, for channel modeling in an outdoor environment scenario, both the near-field and far-field effects can be considered depending upon the relative position of the IRS with respect to transmitter and receiver location.

For a user in an outdoor environment, in particular for an urban terrain characterized with high rise buildings, huge size sign boards along the road can be equipped with IRS panels at appropriate locations to enable virtual line of sight (VLOS) links via IRS panels. For indoor environments, the typical scenarios experiencing high user density

include offices, shopping centres, etc., and in such terrain IRS panels can be deployed on various objects such as walls, ceilings, windows, furnitures to improve the quality of received signal and the coverage area.

2.3.1 Indoor scenarios

Typically, the wireless communication established in an indoor propagation environment is for shorter distances. Further, the variability of the environment is much larger even for a small separation range of transmitter-receiver. Subsequently, the propagation inside a building is strongly influenced by; layout of the building, construction materials, and building type which can be factory, office area, shopping mall etc. The strength of the received signal measured inside a building usually is low, due to the high penetration loss from walls. One of the major requirement of indoor scenario such as; hospitals, factories, security offices is to have a ultra-reliable high-speed communication. In this situation, an IRS-assisted communication setup established will certainly help to improve communication and coverage aspects of indoor wireless system. IRSs indeed have many other applications including military purposes, indoor localization and health monitoring system etc.

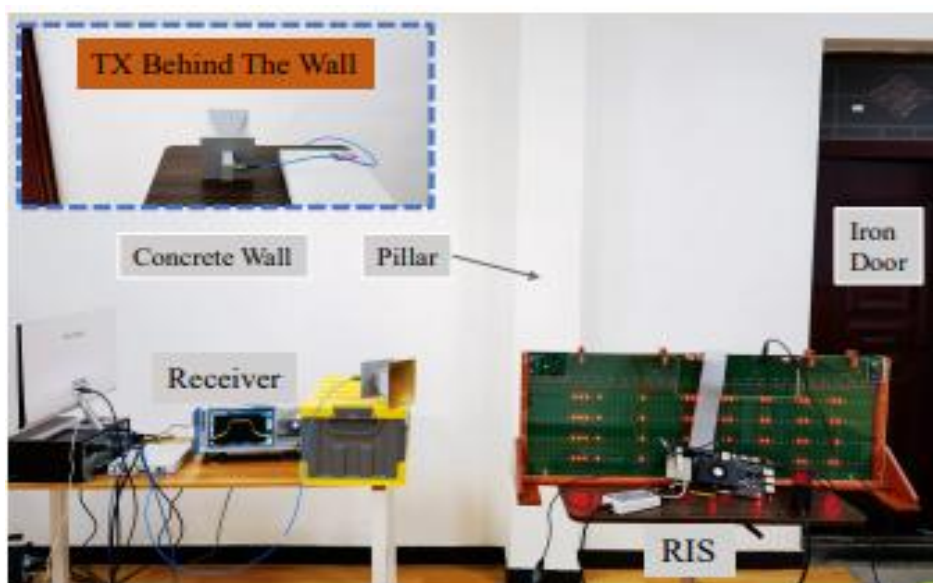


Figure 2.6: A transmission setup for indoor scenario (Pei et al., 2021).

A prototype setup for an IRS-assisted wireless communication in an indoor environment is shown in Figure 2.6 (Pei et al., 2021). The setup depicts for a scenario wherein transmitter and receiver (transceiver) placed in a separate room, so as to comply NLOS norms. In such use case, as the transmitted signal suffers penetration loss, the obtained experimental results demonstrate that received signal strength increases due to the presence of IRS. The effectiveness of the IRS usage in terms of total received signal strength is validated for both, i.e., LOS and NLOS scenarios.

2.3.2 Outdoor scenarios

A prototype setup of over-the-air test for an outdoor terrain equipped with an IRS is shown in Figure 2.7 (Pei et al., 2021). Implications of IRS presence is validated using enhanced received signal strength for a particular experimental setting in which transmitter and the receiver is 500 m space apart and tested for a real-time transmission of a video signal. It is validated that the streaming video is communicated smoothly in the presence of IRS.

In outdoor environment scenarios, ultra-reliable low-latency communication (URLLC) requirement acts as crucial factor for applications that demand stringent latency and reliability requirements such as augmented/virtual reality and autonomous vehicles. IRS can be deployed on the building facade, advertising sign-board, lamppost and also even on the surface of moving vehicles, to have URLLC requirement. The key factor that has to be considered, is to effectively compensate the Doppler spread and delay spread effects, in turn benefits smart transportation applications have stringent URLLC requirements. In these kind of scenarios, the reliable end-to end communication can be achieved by exploiting IRS-assisted links. Thus the usage of IRS-assisted system helps in reducing the packet retransmission and subsequently minimizing the delay which is critical for URLLC applications.

The typical outdoor wireless terrain scenarios used for field measurement with channel parameters and specifications are given in Table 2.3. For the system setup and deployment of wireless communication system, knowing the propagation characteristics

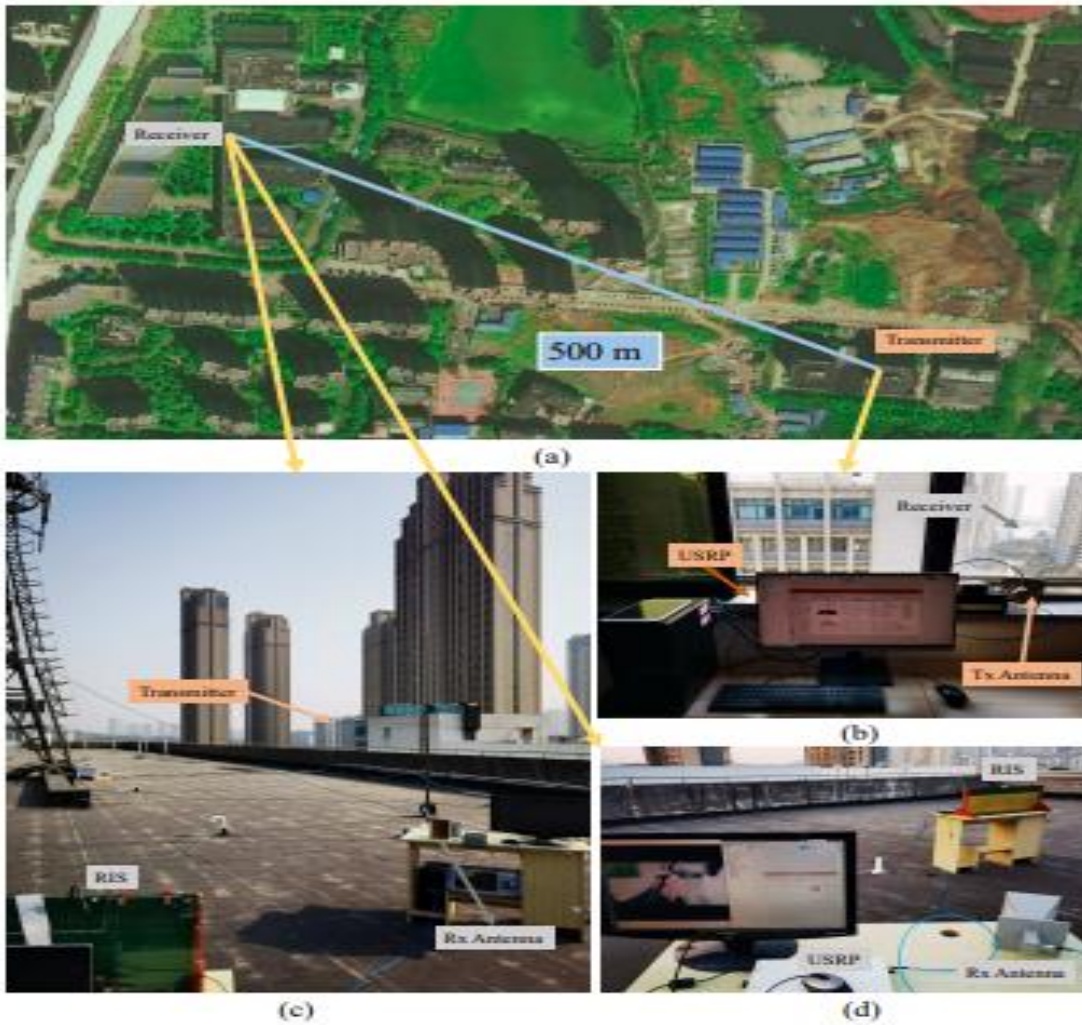


Figure 2.7: A transmission setup for outdoor scenario spanning 500 m (a) location of the transmitter and receiver on the map (b) the transmitter unit (c) the site of the receiver; (d) a snap of the receiver while data transmission. (Pei et al., 2021).

is very important, since user complying to LOS or NLOS with respect to BS makes a big impact for mmWave communication system. Here two major classifications for outdoor scenarios namely; urban microcell (UMi) and urban macrocell (UMa) terrain specifications are considered. In case of UMi scenario, BSs are usually mounted below the rooftop levels of surrounding buildings, for realizing seamless coverage. Whereas, in UMa scenarios with larger inter-site distances and the regions with rich scattering environments, BS heights above 25 m are considered. Overall, the parameters and specifications in Table 2.3 gives an indication of the typical transmitter and receiver

height setups, valid communication range and path loss exponent (PLE) values for a specific outdoor wireless terrain that operates in the mmWave band of frequencies.

Table 2.3: Channel parameters and specifications in outdoor scenarios (Wang et al., 2019)

Area	scenario	frequency (GHz)	Tx height (m)	Rx height (m)	range (m)	PLE
UMi campus	LOS	28/38	5	1.7	14-113	2.7/3.1
	NLOS	28/38	5	1.7	14-113	3.7/3.1
	NLOS	28	15	1.5	98-270	2.7
	LOS	38	8/23/36	1.5	>200	1.9
	NLOS	38	8/23/36	1.5	>200	3.3
UMi street canyon	LOS	28	7/17	1.5	31-54	2.1
	NLOS	28	7/17	1.5	61-186	3.4
	LOS	29	6.5	1.5	35-256	2.2
	NLOS	29	6.5	1.5	35-256	3.1
UMi downtown	LOS	28	8/17	-	55-207	2.1
	NLOS	28	40	1.5	110-135	4.1
UMa open area	LOS	29	-	-	35-256	2.7
	NLOS	29	-	-	35-256	3.4
UMa parking structures	LOS	29	-	-	35-256	2.9
	NLOS	29	-	-	35-256	3.44

2.4 Comprehensive performance metrics

The impact of IRS presence can be validated by various performance metrics which are typically used in a variety of wireless networks scenarios. The performance metrics based on probabilistic analysis are used to characterize the uncertainty associated with an end-to-end link that comprises a transmitter, propagation channel and the receiver architecture. Further, the ergodic metrics are used to characterize the averaged network performance, channel conditions, considering the randomness in network topology, the distribution of reflecting elements, and interference variations, etc,. Performance metrics used for IRS-assisted wireless network include the following:

- Reflection probability: The probability that an IRS can reflect the signals from a

transmitter to an intended receiver.

- Outage or coverage probability: The probability that the SNR estimate at receiver is above or below a stipulated threshold.
- Bit error probability: The probability that the decoded information bits at receiver differs from the transmitted one.
- Ergodic capacity: The expectation of channel capacity measured by Shannon's formula.
- Pairwise error probability which measures the probability that the decoded signal is a certain symbol given the transmitted signal.
- Average area spectral efficiency which is the sum of the capacity of all the communication channels normalized over operating spectral bandwidth for a geographical terrain under investigation.
- Energy efficiency which measures the capacity normalized over the energy consumption of IRS equipped wireless networks.

From the perspective of future wireless network goals, researchers have considered the design objective with IRS assistance to achieve power minimization, rate maximization, energy efficiency maximization, outage minimization, weighted sum-rate maximization, and capacity/rate region characterization. A detailed set of performance metrics considered for analysing the performance of IRS-assisted wireless terrain is given in Table 2.4 and Table 2.5.

Table 2.4: Summary of performance metrics for IRS-assisted wireless networks ([Hassouna, 2022](#))

Sl. No.	Reference	Performance metrics	Design goal
1	(Di Renzo and Song, 2019)	Reflection probability	Establish point-to-point communication with maximizing reflection probability
2	(Khaleel and Basar, 2020)	Bit Error Rate (BER)	Enhance the performance and improve the spectral efficiency
3	(Guo et al., 2020)	Outage Probability	Minimization of outage probability in IRS-assisted MIMO systems
4	(Ferreira et al., 2020)	Bit error probability	To show performance improvement under double-Nakagami fading channels
5	(Jung et al., 2020a)	Achievable rate	To attain asymptotic optimality of IRS for maximizing achievable rate
6	(He et al., 2020)	Achievable rate	To achieve high rate in low SNR regime
7	(Özdoğan et al., 2020)	Achievable rate	Maximize the rate by optimizing phase and proper IRS deployment
8	(Zhang et al., 2020)	Achievable data rate	Maximize the data rate with optimal phase shift calculations
9	(Lyu and Zhang, 2020)	Spatial throughput	Maximize spatial throughput for IRS-aided multiuser environment
10	(Björnson, 2021)	Achievable data rate	Sum rate enhancement IRS-assisted OFDM under mutual coupling

Table 2.5: Summary of performance metrics for IRS-assisted wireless networks, continue from Table 2.4. (Hassouna, 2022)

Sl. No.	Reference	Performance metrics	Design goal
11	(Zhang and Zhang, 2021)	Achievable user rate	Achieve superior rate performance for different IRS deployment strategy
12	(Papazafeiropoulos et al., 2021a)	Coverage probability	To enhance coverage probability of IRS system under spatially correlated channels
13	(Jung et al., 2020b)	Ergodic rate	To show performance of IRS aided comparable to that of massive MIMO
14	(Papazafeiropoulos et al., 2021b)	Sum spectral efficiency	To enhance sum spectral efficiency for IRS-assisted MU-MISO systems
15	(Wu et al., 2021b)	Energy efficiency	To achieve energy efficiency for IRS-assisted cognitive radio networks
16	(Yang et al., 2021c)	Coverage probability and average throughput	Enhance coverage probability and throughput with minimal energy
17	(He et al., 2021)	Downlink rate	To enhance downlink rate for cooperative multi-IRS communications
18	(Du et al., 2021)	Outage probability and bit-error probability	To show that IRS aided system outperforms over AF relay system
19	(El Bouanani et al., 2020)	Outage probability and symbol error probability	To perform wireless power transfer with IRS aided wireless networks
20	(Yue and Liu, 2021)	Outage probability and ergodic rate	Enhance energy efficiency compared to conventional communications.

CHAPTER 3

CHANNEL MODELING AND PERFORMANCE ANALYSIS OF IRS-ASSISTED WIRELESS TERRAIN

3.1 Introduction

Wireless communication system is composed of propagation channel, transceiver units with associated antennas as air interface. Propagation channel is a medium, in which transmitted radio waves propagate and subsequently received by a receiving antenna. During this journey, radiated waves typically undergo attenuation and dispersion phenomena. Considering the operational characteristics of the propagation channel that depend on the geographical features of the wireless terrain, the transceiver should be properly designed to achieve a higher achievable rate and reliable communication.

In general, modeling of a wireless channel incorporates important channel parameters such as path loss exponent, attenuation coefficients and path delays associated with multipath components, and LOS probabilities. The key performance measures for 5G systems are data rate, latency, spectral efficiency, connection density, energy efficiency, reliability, mobility, and coverage. The 5G channel modeling is investigated in different communication scenarios namely, Urban Micro- (UMi) and Urban Macro- (UMa) cellular scenarios, Rural Macro (RMa), indoor office, indoor shopping mall, etc. The UMi scenarios include open square (OS) and street canyon (SC) terrain with high user density ([Docomo, 2016](#)), ([Technical-report, 2017](#)), ([Rappaport et al., 2017](#)).

Passive reflecting surfaces are deployed in radar systems, remote sensing earth observatory platforms, and satellite/deep-space navigation and communication systems, however, usage of passive reflecting surfaces is still limited in the mobile wireless communication paradigm. This is mainly because the traditional reflecting surfaces have

fixed phase shifters, which are unable to regulate the characteristics of wireless channel in a desired manner while considering user mobility as one of the important system parameters. However, the recent advances in RF micro electromechanical systems (MEMS) and metamaterial have made the reconfigurability of reflecting surfaces possible, even by an extent in which phase shifters can be controlled in real-time (Cui et al., 2014), (Tang et al., 2019). With a smart controller, each element of an IRS can independently reflect the incident signal while introducing desired amplitude and phase shift regulations. By appropriately adjusting the phase shifts of the passive elements, the reflected signals can be added coherently at the true location of the receiver to improve the receiving signal strength. Moreover, the received signals at the non-intended receivers can be added destructively to suppress interference, which also provides privacy (Wu and Zhang, 2020). The effectiveness of using IRS for mmWave-non-orthogonal multiple-access (NOMA) systems has resulted in significant sum-rate gains (Zuo et al., 2020).

Conceptually, IRS can be viewed as an ideal phase shifter that introduces phase shift variations which yield enhancement in received signal power. In terms of operational characteristics, as the IRS panel involves passive reflecting elements, it doesn't contribute to noise amplification (Basar et al., 2019). Further IRS also supports full-duplex (FD) transmission while ensuring no mutual interference or crosstalk between the uplink and downlink (Wu et al., 2021a). Thus, offers competitive advantages over traditional active relays, e.g., half-duplex (HD) relay that suffers from low spectral efficiency as well as FD relay that needs sophisticated techniques for self-interference cancellation. To improve network energy efficiency, a scheme that includes usage of precoding at the base station and formation of direction-specific narrow beamforming by the virtue of IRS is investigated in (Huang et al., 2019).

3.2 Channel modelling of wireless terrain

A propagation channel is an integral part of any communication system, be it wired or wireless. A precise mathematical model yields fairly good insight into the channel characteristics that influence the propagation of signals over a given geographical terrain. The commonly used channel model parameters are carrier frequency, bandwidth, the distance between transmitter and receiver, and the associated geographical terrain specifications.

The channel behavior and associated signal propagation mechanism can be analyzed based on LOS probability and Large-scale path loss models. The mobile user frequently satisfies compliance of LOS or NLOS norms with the BS during course of motion in shorter epochs. Conventionally, owing to the presence of surrounding obstructions, statistical models are used to predict the compliance of LOS or NLOS norms. The LOS probability is modeled as a function of the transmitter-receiver (T-R) separation distance, which is frequency-independent, and is solely based on the geometry and layout of service terrain (Sun, 2016). Compared to LOS propagation, NLOS propagation exhibits a higher path loss exponent (PLE) and increased shadowing variance, which leads to an inference that LOS propagation ensures reliable and robust performance in mmWave band (Sun et al., 2015). The characterization of the path loss exponent and delay spread for a mmWave channel operating at 26 GHz is reported based on the Ray Tracing method (da Silva et al., 2019). Usually, large-scale path loss models are used to estimate the strength of mmWave signal with varying distances.

In this section, mathematical analysis and modeling for static and time-varying channels are discussed. Time-invariant (TI) channel model is used for static channel analysis whereas, time-variant (TV) channel model represents a reasonably good approximate analysis of dynamic channels. In many single user use cases, it is presumed that the communication paradigm involves one BS (transmitter) and one mobile unit (receiver). The wireless communication system comprises of N_T transmit antennas and N_R receive antennas at the BS and mobile unit, respectively. The propagation environment characteristics in terms of downlink signal propagation from the BS to the mobile unit

is presumed to have a single LOS propagation component and a scattering cluster having N_{ray} number of NLOS propagation components. The azimuth angles of arrival and departure of the l^{th} ray in the scattering cluster are denoted by ϕ_l^r and ϕ_l^t , respectively. Similarly, the elevation angles of arrival and departure of the l^{th} ray are denoted by θ_l^r and θ_l^t , respectively.

3.2.1 Time-Invariant (TI) channel model

The impulse-response of a TI channel between transmitter and receiver in a matrix form can be given as

$$\mathbf{H}(\tau) = \mathbf{H}_{NLOS}(\tau) + \mathbf{H}_{LOS}(\tau) \quad (3.1)$$

The NLOS component of the impulse response is given by (Buzzi and D'Andrea, 2016)

$$\mathbf{H}_{NLOS}(\tau) = \xi \sum_{l=1}^{N_{ray}} \alpha_l \sqrt{L(r_l)} \mathbf{a}_r(\phi_l^r, \theta_l^r) \times \mathbf{a}_t^H(\phi_l^t, \theta_l^t) h(\tau - \tau_l) \quad (3.2)$$

where α_l is the complex path gain, $L(r_l)$ is the distance dependent attenuation, r_l is the length associated with the propagation path of the l^{th} ray. Usually, in wireless terrain during the course of propagation, signal experiences many obstacles between the BS and a mobile receiver. Considering these obstacles, for transmitting and receiving rays; azimuth and elevation angles are represented by pairs (ϕ_l^t, θ_l^t) and (ϕ_l^r, θ_l^r) , respectively. The factors $\mathbf{a}_r(\phi_l^r, \theta_l^r)$ and $\mathbf{a}_t(\phi_l^t, \theta_l^t)$ represent normalized receive and transmit array response vectors evaluated at corresponding angles, respectively. Propagation delay associated with the l^{th} path is $\tau_l = r_l/c$, where c is speed of light. A normalization factor ξ ensures that the received signal power scales linearly with the product $N_R N_T$, and is given by $\xi = \sqrt{\frac{N_R N_T}{N_{ray}}}$.

The total length of the l^{th} propagation path r_l , is estimated using geometrical considerations and is given by:

$$r_l = r_s + \sqrt{(h_T - h_R + r_s \sin \theta_l^t)^2 + (d - r_s \cos \theta_l^t \cos \phi_l^t)^2} \quad (3.3)$$

Estimate of a propagation path length depends on the Euclidean distance between scattering cluster and receiver, r_s , link length distance d , transmitter antenna height (h_T), and receiver antenna height (h_R).

The attenuation associated with the propagation path of l^{th} ray for the UMi terrain is given by (Buzzi and D'Andrea, 2016),(Alonzo and Buzzi, 2017)

$$L(r_l) = -20 \log_{10} \left(\frac{4\pi}{\lambda} \right) - 10 n \left[1 - b + \frac{bc}{\lambda f_0} \right] \log_{10}(r_l) - X_\sigma \quad (3.4)$$

It has functional dependency on key parameters namely, path loss exponent (n) and zero-mean Gaussian distributed Shadow fading term (X_σ) in logarithmic units having standard deviation (σ), system parameter (b), speed of light (c), fixed reference frequency (f_0) and the operating wavelength (λ) corresponding to carrier frequency. For both the wireless terrain (UMi-OS as well as UMi-SC), values of n and σ are given in Table 3.1 for the LOS and NLOS compliance. Further, in equation (3.4), for outdoor wireless scenarios, system parameter b is treated as zero (Docomo, 2016), (Buzzi and D'Andrea, 2016).

In an UMi scenario, the width of the typical OS area is in the order of 50 to 100 m and it is considerably smaller for SC (Technical-report, 2017). The impulse response

Table 3.1: Pathloss model parameters for UMi-SC and UMi-OS

UMi-SC LOS (n, σ)	UMi-SC NLOS (n, σ)	UMi-OS LOS (n, σ)	UMi-OS NLOS (n, σ)	references
(2.1, 3.76)	(3.17, 8.09)	(1.85, 4.2)	(2.89, 7.1)	(Docomo, 2016)
(1.98, 3.1)	(3.19, 8.2)	(1.85, 4.2)	(2.89, 7.1)	(Buzzi and D'Andrea, 2016) (Alonzo and Buzzi, 2017) (Haneda et al., 2016)
(2, 2.9)	(3.1, 8.1)	(1.9, 4.7)	(2.8, 8.3)	(Sun et al., 2016)
(2.1, 3.2)	(3.4, 8.6)	--	--	(Sun, 2016)

corresponding to LOS component in equation(3.1) is given by (Buzzi and D'Andrea, 2016)

$$\mathbf{H}_{LOS}(\tau) = I_{LOS}(d)\sqrt{N_R N_T}e^{j\eta}\sqrt{L(d)}\mathbf{a}_r(\phi_{LOS}^r, \theta_{LOS}^r) \times \mathbf{a}_t^H(\phi_{LOS}^t, \theta_{LOS}^t)h(\tau - \tau_{LOS}) \quad (3.5)$$

where $I_{LOS}(d)$ is a random variable that takes the value equal to one, if a LOS link exists between transmitter and receiver, η is a uniformly distributed random variable covering angular span in the range $[0, 2\pi)$.

3.2.2 Time-Variant (TV) channel model

This section deals with modeling aspects of wireless communication systems operating over channels that vary in time due to the inherent mobility of a transmitter and/or receiver. Even if both of these entities (transmitter and receiver) are stationary, surrounding temporary obstacles and scatterers may introduce relative velocities. These situations yield temporarily varying wireless channel characteristics due to the Doppler effect, which hinders degree of precision with parameter estimation and degrades detection performance. Owing to the practical relevance, TV channels have attracted considerable interest in the fields of signal processing, communications, propagation, information theory, and mathematics.

In a generic scenario, the transmitter and receiver are considered moving with speed ν^{TX} and ν^{RX} , respectively along the city street/highway. The channel can be modeled as a time-variant system, and its matrix-valued impulse response can be expressed as:

$$\mathbf{H}(t, \tau) = \mathbf{H}_{NLOS}(t, \tau) + \mathbf{H}_{LOS}(t, \tau) \quad (3.6)$$

It's NLOS component is given by ([Buzzi and D'Andrea, 2016](#))

$$\mathbf{H}_{NLOS}(t, \tau) = \xi \sum_{l=1}^{Nray} \alpha_l(t)\sqrt{L(r_l)}\mathbf{a}_r(\phi_l^r, \theta_l^r) \times \mathbf{a}_t^H(\phi_l^t, \theta_l^t)h(\tau - \tau_l)e^{-j2\pi\nu_l t} \quad (3.7)$$

In equation (3.7), in contrast to equation (3.2), the effect of Doppler shift ν_l can be observed due inherent characteristics of a TV channel. Here, the complex path gain (α_l) is evaluated at the discrete-time intervals nT_s on sampling the received signals with uniform period, T_s . The Doppler shift due to receiver mobility for the l^{th} propagation path is given by:

$$\nu_l = -\frac{f}{c}(\nu^{RX} \cos\theta_l^r \cos\phi_l^r) \quad (3.8)$$

here f corresponds to the center frequency of the received signal bandwidth. Equation (3.8) is used to estimate doppler shift associated with l^{th} NLOS signal component.

The impulse response characterization of LOS component in equation (3.6) is given by (Buzzi and D'Andrea, 2016):

$$\mathbf{H}_{LOS}(t, \tau) = I_{LOS}(d) \sqrt{N_R N_T} e^{j\eta(t)} \sqrt{L(d)} \mathbf{a}_r(\phi_{LOS}^r, \theta_{LOS}^r) \times \mathbf{a}_t^H(\phi_{LOS}^t, \theta_{LOS}^t) h(\tau - \tau_{LOS}) e^{-j2\pi\nu_{LOS}t} \quad (3.9)$$

$$\nu_{LOS} = -\frac{f}{c}(\nu^{RX} \cos\theta_{LOS}^r \cos\phi_{LOS}^r) \quad (3.10)$$

In this work, owing to receiver mobility and stationary nature of transmitter (BS); in equations (3.8) and (3.10), only ν^{RX} is considered.

Equations (3.2) and (3.7), infer that the major regulating factor that impacts the impulse response measurement is attenuation associated with the N_{ray} propagation paths corresponding to NLOS components. Thus, it is quite obvious that the performance of received signal strength is governed significantly by the propagation characteristics of NLOS components. These observations project a need to counter the unwarranted received signal strength variation, mainly due to inevitable NLOS components and subsequently enhancing the performance measures namely, achievable rate and coverage. The underlying characteristics of NLOS signal components result in undue signal fading, which can be overcome to some extent by deploying IRS panels in between a BS and mobile receiver at appropriate locations in a wireless terrain.

3.3 IRS panels deployment in wireless terrain

A system consisting of the BS (transmitter) and a mobile unit (receiver) for a downlink communication with a single IRS panel is shown in Figure 3.1. BS is equipped with M antennas and IRS is a planar array having N discrete reflecting elements with an ability to enable desired phase regulation. Owing to the ubiquitous presence of obstacles in the vicinity of a mobile unit and its path locus relative to a BS, the mobile receiver is most likely to experience varying signal strength associated with LOS and NLOS components. The obstacles in the form of buildings or vehicles or foliages, etc., block the direct signal propagation path between BS and receiver, and hinders the performance. For instance, the achievable rate is likely to be affected by the obstacles, since the mobility of the receiver results in complying with LOS or NLOS norms in non-uniform shorter epochs in a sporadic manner.

The performance impairments in the form of undesirable outcomes, such as reduction in throughput and insufficient coverage problems up to some extent can be mitigated by deploying IRS panels. In any localized terrain, IRS panels are deployed at appropriate locations, which enables compliance of LOS norms for some IRS panels with local serving BS. In such circumstances, the NLOS components are processed by IRS panels in a manner that leads to enhanced receiving signal strength at mobile receiver. Usually, IRS panels are mounted on facade of buildings or lamp posts in a given wireless terrain.

3.3.1 Modeling of diverse signal propagation scenarios

It can be observed in Figure 3.1 that, there exist three distinguish channels in an IRS-assisted wireless terrain for a downlink scenario. (i) Channel between a BS and IRS is denoted by $\mathbf{h}_{bi} \in \mathbb{C}^{N \times M}$, (ii) channel between IRS and a mobile receiver is denoted by $\mathbf{h}_{im} \in \mathbb{C}^N$, and (iii) the direct channel that exists between a BS and an arbitrary mobile receiver is denoted by $h_d \in \mathbb{C}$. In this work, M is considered to be equal to one assuming that BS is equipped with a single antenna.

Further, these channel segments are governed by distinguished features. A segment be-

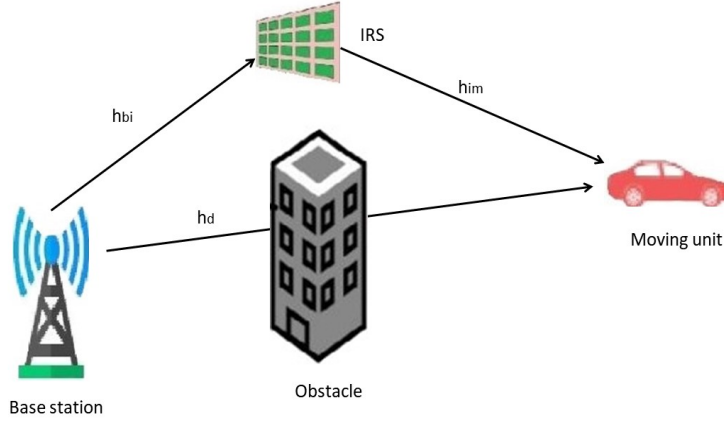


Figure 3.1: IRS-assisted wireless terrain

tween BS and strategically placed IRS panels (reflectors) is treated as TI. The hypothesis for this presumption is that a BS and IRS panels are located at sufficient altitude and thus, presence of any heavy vehicle or any other fixed/mobile obstacles does not intercept progressive signal beam in between a BS and IRS panels. Whereas, the channel segment between a fixed IRS panel and mobile receiver owing to instantaneously changing surrounding geospatial features is considered as TV. LOS component of downlink between BS and the receiver is approximated as TV channel owing to relative motion of mobile receiver. The continuous movement of the receiver yields unpredictable variations in the receiving signal strength.

The phase shift introduced by an IRS panel is denoted by a phase shift matrix

$$\Theta \equiv \text{diag}(\alpha_1 e^{j\theta_1}, \dots, \alpha_N e^{j\theta_N}) \quad (3.11)$$

where $\alpha_n \in [0, 1]$ is the amplitude reflection coefficient and $\theta_n \in [0, 2\pi)$ is the phase shift of reflected signal processed by the n^{th} passive element of an IRS panel.

The array response vector of the IRS $\mathbf{a}(\phi_l^{IRS}, \theta_l^{IRS})$ as given in equation (3.12) is substituted in place of $\mathbf{a}_r(\phi_l^r, \theta_l^r)$ for the BS to IRS link, and in place of $\mathbf{a}_t(\phi_l^t, \theta_l^t)$ for the IRS to mobile receiver link in equations (3.2), (3.5), (3.7) and (3.9). In an IRS panel, for the uniformly distributed passive reflecting elements with an inter-element spacing

of δ , an array response vector is given by

$$\mathbf{a}(\phi_t^{IRS}, \theta_t^{IRS}) = [1, \dots, e^{-jk\delta(u \sin\phi_t^{IRS} \sin\theta_t^{IRS} + v \cos\theta_t^{IRS})}, \dots, e^{-jk\delta((\sqrt{N}-1) \sin\phi_t^{IRS} \sin\theta_t^{IRS} + (\sqrt{N}-1) \cos\theta_t^{IRS})}] \quad (3.12)$$

here $0 \leq u \leq \sqrt{N}-1$ and $0 \leq v \leq \sqrt{N}-1$, assuming a square IRS with \sqrt{N} elements in horizontal and vertical axes, and $k = 2\pi/\lambda$, λ is the operating wavelength.

The overall wireless channel in between a BS and a mobile receiver can be modeled as a superposition of (i) aggregate NLOS component that is characterized by cascade arrangement of BS-IRS link and IRS-mobile receiver link, and (ii) the LOS component featured as a direct link between a BS and a mobile receiver. In aggregate the composite channel is represented as

$$h_{bm} \equiv (\mathbf{h}_{im}^H \mathbf{\Theta} \mathbf{h}_{bi}) + h_d \quad (3.13)$$

3.3.2 Achievable rate

The average achievable rate experienced by a mobile receiver is defined as

$$\mathcal{R} \equiv \mathbb{E}[\log_2(1 + \gamma)] \quad (3.14)$$

where γ is the average value of Signal-to-Noise ratio (SNR) at mobile receiver. In this work, average achievable rate is computed for diverse signal propagation scenarios, which are illustrated next.

- 1) LOS with complying free-space propagation norms :

For a mobile receiver operating in an environment that satisfies the LOS compliance with respect to BS and experiencing free-space gain (h_{fs}), average SNR is

given by

$$\gamma \equiv |h_{fs}|^2 \frac{P_T}{\sigma^2} \quad (3.15)$$

where P_T is transmit power at a BS and σ^2 is the noise power estimate at the mobile receiver.

2a) NLOS under varying fading conditions (without IRS) :

For a mobile receiver served by a BS under NLOS condition in a wireless terrain without IRS and observing channel gain (h_{NLOS}), average SNR is given by

$$\gamma \equiv |h_{NLOS}|^2 \frac{P_T}{\sigma^2} \quad (3.16)$$

2b) NLOS under varying fading conditions (with IRS) :

Considering the preceding use case with IRS equipped wireless terrain and the overall estimated cascaded channel gain ($\mathbf{h}_{im}^H \Theta \mathbf{h}_{bi}$). An usual BS-mobile receiver link (h_d) is considered to experience NLOS norms due to the presence of various static and dynamic obstacles, in such a scenario, average SNR is given by

$$\gamma \equiv |(\mathbf{h}_{im}^H \Theta \mathbf{h}_{bi})|^2 \frac{P_T}{\sigma^2} \quad (3.17)$$

3a) LOS under varying fading conditions (without IRS) :

For the case of mobile receiver served by a BS under LOS condition without IRS, and observing direct channel gain (h_d), average SNR is given by

$$\gamma \equiv |h_d|^2 \frac{P_T}{\sigma^2} \quad (3.18)$$

3b) LOS under varying fading conditions (with IRS) :

Considering the preceding use case for a wireless terrain equipped with IRS, resultant channel gain can be presumed as superposition of cascaded channel gain ($\mathbf{h}_{im}^H \Theta \mathbf{h}_{bi}$) and direct channel gain (h_d). Here, a BS-mobile receiver link (h_d) is presumed to have a LOS path, however, due to local surrounding dynamics of other vehicles/obstacles as perceived by mobile receiver during a few shorter time intervals, mobile receiver experiences fading. To overcome it, IRS panel enables

supplementary channel ($\mathbf{h}_{im}^H \Theta \mathbf{h}_{bi}$), thereby average SNR is approximated by

$$\gamma \equiv |(\mathbf{h}_{im}^H \Theta \mathbf{h}_{bi}) + h_d|^2 \frac{P_T}{\sigma^2} \quad (3.19)$$

Summary of a mathematical framework to estimate the achievable rate is given in Algorithm 1.

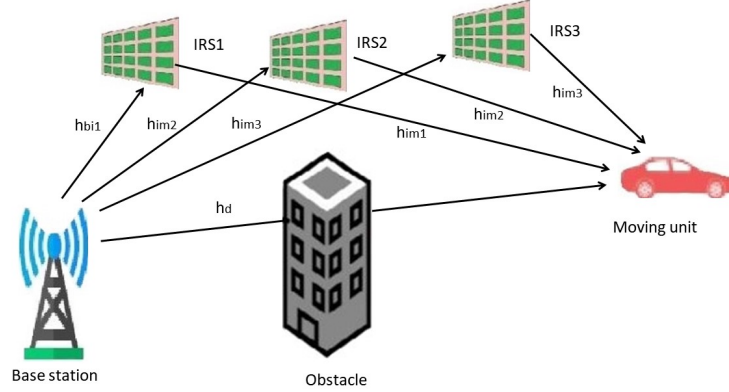
Algorithm 1: Algorithm for computing achievable rate at a mobile receiver for IRS-assisted wireless terrain

Input: Coordinates of a BS, IRS units, Mobile receiver and Transmit signal specifications as given in Table 3.2 and Table 3.3

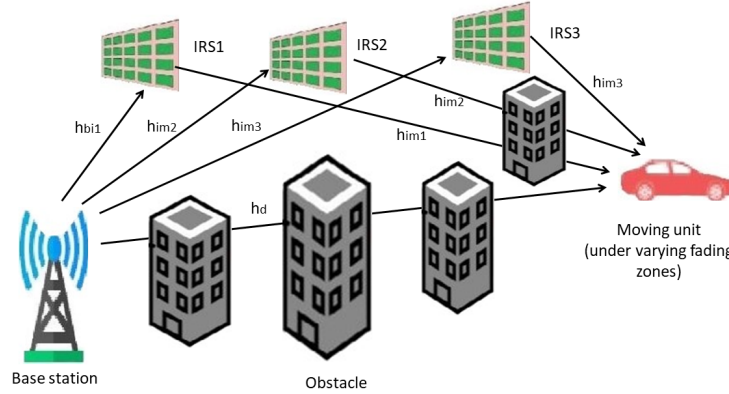
1. Estimating the direct link gain (h_d) using TV channel model as given in equation (3.9)
 2. Estimating the BS-IRS link gain (\mathbf{h}_{bi}) using TI channel model as given in equation (3.5)
 3. Estimating the Doppler shift (ν_l) due to mobile receiver using equations (3.8) and (3.10)
 4. Estimating the IRS- mobile receiver link gain (\mathbf{h}_{im}) using TV channel model using equations (3.7) and (3.9)
 5. In steps 3 and 5, array response vector of the deployed IRS units is estimated using equation (3.12)
 - if** mobile receiver experiences LOS norms with BS in a typical wireless terrain
 - Compute average SNR for LOS without IRS using equation (3.18)
 - Compute phase shift introduced by IRS using equation (3.11)
 - Compute average SNR for LOS with IRS using equation (3.19)
 - else** mobile receiver experiences varying degree of fading, as a result of NLOS compliance for BS-mobile receiver link
 - Compute average SNR for NLOS without IRS using equation (3.16)
 - Compute phase shift introduced by IRS using equation (3.11)
 - Compute average SNR for NLOS with IRS using equation (3.17)
 6. Compute the achievable rate for all the cases using equation (3.14)
-

3.3.3 Coverage enhancement

Deploying IRS panels at appropriate locations not only improves the achievable rate but also ensures coverage area enhancement. With a motive to extend service coverage area, a schematic diagram using multiple geographically distributed IRS panels is shown in Figure 3.2a and 3.2b for UMi-OS and UMi-SC terrain, respectively.



(a)



(b)

Figure 3.2: Coverage enhancement using IRS panels for (a) UMi-OS and (b) UMi-SC

Channels between a BS and multiple IRS units are denoted by $\{\mathbf{h}_{bi1}, \mathbf{h}_{bi2}, \dots\} \in \mathbb{C}^{N \times M}$, and that between IRS units and mobile receiver is denoted by $\{\mathbf{h}_{im1}, \mathbf{h}_{im2}, \dots\} \in \mathbb{C}^N$. Figure 3.2a and 3.2b illustrate the usage of three IRS panels, one in proximity to the BS and the others geographically space apart to extend the coverage range. Also, all these IRS panels need to be placed in strategic locations that satisfy LOS norms with BS. An array of embedded reflecting elements in an IRS panel undergoes tunable phase offset introduced by a smart IRS controller connected to a BS over a backhaul link. Cascaded channel $\{h_{bm}\}$ from a BS to the mobile receiver via multiple IRS panels is estimated and subsequently the achievable rate is obtained by estimating average performance over the distributed participating links.

In this chapter, the achievable rate is considered as a performance measure to evaluate the performance of channel segments for the various case studies. In these case studies; the appropriate channel model (TI/TV) is considered to evaluate the impulse response i.e, $\mathbf{H}(\tau)$ and $\mathbf{H}(t, \tau)$, and subsequently, inference from the channel impulse response is used to estimate the achievable rate at mobile receiver as well as an analysis about the coverage aspect is carried out.

In this work, validation of channel TI/TV impulse response models is exercised for two different geographical terrain, namely UMi-SC (an area having a large number of obstacles) and UMi-OS (an area characterized with relatively low density of vehicles/obstacles). For both of these terrain; various case studies are investigated to assess the performance of a wireless link between a BS and a mobile receiver. The underlying factors for these case studies are wireless terrain with/without IRS, presence of single or multiple IRS panels, IRS panels with varying strength of the number of embedded reflecting elements (EREs), a varying separation between two neighbouring EREs as a multiple of operating wavelength, regulation in BS transmit power and owing to inevitable movement of mobile receiver treating distance as a variable of interest. For a variety of underlying factors, the performance of wireless links is measured in terms of achievable rate (bit/s/Hz) at mobile receiver.

3.4 Simulation results

Wireless terrain under test involve fixed as well as variable network parameters, specifications of these parameters used during the simulation study are given in Table 3.2 and 3.3. In a majority of simulation results, traversing distance, number of active ERE, transmit power level of BS are treated as independent variables/parameters. In case these network specifications are neither independent variables nor regulating parameters, then the considered values are kept constant. In simulation results, value of the transmit power level, number of active ERE deployed in an IRS panel, and separation between two neighbouring EREs is considered as 20 dBm, 64 and $\lambda/2$, respectively.

Table 3.2: Wireless terrain specification having fixed network parameters

Parameter	Value
Carrier frequency	28 GHz
Noise PSD	-174 dBm/Hz
BS coordinates: $(x, y, h)_{BS}$	(0,0,20)
Receiver coordinates: $(x, y, h)_{MU}$	(d,10,1)
IRS panel coordinates: $(x, y, h)_{IRS}$	
IRS_1	(25,5,10)
IRS_2	(50,5,10)
IRS_3	(75,5,10)

Table 3.3: Wireless terrain specification having variable network parameters

Parameter	Value
Transmit power	0 to 40 dBm (Wu, 2019; Wu and Zhang, 2020)
Number of EREs	16 to 256 (Dai et al., 2020)
ERE separation distance	$\lambda, \lambda/2, \lambda/4$ (Adnan et al., 2017)
Receiver speed	24 and 36 km/hr (Bas et al., 2019),(Hur et al., 2018)

Simulation results are analysed for two distinct geographical terrain, namely, UMi-OS and UMi-SC. Further, other characteristics considered in simulation studies are distinct short epochs during which measurement is carried out, i.e., peak business hours or off-peak hours. In all use cases, it is presumed that the mobile receiver traverses away from a centrally located BS. Achievable rate is estimated at every one-meter separation distance for a span of 100 meter and 180 meter omnidirectional locus of mobile receiver movement. Since the performance analysis is confined to a single cell, the impact of interference from neighbouring cells is ignored during an analysis of the results. The spectral efficiency of a downlink for a mobile receiver at different locations for both the geographical terrain is estimated and comparative analysis is reported with an average estimate of 3.087 b/s/Hz (nex, 2015) and 4 b/s/Hz (Bas et al., 2019).

During six different case studies, achievable rate is estimated as the key performance measure. These case studies are characterized with distinct features such as deployment of single or multiple IRS panels in wireless terrain, regulating; transmit power level of BS, number of active EREs and spatial separation between EREs, etc. For both the considered geographical terrain (UMi-OS and UMi-SC), depending upon the current

location and the characteristics of the surrounding environment, the mobile receiver satisfies LOS and NLOS norms with respect to a BS. Moreover, during shorter epochs, presence of heavy vehicles in the vicinity of the mobile receiver leads to a breach of LOS compliance and usually contributes more severe fading during prevailing NLOS norms. A comprehensive analysis of achievable rate variations and its dependence on some key regulating parameters is presented next for six different case studies.

3.4.1 Wireless terrain assisted with a single IRS panel

In this case study, it is presumed that both the geographical terrain are equipped with a single IRS panel and to experience the impact of the sole IRS panel on receiving signal strength at mobile receiver location, four different scenarios are considered. These four scenarios attribute to pairing LOS and NLOS compliance with active or disable state of a single IRS panel. Treating distance between a BS and mobile receiver as an independent variable, achievable rate characteristics corresponding to these four scenarios are shown in Figure 3.3a and Figure 3.3b for UMi-OS and UMi-SC, respectively. Achievable rate characteristics shown in Figure 3.3a and 3.3b have one unique trend; it can be inferred that in aggregate terms achievable rate decays with distance (d). For both the terrain, i.e., UMi-OS and UMi-SC owing to the presence of a single IRS panel at a location, $(25, 5, 10)$; decay characteristics reverses its trend in the close proximity of IRS panel for LOS as well as NLOS compliance. Analysis of these characteristics reveal that the poorest achievable rate attained in an UMi-SC geographical terrain, which is inherently characterized by high-rise buildings and a high density of obstacles in the vicinity of a mobile receiver. This can be validated from the characteristic shown in Figure 3.3b corresponding to NLOS compliance for a UMi-SC terrain without IRS panel. In relative terms, achievable rate performance in UMi-OS terrain for NLOS compliance without having an IRS is marginally better than that obtained in UMi-SC. It attributes to the geometrical characteristics of OS terrain that deprives the presence of high-rise buildings and enjoys a low density of fixed and movable obstacles.

The performance of LOS and NLOS paths can be discriminated by the spatial aspect-

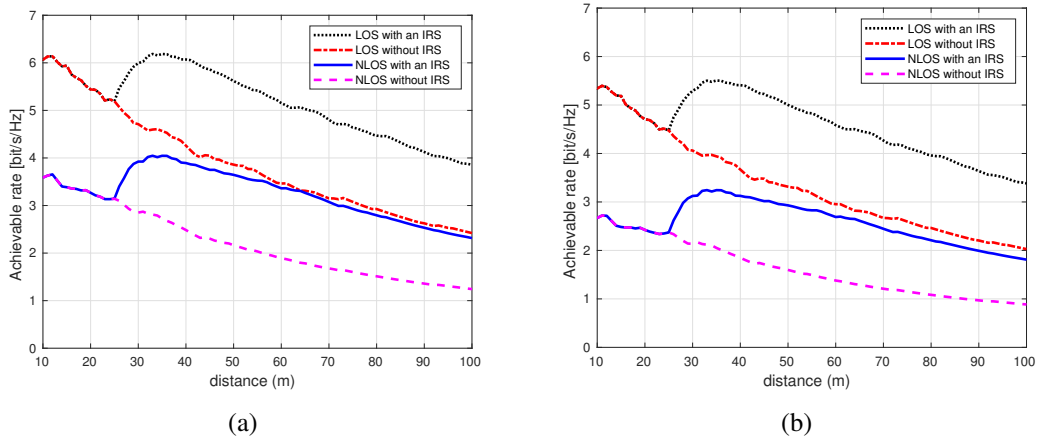


Figure 3.3: Achievable rate for a single IRS-assisted scenario (a) UMi-OS and (b) UMi-SC

driven geometrical specification of surrounding objects. The state of fading zone in NLOS complied geographical smaller areas is considered to be a steady-state, whereas, a terrain that usually satisfies LOS norms (hereafter, it is invariably established between a mobile receiver and BS) may experience varying degrees of fading, sporadically during shorter epochs owing to frequently changing characteristics of surrounding vehicles/obstacles.

For both the geographic terrain, i.e., UMi-OS and UMi-SC, wireless communication, assisted by a single IRS panel under the steady compliance of LOS shows significant improvement in achievable rate compared to exclusive LOS scenario and NLOS with/without IRS scenarios. For both of these terrain; achievable rate characteristics have three different trends corresponding to different positions of the mobile receiver with respect to a BS. For the first interval of displacement $(10 - 25)m$, achievable rate decays from its maximum value almost monotonically, due to a drop in the signal strength of the received signal from BS. During the second interval of displacement $(25 - 40)m$, due to presence of an IRS panel at $(25, 5, 10) m$, achievable rate characteristics reverse its trend and almost attained the initial maximum value as observed at BS. In the third and last displacement interval $(40 - 100)m$, achievable rate monotonically decays with distance. As anticipated the best performance of achievable rate is attained for UMi-OS LOS scenario in the presence of a single IRS panel. In IRS-assisted wire-

less communication, this attribute to distributive manner in which, the channel gain experiences enhancement first in the BS-IRS panel wireless link segment and subsequently in an IRS panel-mobile receiver link segment.

3.4.2 Wireless terrain assisted with a single or multiple IRS panels

This case study presumes that both the geographical terrains are equipped with either a single IRS panel or multiple IRS panels. Empirical observations based on enhancement in achievable rate characteristics by virtue of a single IRS panel envisage a further possibility in rate improvement by deploying multiple IRS panels. The coordinates of IRS panels are given in Table 3.2. Combining IRS panel specifications (single/multiple) with LOS and NLOS compliance results in the estimation of four different achievable rate characteristics shown in Figure 3.4a and Figure 3.4b.

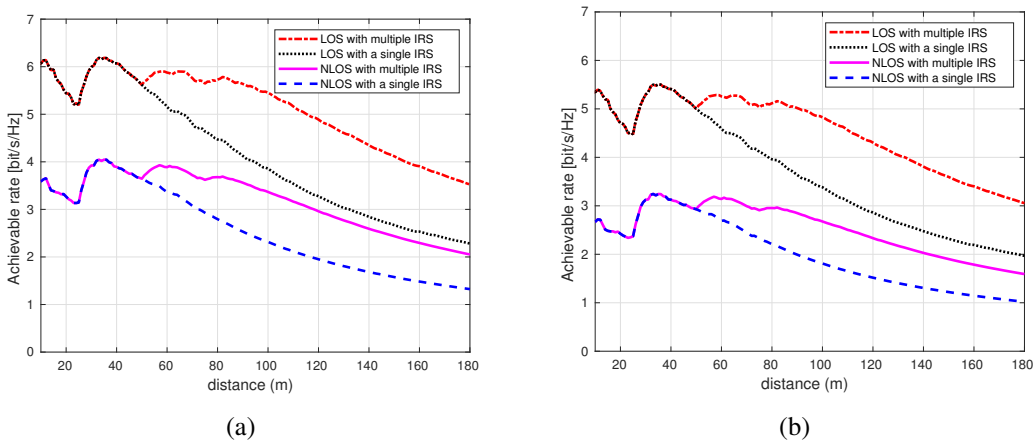


Figure 3.4: Achievable rate for single or multiple IRS-assisted scenarios (a) UMi-OS and (b) UMi-SC

For both of these geographical terrain, achievable rate performance is severely compromised when a mobile receiver fails to satisfy LOS norms with respect to BS. Figure 3.4a and Figure 3.4b yields moderate achievable rate performance under compliance of LOS condition. An interesting observation in Figure 3.4a and Figure 3.4b especially in the vicinity of IRS panels infers that the achievable rate measured at mobile receiver remains approximately constant at a moderately high value. This establishes a hypoth-

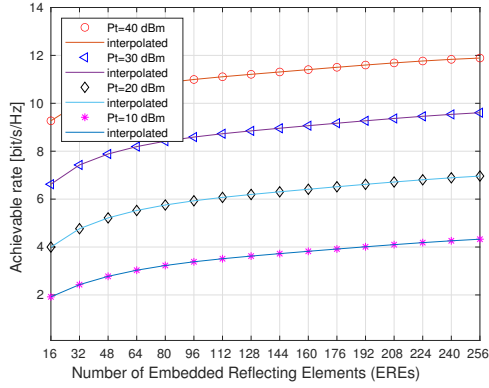
esis that up to a certain extent, irrespective of wireless terrain spatial features, usage of multiple IRS panels mitigates the fading phenomenon and leads to a robust achievable rate performance. In summary, owing to surrounding environment characteristics, achievable rate performance obtained in UMi-OS is better than that secured in UMi-SC.

Further, for both the geographical terrain with respect to the estimated mean value of the acceptable achieved rate, i.e., 3.087 b/s/Hz (nex, 2015) and 4 b/s/Hz (Bas et al., 2019), characteristics in Figure 3.4a and Figure 3.4b reveals that usage of multiple IRS panels (in this work, three IRS panels) result in attaining achievable rate above the chosen threshold value (3.087 b/s/Hz) at a distance of 180 m and 100 m for LOS and NLOS compliance, respectively. This observation establishes an advantage in favour of deploying multiple IRS panels in wireless terrain.

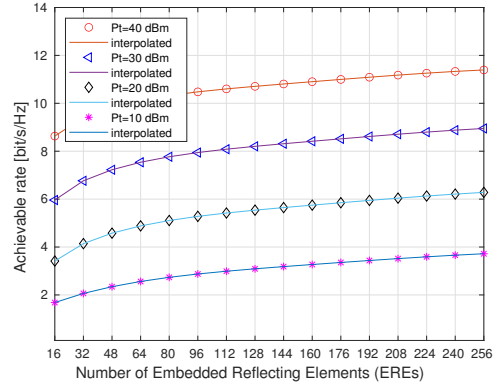
3.4.3 Single IRS panel assisted wireless terrain with the regulation in number of active EREs:

An IRS panel comprises several reflecting elements in an array form. Two fundamental specifications of an IRS panel are its size and the number of active EREs. Spatial precision in beamforming mechanism is introduced by an IRS panel and it depends on active status of EREs, in this case study, the impact of parametric variations in number of EREs on the achievable rate is investigated. The basis for regulation is taken from (Dai et al., 2020) in which a maximum of 256 EREs are considered on a single IRS panel. Maximum signal reflection is achieved when reflection coefficients of all the EREs in an IRS panel are set to maximum value (Wu and Zhang, 2020).

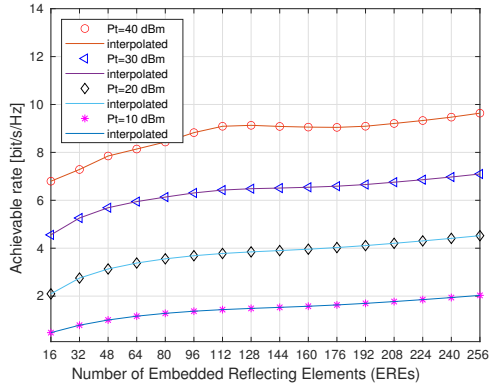
For the UMi-OS and UMi-SC geographical terrain, achievable rate characteristics while regulating number of active EREs are shown in Figure (3.5a-3.5d) for LOS as well as NLOS compliance. For both the terrain; with parametric variations in the form of an increase in BS transmit power levels, achievable rate enhances with an initial increase in the number of participating EREs. Although these characteristics reveal that an, approximately linear rising trend persists for an initial hike in number of active EREs and



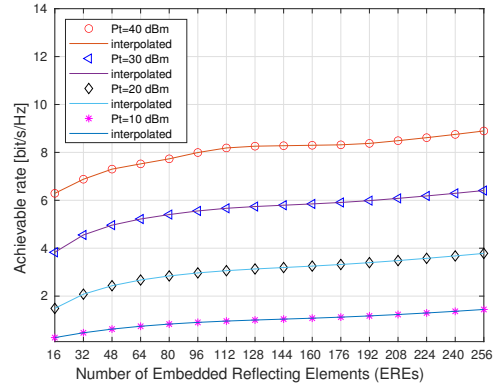
(a)



(b)



(c)



(d)

Figure 3.5: Achievable rate for a single IRS-assisted scenario (a) UMi-OS complying LOS, (b) UMi-SC complying LOS, (c) UMi-OS complying NLOS and (d) UMi-SC complying NLOS

subsequently, achievable rate characteristics corresponding to different transmit power levels attain saturation status for number of EREs ≥ 96 .

3.4.4 Wireless terrain with a single IRS panel and variations in transmit power level:

To analyse the impact of spatial separation (δ) between two adjacent EREs on beam-forming mechanism (it is one of the decisive factors in equation 3.12) and subsequently, its after effects towards achievable rate performance, operating wavelength (λ) is treated as a parameter while regulating the transmit power level of BS. As per the

empirical observations given in (Adnan et al., 2017), for a large antenna array system, maintaining inter-element spacing of order less than $\lambda/2$ yields poor directivity, and to achieve a higher directivity, inter-element spacing must be atleast $\lambda/2$.

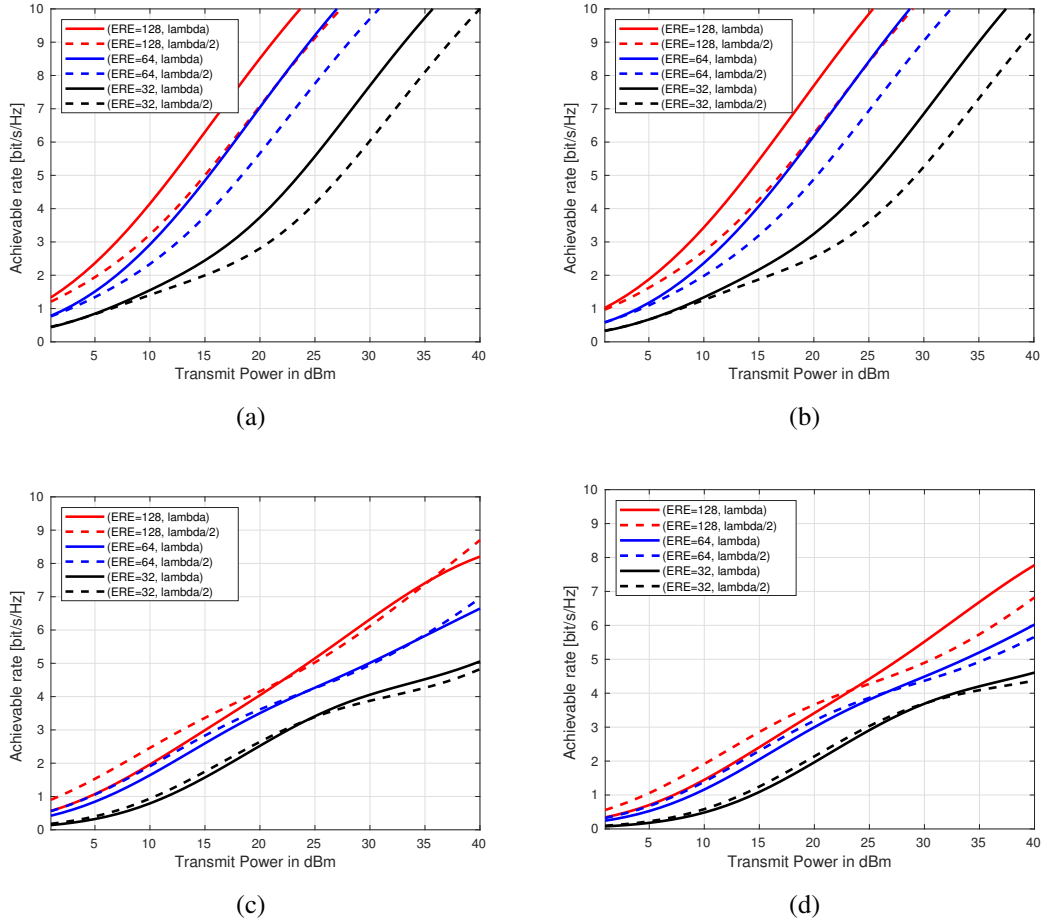


Figure 3.6: Achievable rate for a single IRS-assisted scenario (a) UMi-OS complying LOS, (b) UMi-SC complying LOS, (c) UMi-OS complying NLOS and (d) UMi-SC complying NLOS

Achievable rate characteristics under the LOS and NLOS compliance with varying transmit power of BS, number of active EREs in the participating IRS panels and inter separation distance of EREs are shown in Figure (3.6a-3.6d) for UMi-OS and UMi-SC wireless terrain. These characteristics reveal that for both the geographical terrain achievable rate as perceived by a mobile user enhances with an increase in the number of active EREs and spatial separation maintain between EREs. It can be inferred that to attain a reasonably satisfactory achievable rate, an IRS panel must comprise sufficiently

a large number of active EREs while maintaining appropriate spacing (integer multiple of $\lambda/2$) between participating EREs.

3.4.5 ERE spacing driven distance centric analysis for single IRS panel assisted wireless terrain:

In this case study, observations are drawn for a scenario in which variable/key-parameters, namely, distance-driven locus of a mobile receiver, spatial separation between EREs vary, and the impact of these variations is analysed in terms of the resultant achievable rate. For a traversing span of 100m with respect to a BS, treating three distinct spacing viz, λ , $\lambda/2$, and $\lambda/4$, achievable rate characteristics for UMi-OS and UMi-SC terrain are shown in Figure (3.7a -3.7d) for LOS as well as NLOS compliance. Further, empirical observations about maintaining appropriate spacing between EREs given in (Adnan et al., 2017) can be validated for characteristics associated with $\lambda/4$ spacing in both the geographical terrain, as in most of the distance segments achievable rate falls below the chosen threshold of 3.087 b/s/Hz (nex, 2015). These characteristics reveal that presence of an IRS makes a significant improvement in the achievable rate when a mobile receiver maintains proximity with IRS panel (with location coordinates (25,5,10)) during the course of traversing. Further, it is also observed that as we decrease the spacing between adjacent EREs, achievable rate decays with a nonlinear trend.

3.4.6 Impact of mobile receiver velocity in a single IRS panel-assisted wireless terrain:

Frequent call drops or intermittent loss of services of data network usually attributes to the occurrence of fading phenomenon, which primarily depends on mobile receiver (user) velocity. For both the considered geographical terrain, while introducing parametric variations in mobile receiver velocity, achievable rate characteristics are shown in Figure 3.8. Both of these geographical terrain are equipped with a single IRS panel

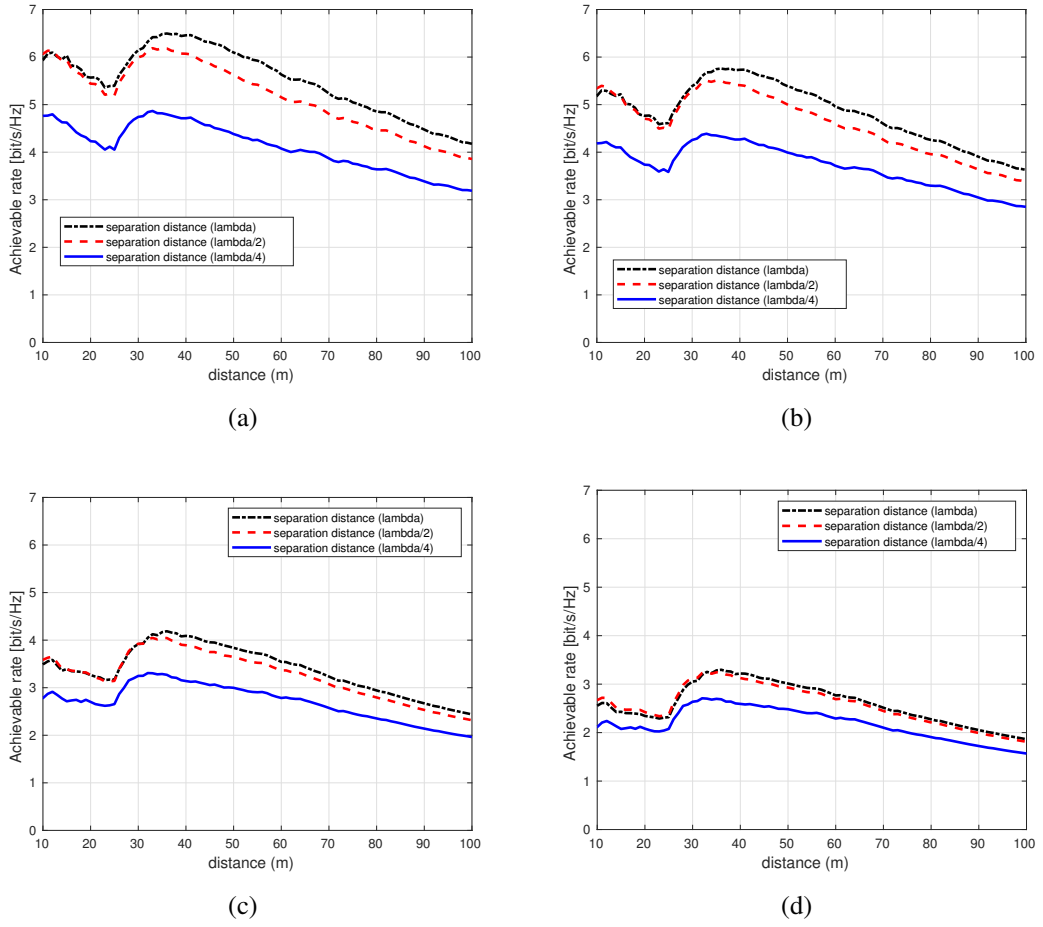


Figure 3.7: Achievable rate for a single IRS-assisted scenario (a) UMi-OS complying LOS, (b) UMi-SC complying LOS, (c) UMi-OS complying NLOS and (d) UMi-SC complying NLOS

having Cartesian coordinates as (25, 5, 10).

These characteristics are obtained for a mobile receiver speed of 24 km/h (Bas et al., 2019) and 36 km/h (Hur et al., 2018) for UMi-OS and UMi-SC while satisfying LOS and NLOS compliance. These characteristics reveal that achievable rate is significantly better at a slower speed of the mobile receiver for both geographical terrain. Moreover, due to the inherent characteristics of local geometrical aspects, it is observed that UMi-OS experiences a better achievable rate than that obtained in UMi-SC.

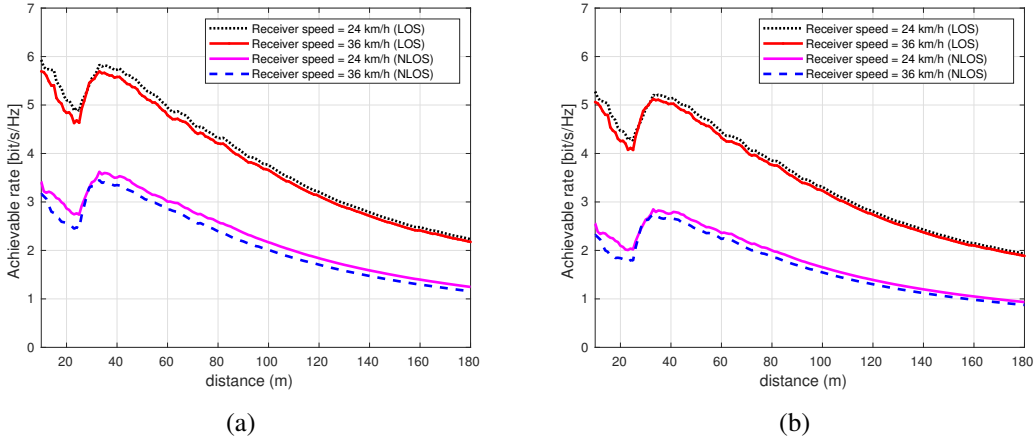


Figure 3.8: Achievable rate for a single IRS-assisted scenario with parametric variation in the receiver speed (a) UMi-OS and (b) UMi-SC

3.5 Summary

In most of the wireless terrain, the presence of obstacles (fixed and/or moveable) is inevitable. Presence of IRS panels ensures alleviating unwarranted degradation in receiving signal strength during shorter epochs especially for the smaller geographical regions that comply the NLOS mode. For various considered scenarios, simulation results reveal that IRS-assisted wireless terrain performance is significantly enhanced with respect to a conventional wireless terrain (terrain without IRS). Further, a comprehensive analysis is presented while exercising regulation in elements such as transmit power of BS, number of EREs embedded on IRS panels, spatial separation between the adjacent EREs, number of IRS panels deployed and the impact of a mobile receiver velocity on the performance of achievable rate. Analysis of achievable rate characteristics with respect to considered regulatory parameters infers many insights and observations that may be of immense interest to wireless service providers. In addition to that, wireless terrain equipped with multiple IRS panels is analysed, herein obtained result demonstrates that irrespective of mobile receiver locations measured achievable rate remains above the chosen threshold of 3.087 b/s/Hz, this may be treated as an enhancement in network reliable coverage.

CHAPTER 4

OUTAGE PROBABILITY ANALYSIS FOR MULTIPLE IRS-ASSISTED WIRELESS NETWORKS

4.1 Introduction

IRS is capable of dynamically altering wireless channels to enhance the QoS experience in terms of performance measures, namely, improved energy and spectral efficiency, data rate optimality, coverage area enhancement, and mitigating deep fading ([Pan et al., 2020](#); [Zou et al., 2020](#); [Basar, 2019](#); [Dhruvakumar and Chaturvedi, 2022](#)).

An analysis of multiple IRS panel assisted wireless terrain to improve the network reliability and connectivity in the presence of random blockages is reported in ([Zhou et al., 2021](#)), where a stochastic optimization problem based on the minimization of sum outage probability is formulated to enhance beamforming robustness. Outage performance analysis of an IRS-assisted wireless communication system with statistical CSI over Rician fading channels is investigated in ([Xu et al., 2022](#)), where, an end-to-end (source to destination) wireless channel is considered as a cascade arrangement of two identical and independently distributed (i.i.d) sub-channels. First channel is the standalone LOS link between a base station and an arbitrary IRS panel, whereas, the second channel is the dominant LOS link between a corresponding IRS panel and a receiver. In particular, both the sub-channels are stochastically modeled as Rician fading channel. Considering this hypothesis, closed-form expression of outage probability is derived. Further, an asymptotic outage probability expression is derived for a wireless terrain experiencing higher value of SNR. In addition, phase regulation is exercised on continuum as well discrete basis while adjusting coding gain and scaling laws.

The performance analysis of an IRS-assisted single-input single-output (SISO) system over the channels experiencing Rayleigh fading is given in ([Zhang et al., 2021](#)).

Here, the outage probability and the ergodic capacity is derived in an exact closed-form expressions, while considering a practical phase shift model. Furthermore, a simplified expressions is derived assuming that an IRS panel comprises of a large number of reflecting elements. In (Zhang et al., 2021), authors expressed apprehension that equipping a wireless terrain with multiple IRS may yield a remarkable improvement in getting a more accurate lower and upper bound estimate of ergodic capacity. Usage of a Rate-Splitting Multiple Access (RSMA) for a wireless terrain equipped with IRS in downlink scenario is investigated in (Bansal et al., 2021). RSMA utilizes rate-splitting at the base station and successive interference cancellation at the users. An analysis of outage probability in a wireless terrain assisted with an IRS panel and experiencing $\kappa - \mu$ fading, is given in (Charishma et al., 2021). Here, the authors considered, phase error that occurs due to quantization at IRS with and without source-destination link and approximation for the outage probability estimate is exercised using three different approaches including moment matching technique.

Shadowing and multipath propagation affect the performance of a wireless communication system in a considerable manner. Usually, the $\kappa - \mu$ shadowed fading accounts for multipath propagation effects and Line-of-Sight (LOS) shadowing (PARIS, 2014)-(Kodide et al., 2016). Performance analysis of wireless networks over fading channels has been addressed in the recent research work (Lopez-Martinez et al., 2017)-(Badarneh et al., 2020). Performance of IRS-assisted communication system influenced by Rayleigh and Ricean fading channels is analyzed with tight bounds and asymptotic results in (Tao et al., 2020). An accurate closed-form approximation for outage probability and average channel capacity of a Rayleigh fading channel for an IRS-assisted wireless terrain is presented in (Yang et al., 2020). An approximate performance evaluation of IRS-empowered systems over Nakagami-m fading channel is given in (Samuh et al., 2021).

The authors in (Trigui et al., 2020) analysed the scaling rates for outage probability and average sum-rate for a single and multiple IRS element over Fox's H fading channel. In most of these methods, performance is measured in terms of outage probability, average channel capacity, and average Bit Error Rate (BER). However, most of these

investigations on IRS-aided communication have considered wireless terrain equipped with a single IRS panel. Wireless terrain equipped with single IRS panels have some limitations, some of these are: (i) In a terrain characterized with high rise buildings and other miscellaneous obstacles, quite often an IRS fails to comply LOS norm with an intended receiver, thereby leads to frequent blind spots creation and (ii) Use cases that impose stringent requirement about latency may not be afford frequent outage owing to presence of single IRS. Thus, wireless terrain equipped with multiple IRS panels can achieve robust signal transmission and attain significant improvement in blind spot phenomenon. Further, looking into coverage span of UMi wireless terrain and the associated geographical features, deployment of multiple IRS panels seems to be a cost effective performance enhancement strategy.

To mitigate the fading, realizing an IRS-aided communication link using a single IRS panel is inadequate in an environment characterized with dense obstacles. In such scenarios, multiple IRS panels can be deployed to ensure reliable connectivity as well as an extended coverage. However, even in IRS-assisted wireless terrain, LOS link between IRS panel and the receiver may undergo frequent sporadic blockage due to heavy vehicles proximity, which in turn results in blind spots creation.

The severity of fading in any localized wireless terrain is non-uniform, this attributes to inherent spatial aspects in close vicinity of receiver and the time sensitive surrounding vehicular-traffic characteristics that lead to presence of temporary blockages in short epochs. In this thesis, to characterize the surrounding dynamics of diverse wireless terrains in a holistic manner, three different fading zones, namely; lightly fading zone, moderately fading zone and severely fading zone are considered. Further, for any urban or semi-urban wireless terrain, data/vehicular traffic pattern varies depending upon the timing of the day. Corresponding to diverse traffic generation characteristics, three distinct observation time-slots viz; peak hours, off-peak hours, and wee hours are considered for wireless links outage analysis.

4.2 System model

In geographical service area segments, for a reliable communication, IRS panels are mounted on the facade of buildings at appropriate locations. These strategically chosen locations enable LOS norms compliance for some of these IRS panels with a local serving BS and thereby facilitate virtual-LOS (VLOS) links between a serving BS and a user. Direct signal propagation path between source(S)/ base station (BS) and destination (D)/receiver is blocked by obstacles in the form of buildings or vehicles or foliage, etc., and hinders achievable performance. For instance, outage probability and ergodic capacity is likely to be affected by the obstacles, since mobility of a receiver results in LOS or NLOS compliance with BS during sporadic short epochs. Thus, a small segment in a geographical region that fails to satisfy LOS compliance and thereby a VLOS link through an IRS panel comes into effect in a manner that leads to an enhanced signal strength at receiver.

The IRS-assisted wireless network consists of a source, a destination, and R number of IRS panels $\{IRS_1, IRS_2, \dots, IRS_R\}$ is shown in Figure 4.1. An IRS is a planar array having N embedded reflecting elements (EREs). These EREs are capable to introduce the desired phase regulation. The direct channel between the source (S) and the destination (D) is denoted by $h_{S,D} \in \mathbb{C}^1$, a channel between S and r^{th} IRS panel is denoted as $\mathbf{h}_r \in \mathbb{C}^{N \times 1}$ and a channel between the r^{th} IRS panel and D is denoted by $\mathbf{g}_r \in \mathbb{C}^{N \times 1}$. It is assumed that small-scale fading coefficients of these three links experience $\kappa - \mu$ fading [Charishma et al. \(2021\)](#).

In this work, the complete knowledge of CSI is assumed to be available at a BS in order to optimize the phase shifts. Let x represents a signal transmitted by a BS and passively reflected to an intended receiver (D) by an arbitrary r^{th} IRS panel, which regulates the phase reflection coefficients to maximize SNR at receiver, thereby improves end-to-end quality of the wireless link. Received signal, y is expressed as [Tao et al. \(2020\)](#)

$$y = \sqrt{P_T} (\mathbf{h}_r^T \Theta_r \mathbf{g}_r + h_{S,D}) x + w \quad (4.1)$$

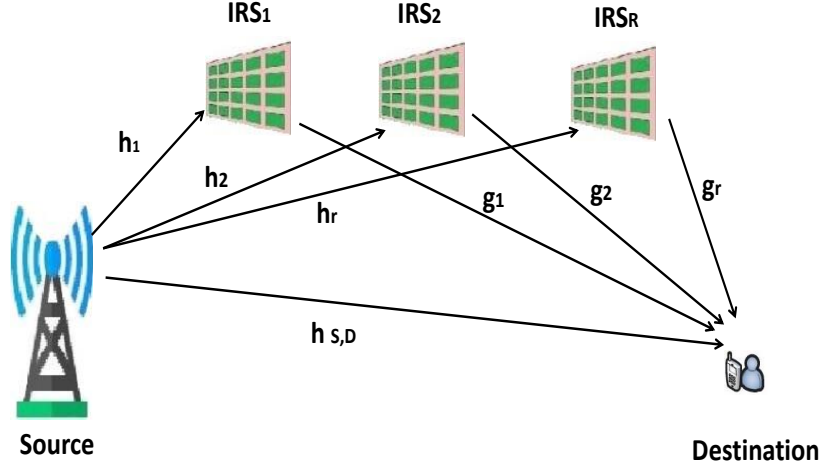


Figure 4.1: Multiple IRS-assisted wireless communication system.

where P_T denotes transmit power level at BS and w represents additive white Gaussian noise (AWGN) with zero mean and variance σ_N^2 during the course of signal propagation, Θ_r is a phase-shift matrix associated with r^{th} IRS panel, and is defined as $\Theta_r = \text{diag}(e^{j\theta_{r,1}}, e^{j\theta_{r,2}}, \dots, e^{j\theta_{r,N}})$, where $r = 1, 2, \dots, R$. Here, $\theta_{r,n}$ is the phase-shift introduced by the n^{th} reflecting element associated with r^{th} IRS panel.

Instantaneous SNR estimate by virtue of beam forwarding from the r^{th} IRS is given by (Charishma et al., 2021):

$$SNR_{IRS} = \frac{P_T |\mathbf{h}_r^T \Theta_r \mathbf{g}_r + h_{S,D}|^2}{\sigma_N^2} \quad (4.2)$$

Considering propagation dynamics through a selected IRS panel and N participating EREs within it, an expression of SNR can be written as (Charishma et al., 2021)

$$SNR_{IRS} = \gamma \left(\left| \sum_{r \in R, n \in N} e^{j\theta_{r,n}} |\mathbf{h}_{r,n}| |\mathbf{g}_{r,n}| + |h_{S,D}| \right|^2 \right) \quad (4.3)$$

where $\gamma = \frac{P_T}{\sigma_N^2}$ is SNR in the vicinity of a BS. In order to maximize received signal power level, the desired phase shifts introduced by n^{th} element of r^{th} IRS panel is

given by

$$\theta_{r,n} = \arg(h_{S,D}) - \arg([\mathbf{h}]_{r,n}[\mathbf{g}]_{r,n}) \quad (4.4)$$

In this work, effect of distance dependent path loss on large-scale fading model is considered for the performance analysis. The distance-dependent path loss is given by [Zhang and Dai \(2021\)](#)

$$L(d) = C_0 \left(\frac{d}{d_0} \right)^{-\nu}, d \in \{d_{SD}, d_{SR}, d_{RD}\} \quad (4.5)$$

where C_0 is path loss at a reference distance $d_0 = 1m$ and ν denotes the path loss exponent. Here d_{SD}, d_{SR}, d_{RD} represents Euclidean distance between BS-receiver, BS-IRS panel, and IRS panel-receiver, respectively, and it is presumed that $C_0 = -30dB$ [Zhang and Dai \(2021\)](#).

Let a random variable Z represents magnitude of end-to-end channel coefficients in IRS-assisted system

$$Z = \left(\sqrt{L_{d_{SR}} L_{d_{RD}}} \sum_{r \in R, n \in N} e^{j\theta_{r,n}} |\mathbf{h}_{r,n}| |\mathbf{g}_{r,n}| + \sqrt{L_{d_{SD}}} |h_{S,D}| \right)^2 \quad (4.6)$$

In this expression, due to coherent combining, pathloss fading coefficients of a direct link and through an IRS reflected link (VLOS) are in-phase. The second term in the equation (4.6) constitutes a sum of identical unit-power double-Nakagami Random Variables. Sum of positive RVs is approximated by a Gamma RV using a causal form of the central limit theorem (CLT) [Papoulis \(1962\)](#). This in-turn, needs the calculation of the first and second moments of the sum.

The mean and variance of sum under unit-power i.i.d. condition is given by

$$\mu_{IRS_r} = \sum_{n=1}^N \mathbb{E} \{ |\mathbf{h}_{r,n}| |\mathbf{g}_{r,n}| \} = N\mu_1$$

$$\mu_{IRS_r}^{(2)} - \mu_{IRS_r}^2 = \sum_{n=1}^N \text{Var} \{|\mathbf{h}_{r,n}| | \mathbf{g}_{r,n}\} = N(1 - \mu_1^2) \quad (4.7)$$

with

$$\mu_1 = \mathbb{E} \{|\mathbf{h}_{r,n}| | \mathbf{g}_{r,n}\} = \mathbb{E} \{|\mathbf{h}_{r,n}|\} \mathbb{E} \{|\mathbf{g}_{r,n}|\} \quad (4.8)$$

as a product of the mean of two independent Nakagami RVs.

Further, the expression for SNR in equation (4.3) can be written in terms of random variable Z as

$$SNR_{IRS} = \gamma Z = \frac{P_T Z}{\sigma_N^2} \quad (4.9)$$

In this work, end-to-end (source-destination) wireless channel segments are modeled as $\kappa - \mu$ shadowed fading channels. The probability density function of the random variable Z , $f_Z(Z)$ is given by [PARIS \(2014\)](#)

$$f_Z(Z) = \frac{\mu^\mu m^m (1 + \kappa)^\mu}{\Gamma(\mu) \bar{Z} (\mu\kappa + m)^m} \left(\frac{Z}{\bar{Z}}\right)^{\mu-1} \exp\left(-\frac{\mu(1 + \kappa)}{\bar{Z}} Z\right) {}_1F_1\left(m, \mu; \frac{\mu^2 \kappa (1 + \kappa)}{\mu\kappa + m} \frac{Z}{\bar{Z}}\right) \quad (4.10)$$

where κ denotes a ratio of total signal power of dominant components to the total power of the scattered waves, μ indicates number of multipath clusters, m is a shadowing parameter and ${}_1F_1(\dots)$ is the confluent hyper-geometric function.

Further, estimate of SNR is carried out using Gamma random variable with shape parameter (α), scale parameter (β) and on exploiting moments. The first and second moments of non-negative random variable Z is given by $\mu_Z = \mathbb{E}\{Z\}$ and $\mu_Z^{(2)} = \mathbb{E}\{Z^2\}$, respectively. The $\kappa - \mu$ shadowed random variable γ can be approximated by the gamma random variable with parameters (α, β), where, these parameters are defined as

$$\alpha = \frac{\mu_Z^2}{\mu_Z^{(2)} - \mu_Z^2}, \quad \beta = \frac{\mu_Z^{(2)} - \mu_Z^2}{\mu_Z}. \quad (4.11)$$

The cumulative distribution function of Z , $F_Z(Z)$ is given by [Kumar and Chouhan](#)

(2015)

$$F_Z(Z) = \frac{Z^\alpha}{\Gamma(\alpha + 1)\beta^\alpha} {}_1F_1\left(\alpha; \alpha + 1; -\frac{Z}{\beta}\right) \quad (4.12)$$

Since the instantaneous SNR estimate of the direct link (BS-receiver) is independent of its value for the r^{th} IRS link, the CDF of the instantaneous SNR for S to D direct link can be expressed as $F_{Z_{S,D}}(Z)$ and is given by

$$F_{Z_{S,D}}(Z) = \frac{Z^{\alpha_{S,D}}}{\Gamma(\alpha_{S,D} + 1)\beta^{\alpha_{S,D}}} {}_1F_1\left(\alpha_{S,D}; \alpha_{S,D} + 1; -\frac{Z}{\beta_{S,D}}\right) \quad (4.13)$$

Similarly, the CDF of instantaneous SNR for a holistic S to D link with an intermediate IRS-assisted link segment is given as

$$F_{Z_{IRS}}(Z) = \frac{Z^{\alpha_r}}{\Gamma(\alpha_r + 1)\beta^{\alpha_r}} {}_1F_1\left(\alpha_r; \alpha_r + 1; -\frac{Z}{\beta_r}\right) \quad (4.14)$$

4.3 Spatial attributes driven channel model

On considering local geometrical features, a fairly good approximated channel model that characterizes propagation behavior of geographical segments under test is presented. Further, during the course of traversing, receiver experiences shadow fading from a BS due to presence of large/small and stationary/movable obstacles in proximity. These underlying observations infer a need to devise a channel model for the given geographical segments while considering randomly varying fading that is inevitable due to random loci of receiver movements.

A wireless channel with increasing shadowing parameter value, m is interpreted as receiver movements from a completely shadowing region to a shadow free region. Whereas, increasing μ value indicates the transition from a small number of scattering clusters to a large number of scattering clusters. Furthermore, enhancement in κ value signifies a transition under which wireless link experiences a migration from a

weak LOS component to a strong LOS component [Chun et al. \(2017\)](#).

4.3.1 IRS panel selection

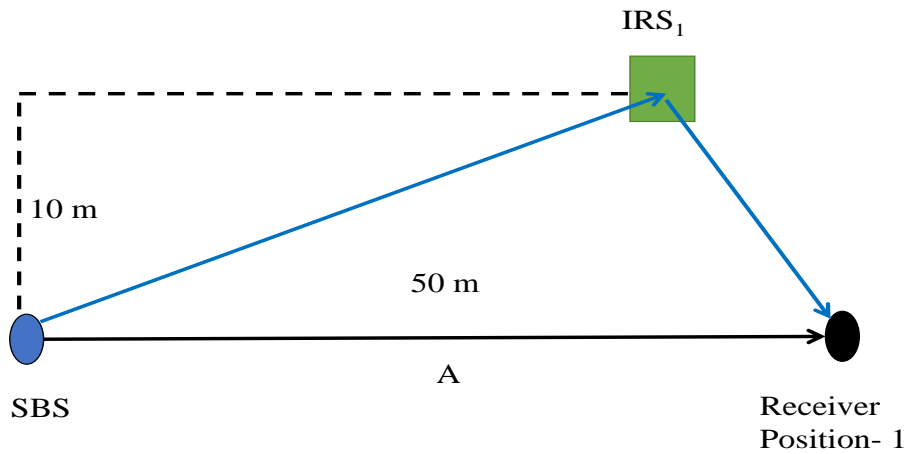
Establishing a particular VLOS end-to-end wireless link through a specific IRS panel depends on location of receiver. Graphical representation containing location attributes of BS, IRS panels and different degree of fading as experienced by a receiver for the considered scenarios are shown in Figure 4.2. For instance, if receiver is within zone A, IRS_1 facilitates VLOS link between a BS and receiver situated at position-1, and thus participates in enhancing QoS performance measures. In a moderately fading zone, receiver as depicted in Figure 4.2b establishes VLOS with BS through IRS_1 or IRS_2 based on VLOS that results in maximizing signal strength at receiver. Whereas, if a receiver is in a severely fading zone, at position-3 in Figure 4.2c, in such circumstances likelihood of LOS link is extremely poor and receiver observes NLOS compliance with BS quite often. In such instances, receiver experiences VLOS with BS through any arbitrary IRS panel from the set (IRS_1, IRS_2, IRS_3) that maximizes signal power at the receiver.

Thus, a strategy to select an arbitrary IRS panel out of total R IRS panels is based on hypothesis that results in signal power maximization at a receiver (γ_{IRS_r}) and is expressed as [Yang et al. \(2021a\)](#)

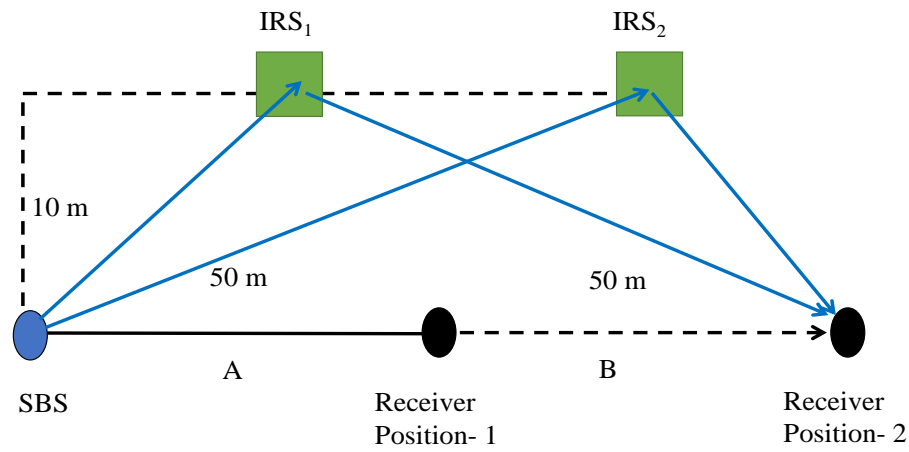
$$r = \arg \max_{r \in \{1, \dots, R\}} \gamma_{IRS} \quad (4.15)$$

In this paper, outage probability and ergodic capacity estimate is performed for three different fading zones based on the surrounding geographical characteristics of obstacles namely;

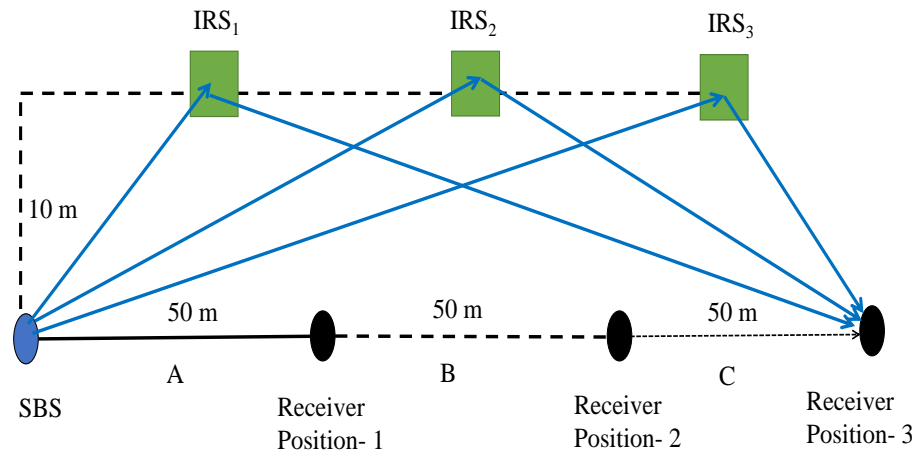
- Lightly fading zone (A): A geographical area characterized with low rise buildings or open square area and having close proximity to BS. This coverage zone is indicated by a regular line in Fig.4.2a, and it signifies high probability of a direct



(a)



(b)



(c)

Figure 4.2: Schematic diagram comprising IRS locations, Receiver positions and viable links in (a) lightly fading zone, (b) moderately fading zone and (c) severely fading zone

LOS link between BS and a receiver.

- Moderately fading zone (B): A geographical area segment characterized with moderate density of buildings and other obstacles along while maintaining a sizeable separation from a BS. This coverage zone is indicated by a dotted line locus in Fig.4.2b. Such a scenario infers moderate probability of a direct LOS link between BS and a receiver.
- Severely fading zone (C): A geographical segment characterized with a large number of high-rise buildings and maintains considerable distance from BS. This geographical segment is indicated by a thin dotted line in Fig.4.2c which manifests a poor likelihood of a direct LOS link between BS and a receiver.

Classification basis owes to channel spatial aspects and further to infuse time-driven data traffic characteristics in the proposed mathematical framework, geographical segments are analysed in short epochs corresponding to distinct vehicular traffic patterns by virtue of time-sensitive traffic characteristics namely; peak hours, off-peak hours, and wee hours.

4.3.2 Outage probability analysis

Outage probability (P_{out}) is defined as likelihood of a phenomenon in which the instantaneous SNR estimate at receiver falls below a predetermined outage threshold (γ_T), subsequently leads to a catastrophic state of wireless link and is expressed as

$$P_{out} = Pr\{\gamma Z \leq \gamma_T\} \quad (4.16)$$

Outage probability $Pr\{\gamma Z \leq \gamma_T\}$ of a multiple IRS-assisted network is estimated using the CDF of total SNR γ_T as [Kodide et al. \(2016\)](#)

$$P_{out} = Pr\{\gamma Z \leq \gamma_T\} = F_{Z_{S,D}}(Z) [F_{Z_{IRS}}(Z)]^r \quad (4.17)$$

where $Pr\{\cdot\}$ denotes the probability, γ is instantaneous SNR estimate and r corresponds to a particular IRS panel which yields maximum SNR at a receiver situated in an arbitrary geographical segment.

Since the instantaneous SNR estimate of a direct link (BS-receiver) is independent of its value for the r^{th} IRS link, the CDF of the instantaneous SNR for S to D direct link can be expressed as $F_{Z_{S,D}}(Z)$ and is given by

$$F_{Z_{S,D}}(Z) = \frac{Z^{\alpha_{S,D}}}{\Gamma(\alpha_{S,D} + 1)\beta^{\alpha_{S,D}}} {}_1F_1\left(\alpha_{S,D}; \alpha_{S,D} + 1; -\frac{Z}{\beta_{S,D}}\right) \quad (4.18)$$

Similarly, the CDF of instantaneous SNR for a holistic S to D link with an intermediate IRS-assisted link segment is given as

$$F_{Z_{IRS}}(Z) = \frac{Z^{\alpha_r}}{\Gamma(\alpha_r + 1)\beta^{\alpha_r}} {}_1F_1\left(\alpha_r; \alpha_r + 1; -\frac{Z}{\beta_r}\right) \quad (4.19)$$

Substituting equations (4.18) and (4.19) in equation (4.17), an approximate closed form expression for outage probability of multiple IRS-assisted system is given as

$$P_{out} \approx \frac{Z^{\alpha_{S,D}}}{\Gamma(\alpha_{S,D} + 1)\beta^{\alpha_{S,D}}} {}_1F_1\left(\alpha_{S,D}; \alpha_{S,D} + 1; -\frac{Z}{\beta_{S,D}}\right) \times \frac{Z^{\alpha_r}}{\Gamma(\alpha_r + 1)\beta^{\alpha_r}} {}_1F_1\left(\alpha_r; \alpha_r + 1; -\frac{Z}{\beta_r}\right) \quad (4.20)$$

4.3.3 Ergodic capacity analysis

Ergodic capacity of a system is determined by averaging the instantaneous capacity over a large number of channel realizations. The ergodic capacity of a system can be expressed as

$$C = \mathbb{E}[\log_2(1 + SNR_{IRS})] = \mathbb{E}[\log_2(1 + \gamma Z)] \quad (4.21)$$

Considering the PDF of γZ , the ergodic capacity is expressed as

$$C = \int_0^\infty \log_2(1+z) f_{\gamma Z}(z) dz \quad (4.22)$$

In terms of CDF, the ergodic capacity is expressed as

$$C = \frac{1}{\ln 2} \int_0^\infty \frac{1}{z+1} \left[1 - F_Z\left(\frac{z}{\gamma}\right) \right] dz \quad (4.23)$$

Further, the ergodic capacity can be approximated using the identity, $(1+z)^{-\zeta} = \frac{1}{\Gamma(\zeta)} G_{1,1}^{1,1} \left(z \middle| \begin{matrix} 1-\zeta \\ 0 \end{matrix} \right)$, where $G_{m,n}^{p,q} \left(z \middle| \begin{matrix} a_1, \dots, a_p \\ b_1, \dots, b_q \end{matrix} \right)$ is the Meiger-G function [Gradshteyn and Ryzhik \(2007\)](#).

$$C \approx \frac{1}{\ln 2} \int_0^\infty G_{1,1}^{1,1} \left(z \middle| \begin{matrix} 0 \\ 0 \end{matrix} \right) \frac{\Gamma\left(\alpha, \frac{z}{\beta\gamma}\right)}{\Gamma(\alpha)} dz \quad (4.24)$$

Considering the equivalence between the incomplete Gamma function and Meiger-G function, i.e., $\Gamma\left(\alpha, \frac{z}{\beta\gamma}\right) = G_{1,2}^{2,0} \left(\frac{z}{\beta\gamma} \middle| \begin{matrix} 1 \\ \alpha, 0 \end{matrix} \right)$, ergodic capacity can be expressed as

$$C \approx \frac{1}{\Gamma(\alpha) \ln 2} \int_0^\infty G_{1,1}^{1,1} \left(z \middle| \begin{matrix} 0 \\ 0 \end{matrix} \right) G_{1,2}^{2,0} \left(\frac{z}{\beta\gamma} \middle| \begin{matrix} 1 \\ \alpha, 0 \end{matrix} \right) dz \quad (4.25)$$

Thus, approximate closed-form expression for ergodic capacity of an IRS-assisted link is given by

$$C \approx \frac{1}{\Gamma(\alpha) \ln 2} \frac{2^{\alpha-1}}{\sqrt{\pi}} G_{3,5}^{5,1} \left(\frac{1}{4\gamma\beta^2} \middle| \begin{matrix} 0, \frac{1}{2}, 1 \\ \frac{\alpha}{2}, \frac{\alpha+1}{2}, 0, \frac{1}{2}, 0 \end{matrix} \right). \quad (4.26)$$

Table 4.1: Geographical segments and wireless channel Parameters.

Parameter	value
Path loss exponent	$\nu=3$
Number of IRS panel	R=3
Number of EREs	N= 32, 64, 128
S to D distance	meter
light fading zone	50
moderate fading zone	100
severe fading zone	150
BS coordinates: $(x, y, h)_{BS}$	(0,0,20)
IRS coordinates: $(x, y, h)_{IRS}$	meter
IRS_1	(50,10,10)
IRS_2	(100,10,10)
IRS_3	(150,10,10)
shadowing parameter	m : Badarneh et al. (2020)Chun et al. (2017)
light fading zone	$m= 50$
moderate fading zone	$m= 5$
severe fading zone	$m= 1.5$
κ factor	20 Chun et al. (2017)
Number of multipath cluster	μ : Chun et al. (2017)
μ in peak hours	$\mu= 5$
μ in off-peak hours	$\mu= 3$
μ in wee hours	$\mu= 1$
Noise power spectral density	-174 dBm/Hz

4.4 Numerical results

In this section, outage probability and ergodic capacity estimate for the geographical segments equipped with multiple IRS panels is presented. For outage probability and ergodic capacity estimate $\kappa - \mu$ shadowed fading channel is considered. All simulation results are obtained on averaging 10^5 Monte Carlo runs.

During simulation study, parametric regulations particularly, the severity of fading zones expressed in terms of shadowing parameter m and time-sensitive vehicular traffic pattern are incorporated using number of multipath clusters μ . Nominal value of these parameters along with service area specific parameters that influence signal propagation phenomenon is given in Table 4.1. The equivalent noise power at receiver is $\sigma_N^2 = N_0 + 10 \log(BW) + NF$, where BW is bandwidth and NF is noise figure. Further, for

three distinct fading zones; to analyse end-to-end wireless link outage probability and ergodic capacity performance, parametric regulation in number of participating EREs and time-sensitive vehicular-traffic pattern are considered and presented as case studies.

4.4.1 Outage probability and Ergodic capacity estimate with regulation in ERE

An outage probability and ergodic capacity estimate for geographical segments experiencing low intensity fading is shown in Figure 4.3. In this case, an IRS panel is considered at a distance of $(50, 10, 10)m$ from BS, and receiver is spotted at position-1 in Figure 4.2a and thus maintains distance of $50 m$ from BS.

Figure 4.3a illustrates the outage probability of an geographical segments with and without IRS. Parametric variations in EREs of an IRS panel are considered for qualitative analysis. Characteristics in Figure 4.3a reveal that the approximation works well for different values of N . Further, it can be observed that the outage probability decreases sharply with increase in SNR, and the decay rate is faster with a larger N .

Figure 4.3b depicts the ergodic capacity of geographical segments with and without IRS. It can be observed that, the ergodic capacity is tightly bound for all configurations, indicating the accuracy of the closed-form expression. Further, it can be inferred that the ergodic capacity increases monotonically with number of ERE, N .

Similar set of observations is presented in Figure 4.4 for the geographical segments exhibiting moderate fading characteristics. Here, coordinates of IRS_1 and IRS_2 are treated as $(50,10,10)$ and $(100,10,10)$, respectively with BS as origin, and receiver is considered at position-2 thus maintaining a distance of $100 m$ from BS as shown in Figure 4.2b. As anticipated, it can be observed that, the ergodic capacity performance degrades compared to light fading zone. The decline in performance can be attributed to distinguished geographical characteristics of a segment in the service area. For ergodic capacity estimate, inference suggests the need for larger number of EREs and is validated for a moderately faded zone (Figure 4.4b) compared to the number of EREs

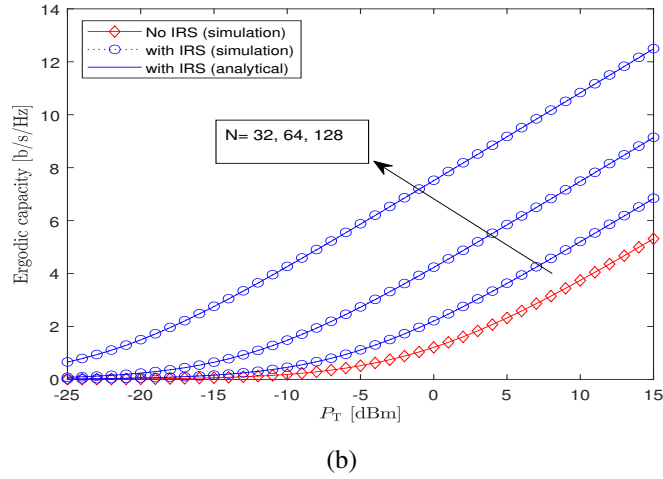
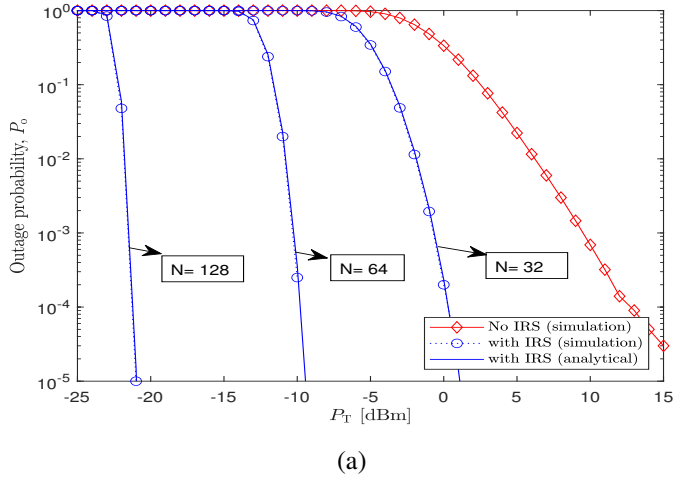
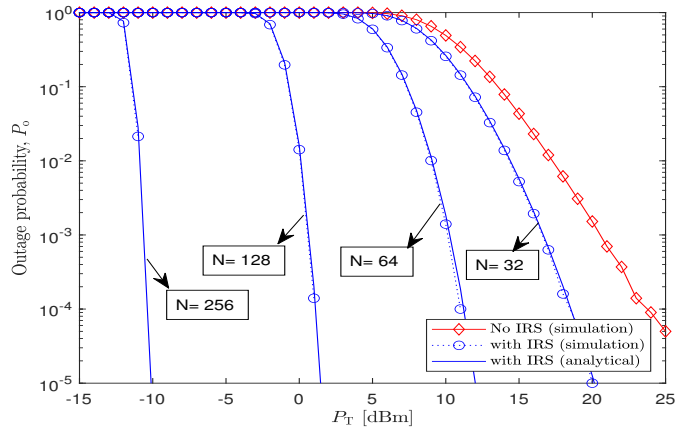


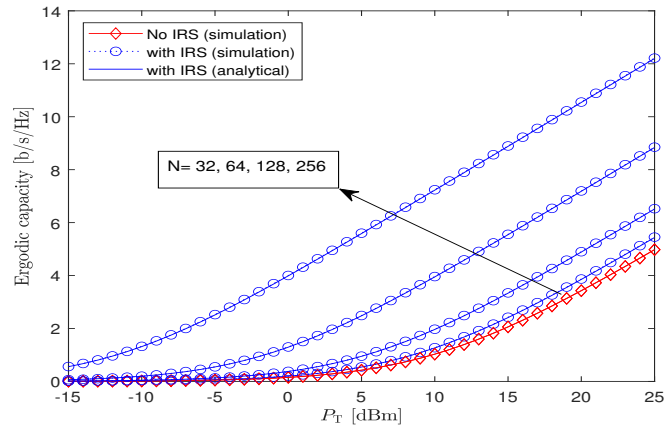
Figure 4.3: Numerical results demonstrating the impact of EREs for light fading zone on (a) Outage probability and (b) Ergodic capacity

required for a lightly faded zone (Figure 4.3b).

Further, outage probability and ergodic capacity estimate for a geographical segment observing relatively severe intense fading is shown Figure 4.5. In this use case, coordinates of IRS_1 , IRS_2 and IRS_3 are treated as (50,10,10), (100,10,10) and (150,10,10), respectively, and receiver is spotted at position-3 (Figure 4.2c) and thus separated by a distance of approximately 150 m from BS. A comparison of various characteristics in Figure 4.5a with that of Figure 4.3a and Figure 4.4a infers a noticeable degradation in network performance in terms of unwarranted enhancement in outage probability estimate. In geographical segments experiencing severe fading, to attain the outage probability of order 10^{-5} , participation of more EREs is required and



(a)



(b)

Figure 4.4: Numerical results demonstrating the impact of EREs for moderate fading zone on (a) Outage probability and (b) Ergodic capacity

it is 256 EREs. Rationale for the performance compromise in terms of unusual higher outage probability is presence of high-rise buildings and high density of surrounding vehicles that causes frequent blind spot formation. This behaviour is quite prominent especially for geographical segments experiencing severe fading. Here, too, analytical result maintains close approximation with the obtained simulation results.

Analysis of outage probability and ergodic capacity estimate for a light fading zone as depicted in Figure 4.3, clearly indicates large number of EREs are redundant, since LOS compliance dominates. Whereas, there is a significant impact of participating EREs on ergodic capacity performance, as receiver satisfies the NLOS compliance most of the time in moderate and severe fading zones as depicted in Figure 4.4 and Figure

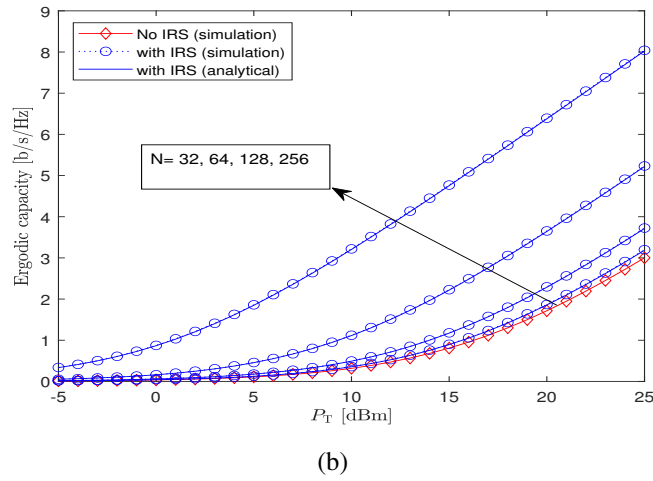
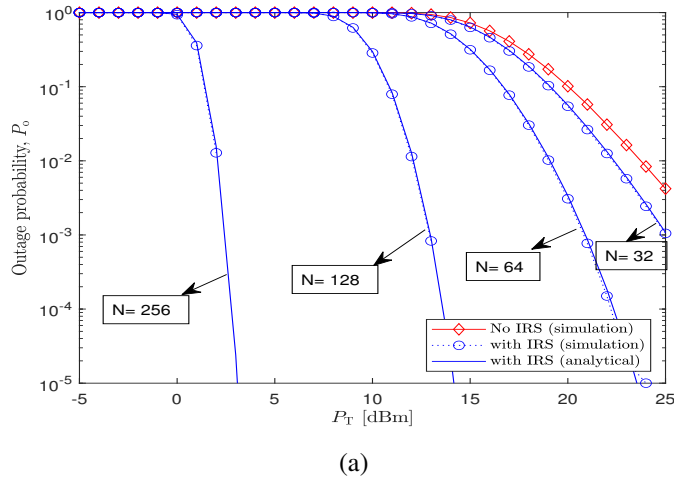


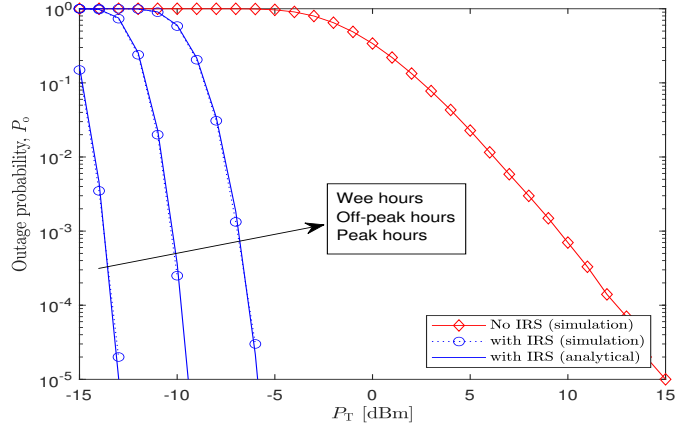
Figure 4.5: Numerical results demonstrating the impact of EREs for severe fading zone on (a) Outage probability and (b) Ergodic capacity

4.5. This attribute justifies the need for a large number of EREs in segments of service area witnessing moderate to severe degree of fading.

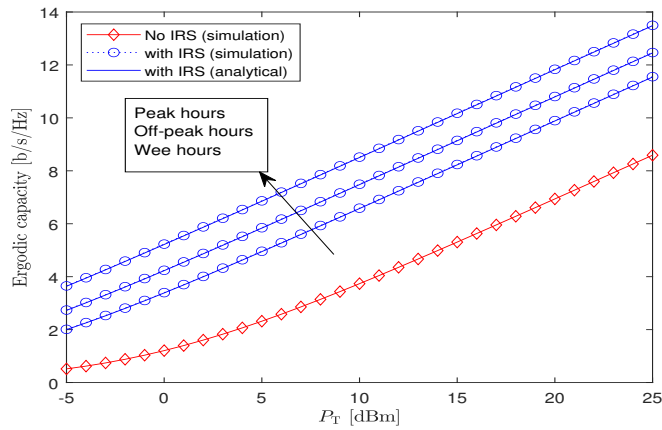
4.4.2 Outage probability and Ergodic capacity dependency on vehicular traffic

Receiver positioning at any arbitrary location in geographical segments experiences various degree of fading during different intervals of a time in day-to-day operation, due to presence of temporary obstacles in close proximity. To ascertain ergodic capacity estimate (as depicted in Figure 4.6, 4.7 and 4.8) dependency on time-sensitive vehicular

traffic only, number of participating EREs are kept constant ($N=64$).



(a)



(b)

Figure 4.6: Numerical results demonstrating the impact of vehicular traffic in wireless terrain equipped with IRS panels having 64 EREs for light fading zone on (a) Outage probability and (b) Ergodic capacity

Outage probability and ergodic capacity characteristics shown in Figure (4.6-4.8) establish dependency on local geographical aspects combined with time-sensitive vehicular traffic. These spatio-temporal aspects are quite generic and inevitable for many outdoor use cases. As an illustration, in wee hours, receiver surrounding is characterized with low density of temporary obstacles (neighbouring vehicles), it results in high ergodic capacity compared to peak and off-peak hours as seen in Figure 4.6, 4.7 and 4.8 for light fading zone, moderate fading zone and severe fading zone, respectively. Further, the performance characteristics depicted in Figure (4.6-4.8) validate that to counter

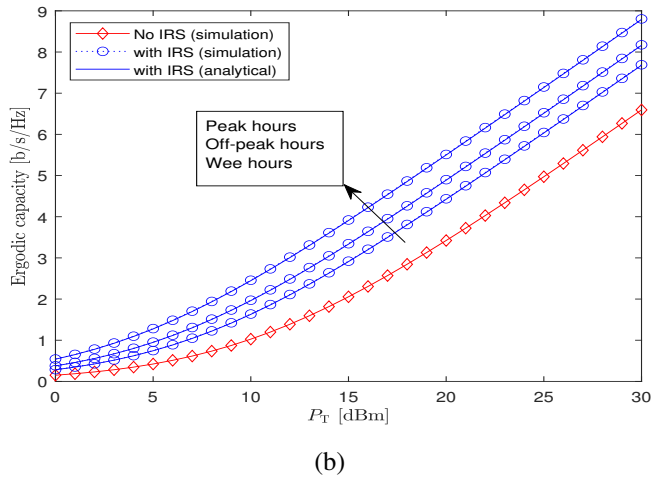
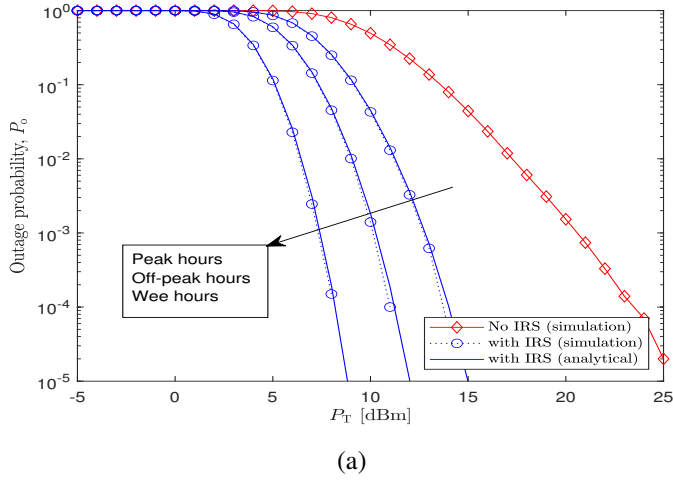
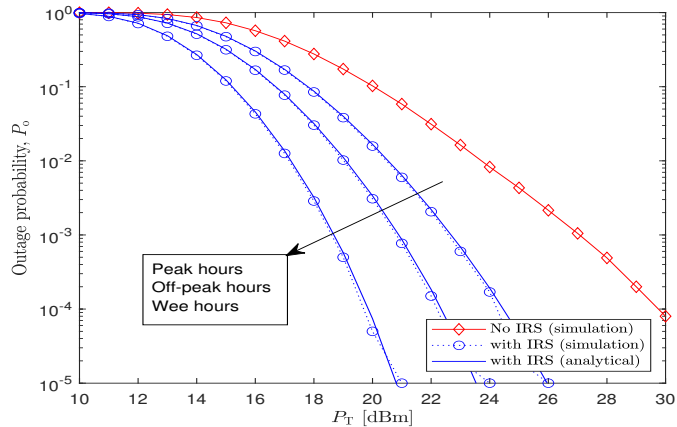


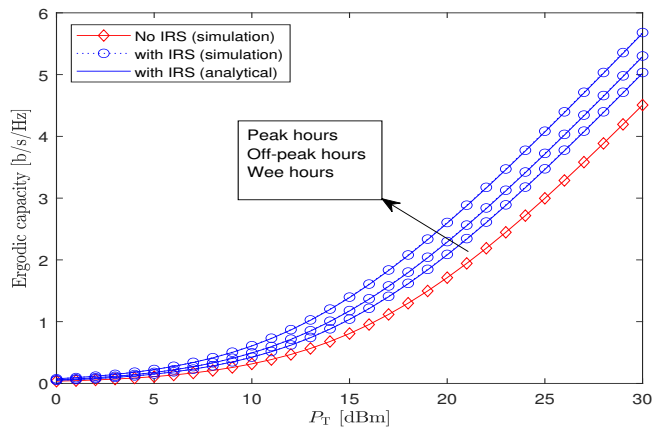
Figure 4.7: Numerical results demonstrating the impact of vehicular traffic in wireless terrain equipped with IRS panels having 64 EREs for moderate fading zone on (a) Outage probability and (b) Ergodic capacity

spatio and temporal factors driven unwarranted fading, usage of IRS panels yield much improved performance compared to the estimate obtained without IRS panels. For instance, during the peak hours of operation in different geographical segments of service area that experience distinct fading phenomenon, to attain the outage probability in the order of 10^{-5} , cellular operators must maintain the transmit power approximately -6 dBm , 15 dBm and 25 dBm for low intensity, moderate intensity and severe intensity of fading, respectively.

Different geographical segments of a service area equipped with IRS panels experience much improved ergodic capacity compared to a scenario wherein IRS panels are



(a)



(b)

Figure 4.8: Numerical results demonstrating the impact of vehicular traffic in wireless terrain equipped with IRS panels having 64 EREs for severe fading zone on (a) Outage probability and (b) Ergodic capacity

not deployed. Although, it can be observed in Figure 4.6b, 4.7b and 4.8b, that the enhancement in ergodic capacity estimate attains different scale. It primarily depends on time driven vehicular traffic characteristics as well as the geometrical attributes in the vicinity of receiver. During the wee hours and off-peak hours relative enhancement is more prominent than the peak hours of operation.

Using these observations, we can infer that IRS panels deployment at appropriate locations in different segments of a service area results in phenomenal improvement in ergodic capacity.

4.5 Summary

In this chapter, an analytical framework is presented to estimate ergodic capacity and outage probability of an end-to-end wireless link that undergoes different fading conditions owing to the localized geometry driven spatial and time-sensitive vehicular traffic attributes. Proposed methodology is validated for geographical segments equipped with multiple IRS panels. During simulation studies, a $\kappa - \mu$ shadowed fading model is adopted. For all the considered use cases, an exact estimate of ergodic capacity and outage probability based on Monte Carlo Simulation is bench-marked with the proposed analytical model driven approximate estimate. The obtained numerical results demonstrate the precision of accuracy in the course of approximation.

In summary, for various geographical and time-sensitive vehicular traffic characteristics, deploying multiple IRS panels ensures an overall improvement in ergodic capacity and outage probability estimate. Adopted $\kappa - \mu$ shadowed fading is approximated by Nakagami-m fading parametric model, and subsequently ergodic capacity and outage probability are estimated. Further, ergodic capacity and outage probability estimate dependency is established while regulating the key system parameters such as provisioning of multiple IRS panels, number of participating EREs, and transmit power. Incorporating these regulatory features and the corresponding enhancement in performance measures are of vital importance for the cellular service providers.

CHAPTER 5

STOCHASTIC MODELING AND COVERAGE ANALYSIS OF IRS-ASSISTED CELLULAR NETWORK WITH INTERFERENCE MITIGATION

5.1 Introduction

The upcoming Sixth generation (6G) wireless technology is expected to provide seamless connectivity by supporting use cases including enhanced blindspots coverage, extreme capacity, connectivity in remote areas and very high mobility. This can be achieved by exploiting advanced technologies such as ultra massive multiple-input multiple-output (MIMO), millimeter wave (mmWave) and TeraHertz (THz) communication, IRS and so on ([Rajatheva et al., 2020](#)). Although, massive MIMO offers high spectrum efficiency owing to large multiplexing gain and antenna array gain, it suffers from high signal processing complexity by virtue of large antenna arrays. Millimeter wave communication can provide large bandwidth and support high data rate, however, its coverage capability is a critical issue in urban environments due to presence of multiple obstacles such as tall buildings, foliage and large moving vehicles ([Samimi and Rappaport, 2014](#)).

Recently, wireless industry and academia has witnessed a considerable interest in IRS enabled wireless communication ([Basar et al., 2019](#); [Wu and Zhang, 2020](#); [Wu et al., 2021a](#)). An IRS is composed of large number of passive, low-cost reflecting elements, each of these elements is able to reflect the incident signal with an adjustable phase shift ([Pei et al., 2021](#)). IRS is capable of dynamically altering wireless channels to enhance the stipulated performance, and has enormous potential in multifacet aspects such as improved energy and spectral efficiency, enhanced data rate, extended coverage,

mitigating deep fading, and Doppler effects (Pan et al., 2020; Zou et al., 2020; Basar, 2021).

Stochastic geometry deals with the study of spatial patterns that are random in nature. Recently, inference based on stochastic geometry finds a prominent place for the analysis of heterogeneous network (HetNet) in cellular communication (Lu et al., 2021). It helps in furnishing some key insights for network design using analytical approaches. In these approaches, usual strategy facilitates a hypothesis in which location of the deployed wireless nodes in a geographical terrain is governed by a point process. Subsequently, the properties of the point process are exploited to analyze the network performance. In this context, performance analysis of IRS-assisted cellular communication using stochastic geometry is still in infancy.

In paper (Lee et al., 2013), authors have performed a holistic comparison of the Poisson Point Process (PPP) and the hexagonal grid models for urban areas, and it is claimed that PPP model is more accurate for coverage probability analysis. Appropriate positioning of the network elements in a cellular communication system using stochastic approach needs precise spatial details and timing information. Typically, any geographical terrain in an urban scenario experiences various degree of fading during different timing intervals and at specific locations. Owing to surrounding geospatial aspects, fading zones can be classified as light fading zone, moderate fading zone and severe fading zone. Similarly, due to heterogeneous behavior of users, data/vehicular traffic patterns can be classified into distinguished time intervals as wee hours, off-peak hours and peak hours, inheriting a unique characteristic; increasing order of users density in short epochs during different time of the day. Usually, users experience localized blindspot in a wireless terrain, one such occurrences may be, during peak hours of a day and in a geographical terrain characterized by a severe fading zone owing to surrounding spatial attributes.

In some of the early investigations, cellular network configuration is considered as homogeneous environment with Macro Base Stations (MBS) and cellular user distribution is treated as uniform and approximated using PPP model. In majority of these

findings, during analytical modeling, spatial attributes of BS and users are not given due considerations. Whereas, in current generation of cellular network, the network architecture comprises of small-cell base stations (SCBS) along with MBS and operates in heterogeneous environment. However, there are scenarios in which not only the user density is high but also some of the geographical segments are characterized with unbalanced distribution of users, thus maintaining different gradient of user density. These geographical segments can be more precisely approximated by Poisson Cluster Process (PCP). Owing to close proximity of BSs and users, and relatively high density of these entities, models based on PCP hypothesis imbibe spatial features of BSs as well as users.

To analyze the behavior of cellular users during wee hours, PPP-based modeling is suitable as the users are randomly distributed. Whereas, during peak hours, users density is exceptionally high and PCP-based models seem to be a good choice, as PCP models are able to capture spatio-temporal behavior more appropriately. Thus, analytical modeling based on stochastic geometry is of particular interest, where the idea is to endow appropriate distributions to estimate locations of different network entities, and subsequently leveraging properties of these distributions to characterize cellular network performance.

Most of the related work on heterogeneous cellular networks based on stochastic geometry consider SCBS as network entity to provide additional capacity along with MBS. During modeling framework, the location aspect of network elements (BSs and users) is modeled using PPP quite often ([Jo et al., 2012](#); [Heath et al., 2013](#); [Dhillon and Andrews, 2014](#)). However, PPP mechanism inherently has shortcomings, for example at a busy traffic junction or any indoor/outdoor scenarios characterized with a relatively higher density of users, for such use cases PPP may lead to poor approximation. All these scenarios quite often experience blindspot and must be dealt with more accurate approximate model.

Considering the realistic scenarios, modeling of networks with blindspots for BS and users involving PCP-based models are given in ([Yang et al., 2021b](#); [Shi et al., 2019](#);

[Afshang and Dhillon, 2018](#)). Key inference in these studies is that PCPs can be defined in terms of PPPs, and PCP-based models are suitable to represent localized spatial behavior in a manner analogous to spatial aspects are incorporated in 3GPP simulation models ([Afshang and Dhillon, 2018](#); [Saha et al., 2018, 2019](#)). A mathematical treatment of downlink analysis for an arbitrary user connected to a BS in HetNet using PCP with maximum power association is given in ([Saha et al., 2019](#)). In ([Mankar et al., 2016](#)), authors have modelled locations of BS using PPP, and users by PCP for coverage probability analysis. PCP can be treated as an outcome of applying homogeneous independent clustering to PPP, which means that the realization of clusters parent points is inferred using PPP.

In ([Zhu et al., 2020](#)), performance analysis of IRS-assisted mmWave networks, using stochastic geometry is investigated to achieve significant enhancement in capacity and energy efficiency. Here, authors presumed that BSs and IRSs are distributed using homogeneous PPP, and channel modeling carried out for direct and IRS-assisted channel. Authors in ([Zhang et al., 2022](#)), have investigated downlink coverage performance of multi-cell non-orthogonal multiple access (NOMA) system assisted by IRS, where BSs and users are modeled by homogeneous PPP, and the closed-form coverage probability expressions is obtained for paired NOMA users in a wireless terrain equipped with a single IRS panel.

Recently, performance analysis of a cellular user with and without IRS assistance is given in ([Shafique et al., 2022](#)). In this, authors proposed approximate expression for performance analysis in terms of measures namely; coverage probability, ergodic capacity, and energy efficiency. In analytical modeling, BSs location is considered as PPP and IRS panels are assumed to be distributed in a finite region as a Binomial Point Process (BPP). Limitation of the proposed framework is a strategy in which network elements are modeled by PPP and BPP, whereas in many practical scenarios, owing to vehicular traffic pattern and the spatial aspects driven degree of fading, PCP along with PPP may yield a better approximation.

So far based on inference drawn from stochastic geometry aspects, this is one of the

early attempt to use IRSs as network element and subsequently, addressing distribution as well as location modeling of IRSs and users by unified approach of PPP/PCP, while exploiting the spatio-temporal behavior of a wireless terrain. In this context, network coverage is significantly improved for a wireless terrain equipped with multiple IRS panels.

5.2 System model

A cellular network scenario consisting of multiple BSs, IRSs and users is shown in Figure 5.1. For an arbitrary user, coverage probability estimate for a downlink is presented. The following assumptions are made while formulating mathematical framework.

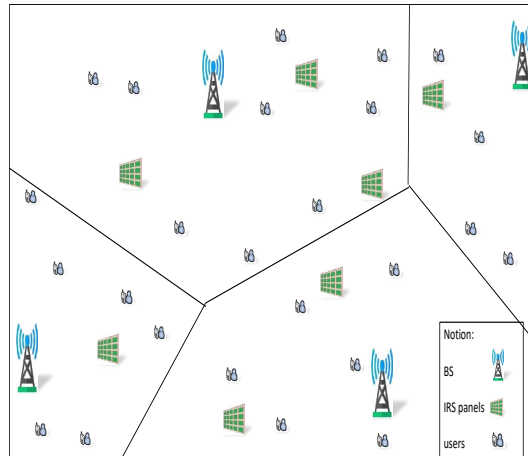


Figure 5.1: A schematic of IRS-assisted cellular network

Assumption 1 (PPP : BS): Base stations locations are modeled using PPP, Φ_b with density λ_b and assumed to have a constant transmit power P_T .

Assumption 2 (PPP/PCP : IRS): IRS panels location is approximated by PPP or PCP. Let \mathcal{R}_P and \mathcal{R}_C denote the indexes of the IRSs which are modeled as per the hypothesis of PPP and PCP, respectively. The basis for modeling IRSs as PPP and PCP depends on the geographical aspects that lead to different degree of fading. The IRS panels distributed using PPP approach is more appropriate for the users in lightly fading zones. Whereas, at certain locations within a wireless terrain experiencing severe fading, clus-

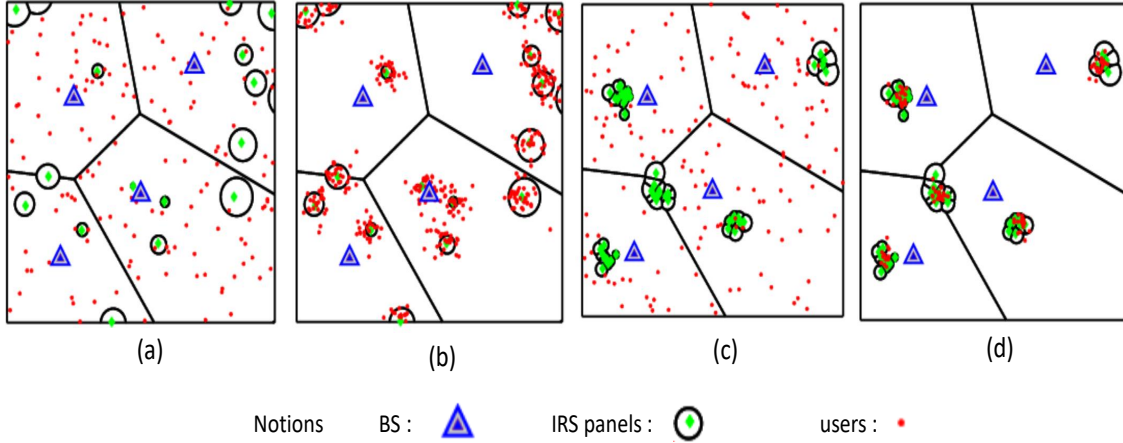


Figure 5.2: Schematics of cellular networks formed by combining PPP and PCP approach for IRS panels and users (a) IRS-PPP, user-PPP (b) IRS-PPP, user-PCP (c) IRS-PCP, user-PPP and (d) IRS-PCP, user-PCP

tered IRS panels modeled using PCP seems more appropriate and may lead to enhancing the QoS experienced by the users. We denote the Poisson processes (point process or cluster process) of the IRSs as Φ_r , where Φ_r is labelled as $\Phi_{\mathcal{R}_P}$ when modelled by PPP which is a function of density $\lambda_{\mathcal{R}_P}$. Otherwise, it is labelled as $\Phi_{\mathcal{R}_C}$ while modeled using PCP.

Assumption 3 (PPP/PCP : user): As a common practice, users are modeled as the point process (Φ_u) irrespective of BS locations and is considered to be stationary. In this work, depending upon the localized spatio-temporal behavior as experienced by different segments of wireless terrain, location of users is approximated by PCP as well as PPP. In realistic scenarios, users can be uniformly distributed or clustered, depending on spatio-temporal state of a wireless terrain. Usually, in wee hours active users spread is governed by uniform distribution, therefore during the short epochs in wee hours users location aspect can be best approximated by PPP. Whereas, during the peak hours of a day or for clustered users appearance in public events (musical concert, political gathering etc.), users presence can be more appropriately approximated by PCP.

In this work, coverage performance analysis of a cellular network is considered for an arbitrary user, which corresponds to a randomly selected point from Φ_u . Without loss of generality, user is assumed to be located at the origin, since Φ_u is stationary.

For the given wireless terrain; from the network topology perspective, based on positioning of IRS panels, location of active users with spatio-temporal behavior generated inference about varying degree of fading and exploiting different underlying stochastic models, four different case studies are presented and depicted in Figure 5.2.

1. Case study-1 (IRS-PPP and users-PPP): In this, IRS panels and users are modeled by PPP. This is the most familiar approach of modelling in cellular networks and is treated as a baseline reference model for comparison with other case studies. This network topology includes independent distribution of uncorrelated IRSs and uniformly distributed users. This model is suitable to approximate a geographical terrain observing light fading during the wee hours.
2. Case study-2 (IRS-PPP and users-PCP): In this, location aspect of IRS panels and users is approximated by PPP and PCP, respectively. This model is suitable for characterizing scenarios having uncorrelated IRS and clustered users. Here, we model the clustered user and IRS locations jointly by considering users whose distribution is governed by PCP and in surrounding terrain IRS panels are deployed based on PPP hypothesis. This configuration mimics network topology having a single IRS panel that serves to many users located in an arbitrary cluster, and thereby leads to relatively fair possibility of blindspot creation in that segment of wireless terrain. This model is suitable for a geographical terrain experiencing light fading during peak/off-peak hours.
3. Case study-3 (IRS-PCP and users-PPP): During this case study location aspect of IRS panels and active users is governed by PCP and PPP, respectively. This scenario may surface when users are spatially apart and no cluster formation takes place with subset of users, however such users are served by IRS panels that belong to a cluster having finite IRS panels as its elements. This model is suitable for a geographical terrain observing severe fading during off-peak hours.
4. Case study-4 (IRS-PCP and users-PCP): In this case study, IRS panels and active users are modeled by PCP. This situation can be envisioned for a wireless terrain

in which closely spaced users are members of clusters and segments in wireless terrain experience moderate to severe fading. To mitigate fading dense deployment of IRS panels is exercised as per the PCP hypothesis. Here, to address modeling aspect of IRS panel and user locations, two PCPs with the same parent PPP but independent and identically distributed (i.i.d.) offspring point processes is considered. This model is more appropriate for a scenario observing moderate to severe fading during short epochs in peak hours of vehicular traffic.

5.2.1 Signal propagation model

An IRS is a planar array having N reflecting elements and each reflecting element is capable to introduce desired phase regulation. The direct channel between a BS and a user is denoted by $h_{BU} \in \mathbb{C}^1$, the channel between a BS and an active IRS panel (any one arbitrary IRS panel out of deployed IRS panels) is denoted as $\mathbf{h}_{BR} \in \mathbb{C}^{N \times 1}$ and the channel between the active IRS and a user is denoted by $\mathbf{h}_{RU} \in \mathbb{C}^{N \times 1}$.

Let s be the signal transmitted by a BS and passively reflected to an intended user by an arbitrary r^{th} IRS, which optimizes the phase reflection coefficient to maximize the SNR estimate at user's location, thereby improves end-to-end quality of a wireless link. The received signal is expressed as

$$s' = \sqrt{P_T} (\mathbf{h}_{RU}^T \mathbf{\Theta}_r \mathbf{h}_{BR} + h_{BU}) s + w \quad (5.1)$$

where P_T denotes transmit power level at BS and w represents additive white Gaussian noise (AWGN) with zero mean and variance N_0 during the course of signal propagation in a channel, $\mathbf{\Theta}_r$ is a phase-shift matrix defined as $\mathbf{\Theta}_r = \text{diag}(e^{j\theta_1}, e^{j\theta_2}, \dots, e^{j\theta_N})$. Here, θ_n is the phase-shift introduced by the n^{th} reflecting element of the r^{th} IRS panel.

We consider two types of downlink for coverage analysis.

- Mode-1 (Direct link): User is connected to BS with one-hop direct link, analogous to conventional cellular communication as shown in Figure 5.3a.

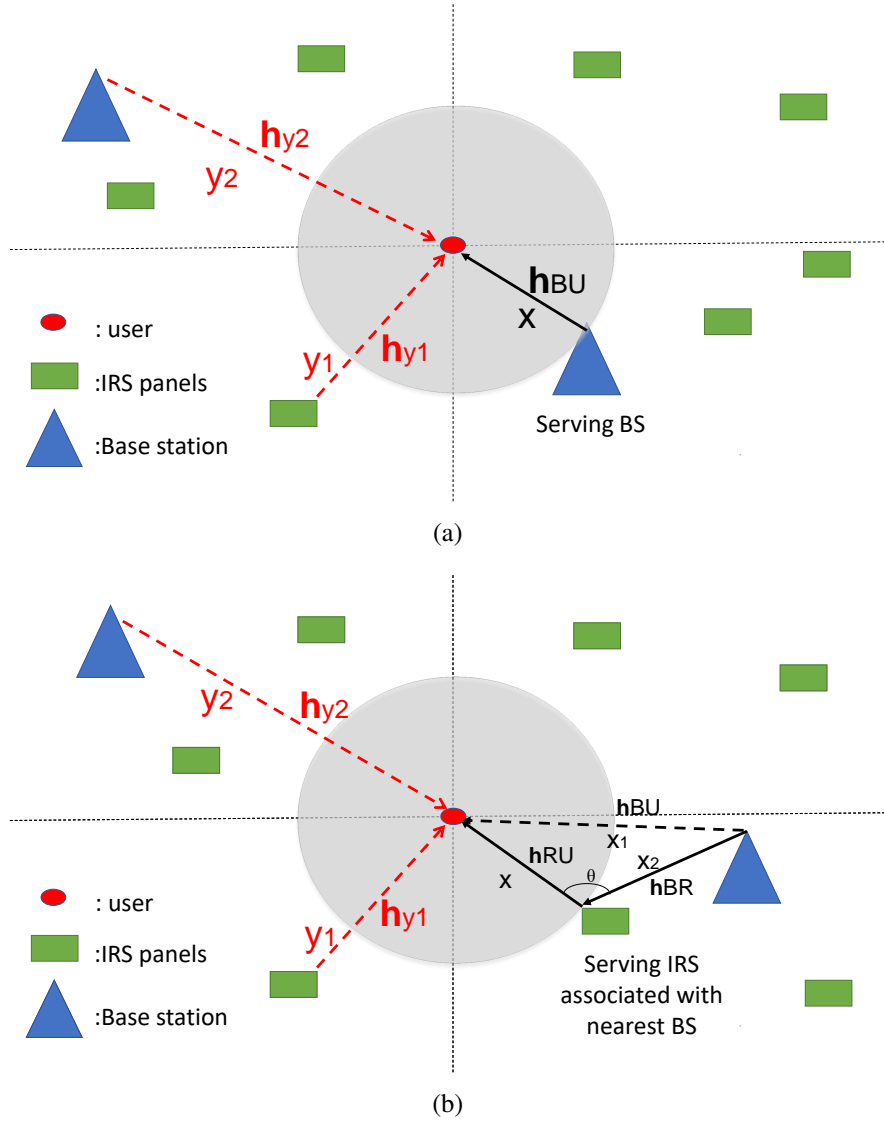


Figure 5.3: Illustration of distance characterization and channel models with reference to a user (a) Mode-1 (Direct link) and (b) Mode-2 (IRS-assisted link)

- Mode-2 (IRS-assisted link): User is connected to BS via IRS-assisted reflected link experiencing two hop count as shown in Figure 5.3b.

Direct link: In this mode, a user is served by a nearest BS. Received signal strength at the user's location is given by (Shafique et al., 2022)

$$S_{d_x} = P_T \beta^2 |h_x|^2 x^{-\alpha} \quad (5.2)$$

here P_T is transmission power of the BS, β is channel power gain of free-space path loss

model, $|h_x|$ is magnitude gain of small scale fading channel, α is path-loss exponent and x is Euclidean distance between a user and the nearest serving BS.

Here, the interference experienced by an arbitrary user is estimated by considering the aggregate interference from BSs excluding interference caused by the nearest serving BS and all IRS panels. The aggregate interference due to BSs is given by (Shafique et al., 2022)

$$\hat{I}_b = \sum_{j \in \Phi_b \setminus x} P_T \beta^2 |h_{y_j}|^2 y_j^{-\alpha} \quad (5.3)$$

here h_{y_j} and y_j is gain of small-scale fading channel and distance between a user to interfering BSs, respectively. In this mode, signal strength associated with reflected links from IRS panels are assumed to be so minimal that the reflected links are treated as weak links, and hence their contribution in signal transmission is marginalized.

Considering the aggregate interference due to all IRS panels, it can be estimated as (Shafique et al., 2022)

$$\hat{I}_r = \sum_{j \in \Phi_b} \sum_{i \in \Phi_r} P_T \beta^2 |\mathbf{h}_{RU_{j,r}}^H \Theta_i \mathbf{h}_{BR_{r,i}}|^2 y_j^{-\alpha} \quad (5.4)$$

here h_{RU_i} and h_{BR_i} are fading channel gain between interfering IRS-user link and between BS-interfering IRS link, respectively. Θ_i is a phase-shift matrix of the interfering IRS and is given by $\Theta_i = \text{diag}(e^{j\theta_{i1}}, e^{j\theta_{i2}}, \dots, e^{j\theta_{iN}})$.

The SINR experienced at user's location served by BS located at distance x in direct transmission mode is given by

$$\text{SINR}_d(x) = \frac{S_{d_x}}{N_0 + \hat{I}_b + \hat{I}_r} \quad (5.5)$$

IRS-assisted link: In this mode, a user is served by the nearest IRS having close proximity with a local BS. The received signal power as perceived by user from a serving BS through IRS is given by

$$S_{r_x} = P_T \beta^2 |\mathbf{h}_{RU_x}^H \Theta_x \mathbf{h}_{BR_{x_2}}|^2 x^{-\alpha} \quad (5.6)$$

here h_{RU_x} is Rayleigh fading channel gain of nearest serving IRS- user link and $h_{BR_{x_2}}$ is channel gain of serving BS-IRS link, and x is Euclidean distance between user and the nearest IRS. Θ_x is a phase-shift matrix of the nearest serving IRS panel and is given by $\Theta_x = \text{diag}(e^{j\theta_{x1}}, e^{j\theta_{x2}}, \dots, e^{j\theta_{xN}})$.

Interference at user's location is estimated by considering the aggregate interference due to BSs (excluding the IRS paired with serving BS and all other IRSs) and is given by

$$I_b = \sum_{y \in \Phi_b \setminus x_1} P_T \beta^2 |h_y|^2 y^{-\alpha} \quad (5.7)$$

here h_y and y are small-scale fading channel gain and the distance between user and non-serving BSs. Here, distance between user and serving BS is considered as x_1 , and distance between serving BS and associated IRS is x_2 . Further, the geometrical distance between user and BS paired with serving IRS is given by : $x_1 = \sqrt{x^2 + x_2^2 - 2xx_2 \cos(\theta)}$.

Considering the aggregate interference due to all IRS panels, excluding the interference from the serving IRS panel (as signal reflected from the serving IRS is the desired information signal), aggregate interference due to IRS panels is given by

$$I_r = \sum_{j \in \Phi_b} \sum_{i \in \Phi_r \setminus x} P_T \beta^2 |\mathbf{h}_{RU_{j,r}}^H \Theta_r \mathbf{h}_{BR_{r,i}}|^2 y_j^{-\alpha} \quad (5.8)$$

The SINR experienced by an arbitrary user served by an IRS panel located at distance x in IRS-assisted mode is given by

$$\text{SINR}_r(x) = \frac{S_{r_x}}{N_0 + I_b + I_r} \quad (5.9)$$

Coverage analysis for an arbitrary selected user that corresponds to mapping a point at random from Φ_U , served by nearest BS or IRS is performed. In this work, user's location is considered at the origin without loss of generality.

By defining the SINR threshold (γ) for reliable connectivity, coverage probability is

defined as:

$$P_c = \mathbb{P} \left[\{ \text{SINR}_{d/x}(x) > \gamma \} \right]. \quad (5.10)$$

5.3 Point process functionals

In this section, a point process Ψ is described with two important functions of Ψ , namely; sum-product functional (SPFL) and probability generating functional (PGFL) and extend it to original and reduced Palm distributions. The considered Ψ can be either a PPP, PCP or its associated offspring process.

Definition 1: Poisson Cluster Process: A PCP $\Phi_u(\lambda_P, f, \bar{m})$ is defined as (Saha et al., 2019)

$$\Phi_u = \bigcup_{z \in \Phi_P} z + \mathcal{B}^z, \quad (5.11)$$

where Φ_P indicates the parent PPP with density λ_P , \mathcal{B}^z represents the offspring point process which corresponds to center of a cluster at $z \in \Phi_P$. The offspring PP is defined as i.i.d sequence of random vectors $\{s \in \mathcal{B}^z\}$, where s follows a probability density function $f(s)$. The number of points in \mathcal{B}^z is indicated by m , where $m \sim \text{Poisson}(\bar{m})$.

Definition 2: Sum-Product Functional: SPFL of a PP, Ψ is defined as (Saha et al., 2018):

$\mathbb{E} \left[\sum_{x \in \Psi} g(x) \prod_{y \in \Psi \setminus \{x\}} v(x, y) \right]$ where $g(x) : \mathbb{R}^2 \mapsto [0, 1]$ and $v(x, y) : \mathbb{R}^2 \times \mathbb{R}^2 \mapsto [0, 1]$ are measurable.

Definition 3: Probability Generating Functional: PGFL of a PP, Ψ evaluated at $v(x, y)$ is defined as:

$$G(v(x, y)) = \mathbb{E} \left[\prod_{y \in \Psi} v(x, y) \right], \quad (5.12)$$

Further, PGFL of Ψ for cases under the condition of excluding a point of Ψ at x or under its reduced palm distribution is defined as

$$\tilde{G}(v(x, y)) = \mathbb{E}_x^! \left[\prod_{y \in \Psi} v(x, y) \right] = \mathbb{E} \left[\prod_{y \in \Psi \setminus \{x\}} v(x, y) \right]. \quad (5.13)$$

where $\mathbb{E}_x^!(\cdot)$ represent the conditional expectation over a point process.

The general definition comprising of SPFL and PGFL of a PP, Ψ discussed in this section is extended for PPP and PCP model.

Sum-Product functional: The SPFL of Ψ when it is modeled by a PPP having density λ is given by (Stoyan et al., 2013)

$$\mathbb{E} \left[\sum_{x \in \Psi} g(x) \prod_{y \in \Psi \setminus \{x\}} v(x, y) \right] = \lambda \int_{\mathbb{R}^2} g(x) \tilde{G}(v(x, y)) dx, \quad (5.14)$$

here $\tilde{G}(v(x, y))$ is PGFL of Ψ with respect to its reduced palm distribution and approximated as $\tilde{G}(v(x, y)) \approx G(v(x, y))$, by Slivnyak's theorem (Stoyan et al., 2013).

SPFL of Ψ when it is modeled by a PCP can be expressed as (Saha et al., 2018):

$$\mathbb{E} \left[\sum_{x \in \Psi} g(x) \prod_{y \in \Psi \setminus \{x\}} v(x, y) \right] = \iint_{\mathbb{R}^2 \times \mathbb{R}^2} g(x) \tilde{G}(v(x, y)|z) \Lambda(dx, dz), \quad (5.15)$$

here $\tilde{G}(v(x, y)|z) = G(v(x, y)) \tilde{G}_c(v(x, y)|z)$, denotes PGFL of Ψ when a point $x \in \Psi$ with cluster center at z is excluded from Ψ . Here, $\wedge(\cdot)$ denotes density measurement of Ψ , and \tilde{G} denotes PGFL of Ψ under its reduced palm distribution.

SPFL of Ψ when $\Psi = z + \mathcal{B}^z$, i.e., the offspring PP of a PCP centered at z can be expressed as (Stoyan et al., 2013):

$$\begin{aligned} \mathbb{E} \left[\sum_{x \in \Psi} g(x) \prod_{y \in \Psi \setminus \{x\}} v(x, y) \right] &= \int_{\mathbb{R}^2} g(x) \exp \left(-\bar{m} \int_{\mathbb{R}^2} (1 - v(x, y)) \bar{f}(y|z) dy \right) \\ &\times \left(\bar{m} \int_{\mathbb{R}^2} v(x, y) \bar{f}(y|z) dy + 1 \right) \bar{f}(x|z) dx. \end{aligned} \quad (5.16)$$

Probability Generating Functional: PGFL of Ψ when it is modeled by a PPP with density λ is given by (Haenggi, 2012)

$$G(v(x, y)) = \exp \left(-\lambda \int_{\mathbb{R}^2} (1 - v(x, y)) dy \right). \quad (5.17)$$

PGFL of Ψ when it is approximated by a PCP, given by (Haenggi, 2012)

$$G(v(x, y)) = \exp \left(- \lambda_p \int_{\mathbb{R}^2} \left(1 - \exp \left(- \bar{m} \times \left(1 - \int_{\mathbb{R}^2} v(x, y) \bar{f}(y|z) dy \right) \right) \right) dz \right). \quad (5.18)$$

PGFL of Ψ when $\Psi = z + \mathcal{B}^z$ conditioned on the removal of a point at x is approximated as

$$\tilde{G}_c(v(x, y)|z) \approx G_c(v(x, y)|z), \quad (5.19)$$

where $G_c(v(x, y))$ is PGFL of $z + \mathcal{B}^z$ which is given by

$$G_c(v(x, y)|z) = \exp \left(- \bar{m} \left(1 - \int_{\mathbb{R}^2} v(x, y) \bar{f}(y|z) dy \right) \right). \quad (5.20)$$

5.3.1 Coverage probability analysis

In this section, coverage probability is estimated for a scenario in which clustered network elements (users and/or IRS panels) are modeled as Neyman-Scott cluster process, and subsequently for a particular usecase clustered users and/or IRS panels are distributed as per the Thomas Cluster Process (TCP). According to Neyman-Scott Cluster Process hypothesis, it is presumed that a user connects to a specific BS/IRS that maximize SINR, and coverage probability can be expressed as (Saha et al., 2018):

$$P_c = \sum_{r \in \mathcal{R}} P_{cr} = \sum_{r \in \mathcal{R}} \mathbb{E} \left[\sum_{x \in \Phi_r} \prod_{j \in \mathcal{R} \setminus \{r\}} G_j(v_{r,j}(x, y)) \times \prod_{y \in \Phi_r \setminus \{x\}} v_{r,r}(x, y) \right] \quad (5.21)$$

with

$$v_{i,j}(x, y) = \frac{1}{1 + \gamma_i \frac{P_j}{P_i} \left(\frac{\|x\|}{\|y\|} \right)^\alpha}, \quad (5.22)$$

here P_{cr} denotes per-tier coverage probability, and specifically represents the joint probability of an event that the serving IRS belongs to Φ_r . Here γ_i is the SINR threshold defined for successful connection, P_j and P_i is transmit power of BS and IRS, respectively, and $\|x\|$ and $\|y\|$ are the norm distances of nearest serving and interfering BS/IRS re-

spectively.

PGFL of Φ_0 for case study-1 and 3 is $G_0(v_{r,0}(x, y)) = 1$. For case study-2 and 4, the expression of PGFL for Φ_0 is given by

$$G_0(v_{r,0}(x, y)) = \int_{\mathbb{R}^2} \frac{1}{1 + \frac{P_0 \gamma_r}{P_r} \|x\|^\alpha \|y\|^{-\alpha}} f_0(y) dy, \quad (5.23)$$

$$G_0(v_{r,0}(x, y)) = \int_{\mathbb{R}^2} G_{c_0}(v_{r,0}(x, y)|z') f_0(z') dz', \quad (5.24)$$

For a scenario, in which IRS panels are distributed as per PCP hypothesis, $r \in \mathcal{R}_C$, per-tier coverage can be expressed as

$$P_{c_r} = \iint_{\mathbb{R}^2 \times \mathbb{R}^2} G_r(v_{r,r}(x, y)) \tilde{G}_{c_r}(v_{r,r}(x, y)|z) \times \prod_{j \in \mathcal{R} \setminus \{r\}} G_j(v_{r,j}(x, y)) \Lambda_r(dx, dz), \quad r \in \mathcal{R}_C, \quad (5.25)$$

whereas, situations in which IRS panels location is approximated by PPP, $r \in \mathcal{R}_P$, per-tier coverage is expressed as

$$P_{c_r} = \lambda_r \int_{\mathbb{R}^2} \prod_{j \in \mathcal{R}} G_j(v_{r,j}(x, y)) dx, \quad r \in \mathcal{R}_P, \quad (5.26)$$

On obtaining estimate of per-tier coverage P_{c_r} , evaluation of nearest tier coverage P_{c_0} is initiated for different use cases as follows:

For the case studies-1 and 3, with user distribution complying PPP, $P_{c_0} = 0$, for $\Phi_0 = \emptyset$

For the case study-2, when $\Phi_0 = \{z_0\}$

$$P_{c_0} = \int_{\mathbb{R}^2} \prod_{j \in \mathcal{R} \setminus \{0\}} G_j(v_{0,j}(z_0, y)) f_0(z_0) dz_0 \quad (5.27)$$

Finally, for the case study-4, when $\Phi_0 = \mathcal{B}_q^{z_0}$

$$P_{c_0} = \int_{\mathbb{R}^2} \int_{\mathbb{R}^2} \exp \left(-\bar{m}_0 \int_{\mathbb{R}^2} (1 - v_{0,0}(x, y)) \bar{f}_0(y|z_0) dy \right) \left(\bar{m}_0 \int_{\mathbb{R}^2} v_{0,0}(x, y) \bar{f}_0(y|z_0) dy + 1 \right) \\ \times \prod_{j \in \mathcal{R} \setminus \{0\}} G_j(v_{0,j}(x, y)) \bar{f}_0(x|z_0) f_0(z_0) dx dz_0 \quad (5.28)$$

5.3.2 Thomas Cluster Process (TCP)

A comprehensive analysis of coverage probability when all IRS panels' location is approximated by TCP framework is given next.

Definition(TCP): A PCP Ψ is called a TCP if distribution of the offspring points in \mathcal{B}^z is Gaussian around a cluster center at origin,

$$f_r(\mathbf{s}) = f_r(s, \theta_s) = \frac{s}{\sigma_r^2} \exp \left(-\frac{s^2}{2\sigma_r^2} \right) \frac{1}{2\pi} \quad (5.29)$$

where $s > 0$ and $0 < \theta_s \leq 2\pi$

The conditional PDF of x can be written as (Afshang et al., 2016)

$$\int_0^{2\pi} \bar{f}_r(x, \theta_x|z) d\theta_x = \frac{x}{\sigma_r^2} \exp \left(-\frac{x^2 + z^2}{2\sigma_r^2} \right) I_0 \left(\frac{xz}{\sigma_r^2} \right) \quad (5.30)$$

where $x > 0, z > 0$ and $I_0(\cdot)$ is the modified Bessel function of the first kind with zero mean.

PGFL of TCP, Φ_j evaluated at $v_{r,j}(x, y)$ is given by:

$$G_j(v_{r,j}(x, y)) = \exp \left(-2\pi \lambda_{p_j} \int_0^\infty (1 - \exp(1 - \bar{m}_j \int_0^\infty (1 - v_{r,j}(x, y)) \Omega_j(y, z) dy)) z dz \right) \quad (5.31)$$

PGFL of offspring point process of TCP, evaluated at $v_{r,j}(x, y)$ is given by:

$$G_{c_j}(v_{r,j}(x, y)|z) = \exp \left(-\bar{m}_j \int_0^\infty (1 - v_{r,j}(x, y)) \Omega_j(y, z) dy \right) \quad (5.32)$$

PGFL of Φ_0 is computed for case study-1 and 3, which attains zero value, i.e., $G_0(v_{r,0}(x, y)) = 0$.

$$G_0(v_{r,0}(x, y)) = \int_0^\infty \frac{1}{1 + \frac{P_0 \gamma_r}{P_r} \left(\frac{x}{y}\right)^{-\alpha}} \frac{y}{\sigma_0^2} \exp\left(-\frac{y^2}{2\sigma_0^2}\right) dy. \quad (5.33)$$

$$G_0(v_{r,0}(x, y)) = \int_0^\infty G_{c_0}(v_{r,0}(x, y)|z_0) \frac{z_0}{\sigma_0^2} \exp\left(-\frac{z_0^2}{2\sigma_0^2}\right) dz_0. \quad (5.34)$$

Equations (5.33) and (5.34) yields PGFL estimate of Φ_0 for case study-2 and 4, by substituting equation (5.29) with parametric setting $r = 0$ in equation (5.23) and equation (5.24), respectively.

Per-tier coverage probability for $r \in \mathcal{R}_C$, when all IRS panels are modeled as TCPs can be expressed as:

$$P_{c_r} = 2\pi \lambda_{p_k} \bar{m}_k \int_0^\infty \int_0^\infty \prod_{j \in \mathcal{R}} G_j(v_{r,j}(x, y)) G_k(v_{r,r}(x, y)) \times G_{c_r}(v_{r,r}(x, y|z)) \Omega_r(x, z) dx dz. \quad (5.35)$$

Using equation (5.35), per-tier coverage probability for nearest serving IRS P_{c_0} is computed for all the case studies, assuming all IRS panels are modeled as TCPs. $P_{c_0} = 0$, for the case study-1 and 3, wherein users are uniformly distributed. For case study-2 and 4, P_{c_0} can be expressed as:

$$P_{c_0} = \int_0^\infty \prod_{j \in \mathcal{R} \setminus \{0\}} G_j(v_{0,j}(z_0, y)) \bar{f}_0(z_0) dz_0 \quad (5.36)$$

$$P_{c_0} = \int_0^\infty \int_0^\infty \prod_{j \in \mathcal{R} \setminus \{0\}} G_j(v_{0,j}(x, y)) \exp(-\bar{m}_r \int_0^\infty (1 - v_{0,0}(x, y)) \Omega_0(y, z_0) dy) \times \left(\bar{m}_0 \int_0^\infty v_{0,0}(x, y) \Omega_0(y, z_0) dy + 1 \right) \Omega_0(x, z_0) dx \times \frac{z_0}{\sigma_0^2} \exp\left(-\frac{z_0^2}{2\sigma_0^2}\right) dz_0 \quad (5.37)$$

Pseudocode to estimate SINR for Mode-1 (Direct link) and for Mode-2 (IRS-assisted link) is presented in Algorithm-2 and Algorithm-3, respectively.

Algorithm 2: Algorithm for computing SINR for Mode-1 users (Direct link)

Input: Direct channel coefficient h_{BU} , with BS-user distance, transmit power and path loss exponent

Initialize: BS Φ_b , IRS Φ_r and user Φ_u .

1. Choose an arbitrary user reference location at origin
2. Identify nearest serving BS for user with distance estimate x and other BSs with distance estimate y_j
3. Compute the signal power received at user's location from the serving BS using equation (5.2)
4. Compute the aggregate interference from all BSs, excluding from nearest serving BS using equation (5.3)
5. Compute the aggregate interference from all IRSs using equation (5.4)
6. Compute the SINR experienced by user via direct link using equation (5.5)

Output: $SINR_d(x)$

Algorithm 3: Algorithm for computing SINR for Mode-2 users (IRS-assisted link)

Input: Channel coefficients \mathbf{h}_{BR} , \mathbf{h}_{RU} , IRS-user distance, transmit power and path loss exponent

Initialize: BS Φ_b , IRS Φ_r and user Φ_u .

1. Choose an arbitrary user reference location at origin
2. Identify nearest serving IRS for user with distance estimate x and other IRSs with distance estimate y_j
3. Compute the signal power received at user's location from the serving IRS using equation (5.6)
4. Compute the aggregate interference from all BSs, excluding the BS in close proximity with serving IRS using equation (5.7)
5. Compute the aggregate interference from all IRS panels, excluding the nearest serving IRS using equation (5.8)
6. Compute the SINR experienced by user via IRS-assisted link using equation (5.9)

Output: $SINR_r(x)$

5.4 Results and discussion

Coverage probability estimate for four use cases based on the stochastic modeling framework in which location of IRS panels and users is approximated by mixture of

PPP and PCP is performed and analysed. Advantage of IRS panels deployment is validated by comparing coverage probability outcome of direct link with IRS-assisted link. The proposed analytical framework is validated using Monte Carlo simulations with 10^4 iterations. For all these scenarios, numerical results demonstrate the precision of approximation accuracy attained.

The height of BSs, IRSs, and users is considered as 30 m, 10 m, and 1.5 m, respectively. BSs, IRSs and users point processes are generated for a circular shaped disc of coverage area 1 km^2 . A wireless terrain considered has phenomenal fading due to substantial number of obstacles, and it contributes to large PLE ($\alpha = 4$), a typical value for outdoor scenario (Lee et al., 2013). PLE of the IRS-aided links can be considered closer to free-space path loss, by deploying IRSs at appropriate close by locations. In this work, we consider PLEs of the BS-IRS link and the IRS-user link as 2 and 3, respectively (Yang et al., 2021b).

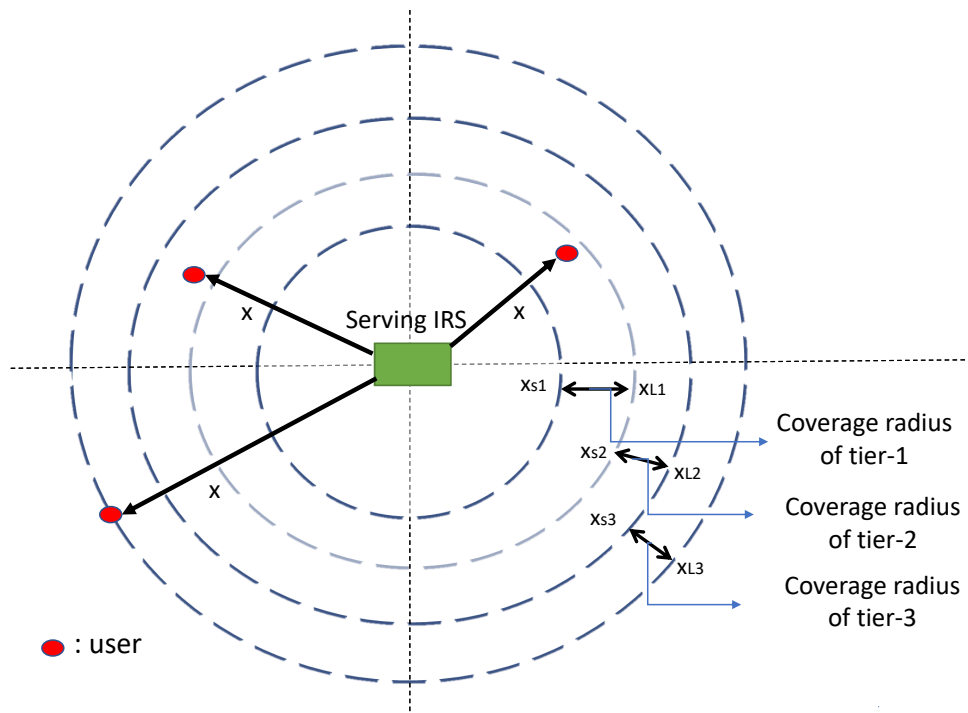


Figure 5.4: A pictorial representation of varying cluster size (σ) with respect to a serving IRS panel

For an arbitrary user served by a BS in a VLOS mode via IRS panel, notion of cluster size (σ) is depicted in Figure 5.4. Here, σ represents the standard deviation of Euclidean

distance between a user located at arbitrary location and a serving IRS. Depending upon the location of a user, as an illustration, segment of the wireless terrain is shown with concentric circles in Figure 5.4 having three different tier of coverage radius, while keeping serving IRS at a centre stage. A User may be situated in any one of these coverage zones at an arbitrary time. In the result section, three different coverage radii are considered maintaining σ as 10 m, 20 m and 30m. These coverage radii are interpreted as cluster size.

As the cluster size increases corresponding to position of the user, it leads to higher Euclidean distance between a serving IRS and a user and as a result likelihood of the user association with that particular serving IRS diminishes. As a consequence of this, received signal strength as perceived by an arbitrary user is compromised.

5.4.1 Impact of varying cluster size on Coverage probability

We consider different case studies based on the stochastic modeling framework, in which IRS panels and users location is governed by PPP and PCP, and coverage probability analysis is performed. Here, case study-1 considers modeling IRSs as well as users using PPP and is treated as the baseline approach to compare coverage probability outcomes with that obtained for other case studies. As urban and semi-urban wireless terrains are characterized with different user density and distribution statistics, in the reported case studies, coverage probability estimate as a performance measure is analyzed with varying cluster size.

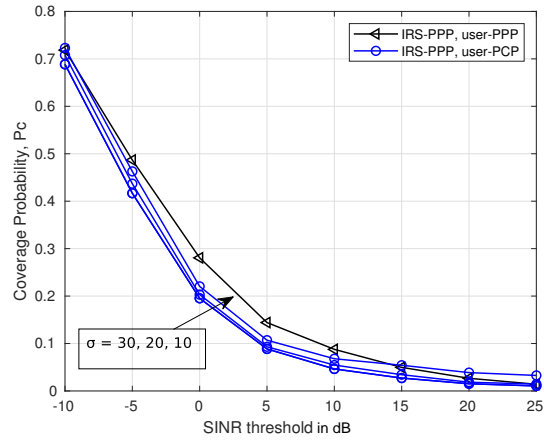
In Figure 5.5a, coverage probability is sketched for case study-2 (IRSs-PPP, users-PCP), with different cluster sizes of Φ_u and is compared with baseline case. It is observed that irrespective of cluster size, coverage probability characteristics obtained in case study-2 is inferior to that secured in baseline case. However, on decreasing the cluster size coverage probability estimate approximates a trend obtained in baseline case. Rationale behind the compromised performance is a significant proportion of users who belong to PCP hypothesis driven geographical positions experience poor coverage from a topological arrangement in which BSs and IRS panels are distributed as per the PPP.

Analogy of case study-2 can be established with a scenario in which a few localized geographical pockets that usually observe mild fading may experience relatively high degree of network congestion owing to high density of users especially during short epochs in peak hours.

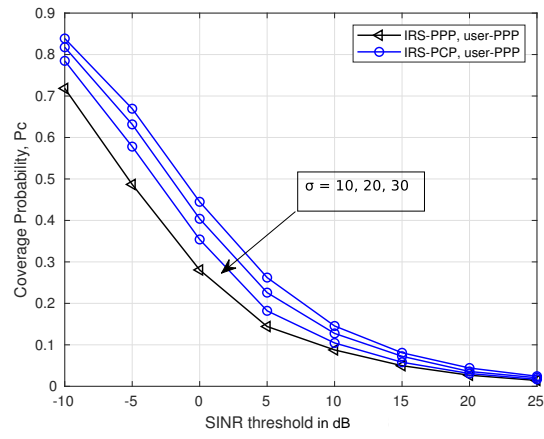
Coverage probability characteristics for case study-3 (IRSs-PCP, users-PPP) with parametric variation in cluster size are shown in Figure 5.5b. These characteristics manifest a contrasting trend as compared to coverage probability obtained in case study-2. It can be observed that coverage probability estimate converges with characteristics that obtained in baseline case with increase in cluster size. These observations lead to inference that in a terrain that characterize with randomly distributed users, degree of reliable coverage can be enhanced when IRS panels deployment follows distribution as per the PCP hypothesis. Further, another interesting reasoning in the support of observed pattern is an underlying mechanism in which formation of clusters by virtue of closely spaced IRS panels enforces better coverage for an arbitrary user. In any wireless terrain this resembles with a scenario in which dense deployment of IRS panels facilitates relatively better coverage in certain geographical locations that experience severe fading owing to surrounding spatial attributes during the off-peak/week hours.

For a scenario described in case study-4 (IRSs-PCP, users-PCP), coverage probability characteristics are shown in Figure 5.5c. An interesting observation manifest that there is a remarkable improvement in coverage probability for a broad span (entire dynamic range) of SINR threshold. Even for the demanding value of SINR threshold (5 to 15 dB) and larger cluster size ($\sigma=30$), coverage probability attained in this case maintains a substantiate margin of 0.2, 0.15 and 0.2 with respect to, case study-2 having $\sigma=30$, case study-3 for $\sigma=30$ and the case study-1 (baseline), respectively. The genesis for an enhanced coverage probability is proximity of dense IRS panels clusters to geographical segments of a wireless terrain characterized with relatively high density of closely spaced users.

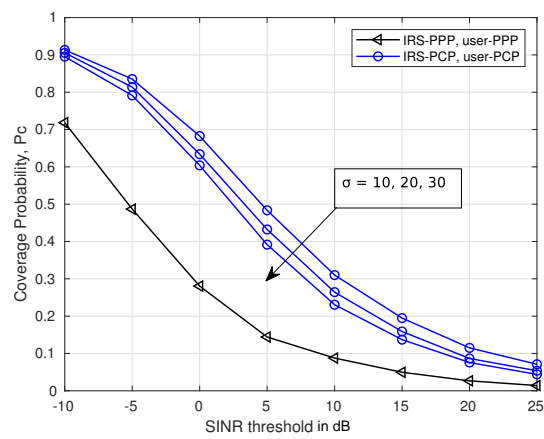
Case study-4 seems approximate the following scenarios: (i) a busy traffic junction in urban environment during peak hours, and (ii) any short duration events that observe



(a)



(b)



(c)

Figure 5.5: Coverage probability with cluster size (σ) regulation (a) IRS-PPP, user-PCP (b) IRS-PCP, user-PPP and (c) IRS-PCP, user-PCP

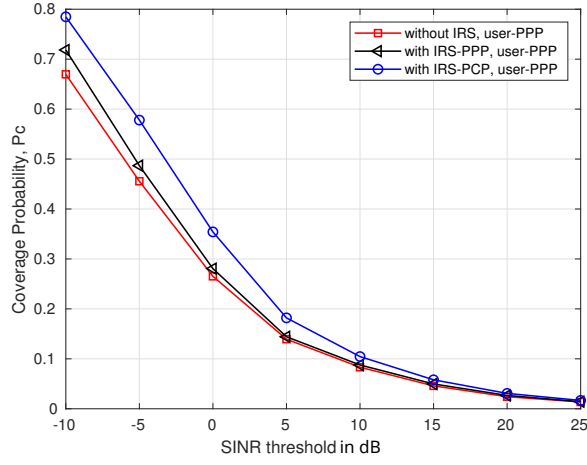
high density of user especially during a concert and sport activities etc.

In summary, these observations infer that depending upon different spatial and temporal dynamics of a wireless terrain, for a better coverage perspective, IRS panels deployment can be exercised based on appropriate process, namely PPP and PCP. The considered approach of modeling users as PPP and PCP appears quite normal as these models resemble the different users centric scenarios with reasonable good degree of approximation. Further, looking into the diversified spatio-temporal characteristics of a particular wireless terrain, no single stochastic approach suffices and usage of a specific model i.e., PPP or PCP should be exercised in context of users and wireless terrain specific spatial attributes.

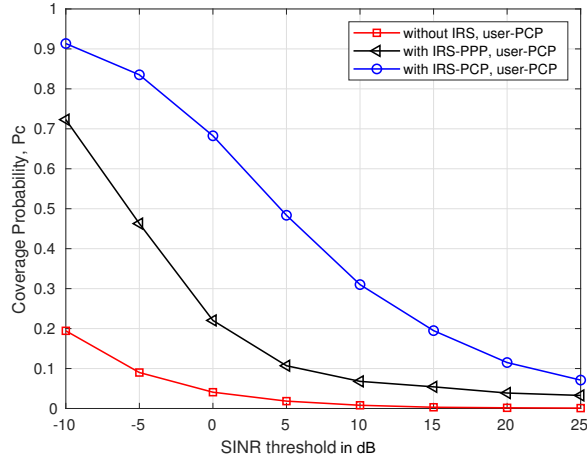
5.4.2 Impact of IRS-assistance on Coverage probability

To understand the impact of multiple IRS panels presence on overall signal propagation process in a given wireless terrain and subsequent leverage in terms of mitigating fading, estimate of coverage probability is presented in Figure 5.6. Broadly, characteristics shown in Figure 5.6 correspond to LOS mode (direct-link) and the VLOS mode (IRS-assisted link). Presence of multiple IRS panels demonstrates a marginal improvement or a significant enhancement in coverage probability depending upon distribution statistics of users and deployment strategy of IRS panels based on either PCP or PPP model. Although coverage probability characteristics shown in Figure 5.6a and Figure 5.6b validate that PCP driven deployment of IRS panels is always advantageous irrespective of spatio-temporal behavior of wireless terrain and distribution of users within it.

In quite a large number of scenarios users are uniformly distributed across the wireless terrain, in such circumstances users location can be approximated by PPP. For this particular kind of users positioning, coverage probability performance is shown in Figure 5.6a. Characteristics shown in Figure 5.6a reveal a significant enhancement in coverage probability on using IRS panels placement strategy based on PCP model. In Figure 5.6a and Figure 5.6b, all the coverage probability characteristics are obtained for a fixed



(a)



(b)

Figure 5.6: Coverage probability with cluster size (σ) regulation (a) Sparsely distributed users-PPP and (b) closely spaced users-PCP

value of cluster size, here it is treated as $\sigma = 10$.

In contrary to scenarios in which users are sparsely located, quite often network service providers are supposed to ensure reliable connectivity and coverage as these terrain are characterized with small or moderate size geographical segments having high density of users during short sporadic time intervals. In Figure 5.6b, coverage probability is presented for the following three use cases (i) a wireless terrain without IRS panels, (ii) a wireless terrain having IRS panels distribution as per PPP and (iii) a wireless terrain equipped with IRS panels based on inference drawn from PCP. In all these use cases,

owing to demographic attributes of users distribution, users location is modeled as per the PCP hypothesis. Here, compared to a wireless terrain without IRS panel, terrain which have provision for IRS panels and their location is inferred from either PPP or PCP model, yield a quite significant improvement in coverage probability. Thus, IRS-assisted links outperform line of sight (direct link) mode. Furthermore, the characteristics shown in Figure 5.6b can be bisected into the following two regions: (i) Region-1: lower value of SINR threshold ranging $-10 \text{ dB} \leq \gamma \leq 10 \text{ dB}$ and (ii) Region-2: higher value of SINR threshold ranging $10 \text{ dB} < \gamma \leq 25 \text{ dB}$. During Region-1; the performance of a wireless terrain equipped with multiple IRS panels is phenomenal as compared to a terrain without IRS panels. Whereas, in Region-2 the performance is slightly compromised owing to higher SINR threshold.

5.5 Summary

In this chapter, coverage probability performance of a direct link (in the absence of IRSs) and a VLOS (for a terrain equipped with IRSs) link is estimated and analysed for an urban wireless terrain. Looking into diversified spatial characteristics in different geographical segments of a wireless terrain during distinct temporal attributes, a single stochastic model is not able to capture the distribution of users and inference about the IRS panels deployment with reasonable approximation. To accommodate terrain geometry driven spatial characteristics and the user's distribution as well as temporal aspects-based users' density for an urban terrain in a holistic manner, stochastic models based on PPP and PCP are proposed to approximate the users spatial distribution and IRS panels deployment in realistic scenarios. Euclidean distance of a serving IRS with a user located at an arbitrary location varies randomly, a statistical measure in terms of standard deviation of the Euclidean distance (σ) is considered as cluster size. Coverage probability is estimated for four different case studies, in which users and IRS panels are distributed as per the PPP and PCP hypothesis and cluster size is treated as a parameter to observe the performance regulation. Broadly, obtained results indicate that the urban terrain equipped with IRS panels yields a significant enhancement in

coverage probability in all these case studies. Further, an important inference can be drawn that for segments of a wireless terrain which are characterized with high density driven cluster topology of users, provisioning of IRS panels as per the PCP hypothesis always yields quite a significant improvement in coverage probability over a broad span of SINR threshold.

CHAPTER 6

CONCLUSION AND FUTURE WORK

In last few years, wireless industry and academia has witnessed a significant interest in the form of several research studies exploring performance enhancement for IRS assisted wireless communication. Comprehensively, the overall work confined to IRS assistance can be fragmented at different levels of implementation. The first set of works can be confined to channel modeling aspect of IRS-assisted system which is different from conventional wireless network. Furthermore, the indepth investigation emphasizes performance evaluation of IRS-assisted networks in terms of various performance metrics. However, validating the impact of IRSs on communication performance is still an open problem. In this thesis, an attempt is made to model the channel behaviour of IRS-assisted wireless terrain, considering the inevitable mobility aspect of receiver. Majority of the reported channel modeling work is limited to stationary receiver. Subsequently, in this thesis, performance measures of IRS-assisted wireless terrain are estimated and the enhanced performance is validated in terms of key measures such as Achievable rate, Outage probability, Ergodic capacity and Coverage probability analysis.

6.1 Conclusion

In this thesis, channel modeling for IRS-assisted UMi wireless terrain is carried out, while prioritizing the time-varying (TV) channel between IRS and user due to mobility of receiver. Further, a time-invariant (TI) channel model between a BS and IRS panels is characterized and the impact of single as well as multiple IRS panels are considered for Achievable rate analysis of wireless terrain that satisfy for LOS and NLOS norms. During simulation, two distinct wireless terrain namely UMi-open square and UMi-street canyon are considered. Subsequently, Achievable rate analysis is extended with parametric variations in transmitted power, number of EREs, separation distance between

EREs, and receiver speed. Further, outage probability analysis for an arbitrary user at three different fading zones, namely; lightly fading zone, moderately fading zone and severely fading zone is performed. In addition to it, spatio and temporal characteristics driven different vehicular traffic patterns, namely; peak hours, off-peak hours and wee hours are considered. Furthermore, coverage probability analysis of IRS-assisted system modeled using stochastic approach is considered. Here, in order to accommodate diversified spatial and temporal characteristics of terrain, usage of Poisson Point Process (PPP) and Poisson Cluster Process (PCP) is proposed to model the users' distribution and IRS panels deployment. Coverage probability is estimated to validate the proposed stochastic models, while regulating the cluster size. In addition to these aspects, the efficacy of IRSs equipped wireless terrain is demonstrated in terms of enhanced coverage probability for the broad ranging SINR threshold.

6.2 Future work

Research work carried out in this thesis explore leverage of deploying single/multiple IRS panel(s) in outdoor wireless terrain observing presence of single user. Based on inferences drawn from use cases involving single user, work can be extended to consider multiple users in wireless terrain and subsequently estimating different performance metrics for multi-user scenarios. Modeling aspect of multi-user scenarios involves complex mathematical framework for beamforming optimization and the precise channel estimate. As users of multiple IRS panels lead to an enhanced state of performance measures, it triggers the deployment of IRS panels at appropriate locations can be addressed as resource allocation framework. Further, more comprehensive channel models suitable for vehicle-to-everything (V2X) scenarios in wireless terrain equipped with IRS panels may lead to important observations for the service provider. For a wide variety of practical applications supported by V2X scenarios, the performance measures namely, latency and connection reliability are of primary consideration.

LIST OF PUBLICATION BASED ON THESIS

Peer reviewed International Journals

1. T Dhruvakumar, and Ashvini Chaturvedi. "Intelligent Reflecting Surface assisted millimeter wave communication for achievable rate and coverage enhancement." Vehicular Communications, Volume 33, January 2022, Article number 100431, pp 1-13.

Papers under review

1. T Dhruvakumar, Ashvini Chaturvedi, "Ergodic Capacity and Outage Probability Analysis for Multiple Intelligent Reflecting Surface Assisted Wireless Networks", Vehicular Communication.
2. T Dhruvakumar, Ashvini Chaturvedi, "Stochastic modeling under the influence of varying fading for IRS assisted downlink coverage analysis", IEEE Transactions on Vehicular Technology.

CURRICULUM VITAE

Name Dhruvakumar T

Address House no: 904,
11th cross,
Gangothrinagar,
Tumkur-572103
Karnataka, India

E-mail dhruvakumar.t@gmail.com

Qualification • M.Tech | Digital Electronics and Communication Engineering |
AMC Engineering College, Bangalore, Karnataka

• B.E | Electronics and Communication Engineering |
SSIT, Tumkur, Karnataka

Experience • Assistant Professor |
Siddaganga Institute of Technology, Tumkur

REFERENCES

- (2015), “A deliverable by the NGMN alliance: NGMN 5G white paper.” URL https://www.ngmn.org/wp-content/uploads/NGMN_5G_White_Paper_V1_0.pdf.
- Adnan, Noor Hidayah Muhamad, Islam Md Rafiqul, and AHM Zahirul Alam (2017), “Effects of inter element spacing on large antenna array characteristics.” *2017 IEEE 4th International Conference on Smart Instrumentation, Measurement and Application (ICSIMA)*, 1–5, IEEE.
- Afshang, Mehrnaz and Harpreet S. Dhillon (2018), “Poisson cluster process based analysis of hetnets with correlated user and base station locations.” *IEEE Transactions on Wireless Communications*, 17, 2417–2431.
- Afshang, Mehrnaz, Harpreet S Dhillon, and Peter Han Joo Chong (2016), “Modeling and performance analysis of clustered device-to-device networks.” *IEEE Transactions on Wireless Communications*, 15, 4957–4972.
- Alodadi, Khaled, Ali H Al-Bayatti, and Nasser Alalwan (2017), “Cooperative volunteer protocol to detect non-line of sight nodes in vehicular ad hoc networks.” *Vehicular Communication*, 9, 72–82.
- Alonzo, Mario and Stefano Buzzi (2017), “Cell-free and user-centric massive MIMO at millimeter wave frequencies.” *2017 IEEE 28th Annual International Symposium on Personal, Indoor, and Mobile Radio Communications (PIMRC)*, 1–5.
- ariadne (2020), “Artificial intelligence aided d-band network for 5G long term evolution.” Available:<https://www.ict-ariadne.eu/>.
- Badarneh, Osamah S., Sami Muhaidat, and Daniel B. da Costa (2020), “The α - η - κ -f composite fading distribution.” *IEEE Wireless Communications Letters*, 9, 2182–2186.

Bansal, Ankur, Keshav Singh, Bruno Clerckx, Chih-Peng Li, and Mohamed-Slim Alouini (2021), “Rate-splitting multiple access for intelligent reflecting surface aided multi-user communications.” *IEEE Transactions on Vehicular Technology*, 70, 9217–9229.

Bas, Celalettin Umit, Rui Wang, Seun Sangodoyin, Dimitris Psychoudakis, Thomas Henige, Robert Monroe, Jeongho Park, Charlie Jianzhong Zhang, and Andreas F. Molisch (2019), “Real-time millimeter-wave MIMO channel sounder for dynamic directional measurements.” *IEEE Transactions on Vehicular Technology*, 68, 8775–8789.

Basar, Ertugrul (2019), “Reconfigurable intelligent surfaces for doppler effect and multipath fading mitigation.” *arXiv preprint arXiv:1912.04080*.

Basar, Ertugrul (2021), “Reconfigurable intelligent surfaces for doppler effect and multipath fading mitigation.” *Frontiers in Communications and Networks*, 2, URL <http://dx.doi.org/10.3389/frcmn.2021.672857>.

Basar, Ertugrul, Marco Di Renzo, Julien De Rosny, Merouane Debbah, Mohamed-Slim Alouini, and Rui Zhang (2019), “Wireless communications through reconfigurable intelligent surfaces.” *IEEE Access*, 7, 116753–116773.

Belmekki, Baha Eddine Youcef, Abdelkrim Hamza, and Benoit Escrig (2020), “On the performance of 5G non-orthogonal multiple access for vehicular communications at road intersections.” *Vehicular Communication*, 22, 1–12.

Björnson, Emil (2021), “Optimizing a binary intelligent reflecting surface for OFDM communications under mutual coupling.” *arXiv preprint arXiv:2106.04280*.

Buzzi, Stefano and Carmen D’Andrea (2016), “On clustered statistical MIMO millimeter wave channel simulation.” *arXiv preprint arXiv:1604.00648*.

Charishma, Mavilla, Athira Subhash, Shashank Shekhar, and Sheetal Kalyani (2021), “Outage probability expressions for an IRS-assisted system with and without source-destination link for the case of quantized phase shifts in $\kappa - \mu$ fading.” *IEEE Transactions on Communications*, 70, 101–117.

Chun, Young Jin, Simon L Cotton, Harpreet S Dhillon, F Javier Lopez-Martinez, Jose F Paris, and Seong Ki Yoo (2017), “A comprehensive analysis of 5G heterogeneous cellular systems operating over $\kappa - \mu$ shadowed fading channels.” *IEEE Transactions on Wireless Communications*, 16, 6995–7010.

cordis (2020), “Harnessing multipath propagation in wireless networks: A meta-surface transformation of wireless networks into smart reconfigurable radio environments.” Available: <https://cordis.europa.eu/project/id/891030>.

Cui, T J, M Q Qi, X Wan, J Zhao, and Q Cheng (2014), “Coding metamaterials, digital metamaterials and programmable metamaterials.” *Light, Sci. Appl*, 3, 2843–2860.

da Silva, Higo Thaian Pereira, Marcelo Sampaio de Alencar, and Karcus Day Rosario Assis (2019), “Path loss and delay spread characterization in a 26 GHz mmwave channel using the ray tracing method.” *2019 SBMO/IEEE MTT-S International Microwave and Optoelectronics Conference (IMOC)*, 1–3.

Dai, Linglong, Bichai Wang, Min Wang, Xue Yang, Jingbo Tan, Shuangkaisheng Bi, Shenheng Xu, Fan Yang, Zhi Chen, Marco Di Renzo, et al. (2020), “Reconfigurable intelligent surface-based wireless communications: Antenna design, prototyping, and experimental results.” *IEEE Access*, 8, 45913–45923.

Dajer, Miguel, Zhengxiang Ma, Leonard Piazzzi, Narayan Prasad, Xiao-Feng Qi, Baoling Sheen, Jin Yang, and Guosen Yue (2021), “Reconfigurable intelligent surface: Design the channel – a new opportunity for future wireless networks.” *Digital Communications and Networks*, URL <https://www.sciencedirect.com/science/article/pii/S2352864821000912>.

Dhillon, Harpreet S. and Jeffrey G. Andrews (2014), “Downlink rate distribution in heterogeneous cellular networks under generalized cell selection.” *IEEE Wireless Communications Letters*, 3, 42–45.

Dhruvakumar, T and Ashvini Chaturvedi (2022), “Intelligent reflecting surface assisted millimeter wave communication for achievable rate and coverage enhancement.” *vehicular Communications*, 33, 100431.

Di Renzo, Marco, Konstantinos Ntontin, Jian Song, Fadil H. Danufane, Xuewen Qian, Fotis Lazarakis, Julien De Rosny, Dinh-Thuy Phan-Huy, Osvaldo Simeone, Rui Zhang, Meroaune Debbah, Geoffroy Lerosey, Mathias Fink, Sergei Tretyakov, and Shlomo Shamai (2020), “Reconfigurable intelligent surfaces vs. relaying: Differences, similarities, and performance comparison.” *IEEE Open Journal of the Communications Society*, 1, 798–807.

Di Renzo, Marco and Jian Song (2019), “Reflection probability in wireless networks with metasurface-coated environmental objects: An approach based on random spatial processes.” *EURASIP Journal on Wireless Communications and Networking*, 2019, 1–15.

Docomo (2016), “White paper on ”5G channel model for bands up to 100 GHz”. Technical report, 2016.[online].” Available: <http://www.5gworkshops.com/5GCM.html>.

DoCoMo, NTT (2018), “Metawave announce successful demonstration of 28 ghz-band 5G using world’s first meta-structure technology.”

Docomo, NTT (2020), “DOCOMO conducts world’s first successful trial of transparent dynamic metasurface.”

Du, Hongyang, Jiayi Zhang, Julian Cheng, and Bo Ai (2021), “Millimeter wave communications with reconfigurable intelligent surfaces: Performance analysis and optimization.” *IEEE Transactions on Communications*, 69, 2752–2768.

El Bouanani, Faissal, Sami Muhaidat, Paschalis C Sofotasios, Octavia A Dobre, and Osamah S Badarneh (2020), “Performance analysis of intelligent reflecting surface aided wireless networks with wireless power transfer.” *IEEE Communications Letters*, 25, 793–797.

Elbir, Ahmet M. and Kumar Vijay Mishra (2020), “A survey of deep learning architectures for intelligent reflecting surfaces.” *ArXiv*, abs/2009.02540.

ElMossallamy, Mohamed A., Hongliang Zhang, Lingyang Song, Karim G. Seddik, Zhu Han, and Geoffrey Ye Li (2020), “Reconfigurable intelligent surfaces for wireless com-

munications: Principles, challenges, and opportunities.” *IEEE Transactions on Cognitive Communications and Networking*, 6, 990–1002.

Ferreira, Ricardo Coelho, Michelle SP Facina, Felipe AP De Figueiredo, Gustavo Fraidenraich, and Eduardo Rodrigues De Lima (2020), “Bit error probability for large intelligent surfaces under double-nakagami fading channels.” *IEEE Open Journal of the Communications Society*, 1, 750–759.

Feteiha, Mohamed and Hossam S Hassanein (2016), “Decode-and-forward cooperative vehicular relaying for LTE-A MIMO-downlink.” *Vehicular Communication*, 3, 12–20.

Gradshteyn, Izrail Solomonovich and Iosif Moiseevich Ryzhik (2007), *Table of integrals, series, and products*. Academic press.

greenerwave (2020), “A technological platform to simplify all em infrastructures: Replacing hardware complexity by algorithms.” Available:<https://greenerwave.com/our-technology/>.

Guo, Chang, Ying Cui, Feng Yang, and Lianghai Ding (2020), “Outage probability analysis and minimization in intelligent reflecting surface-assisted MISO systems.” *IEEE Communications Letters*, 24, 1563–1567.

Haenggi, Martin (2012), *Stochastic geometry for wireless networks*. Cambridge University Press.

Haneda, Katsuyuki, Jianhua Zhang, Lei Tan, Guangyi Liu, Yi Zheng, Henrik Asplund, Jian Li, Yi Wang, David Steer, Clara Li, Tommaso Balercia, Sunguk Lee, YoungSuk Kim, Amitava Ghosh, Timothy Thomas, Takehiro Nakamura, Yuichi Kakishima, Tetsuro Imai, Haralabos Papadopoulos, Theodore S. Rappaport, George R. MacCartney, Mathew K. Samimi, Shu Sun, Ozge Koymen, Sooyoung Hur, Jeongho Park, Charlie Zhang, Evangelos Mellios, Andreas F. Molisch, Saeed S. Ghassamzadeh, and Arun Ghosh (2016), “5G 3GPP-like channel models for outdoor urban microcellular and macrocellular environments.” *2016 IEEE 83rd Vehicular Technology Conference (VTC Spring)*, 1–7.

Hassouna, Saber (2022), “A survey on intelligent reflecting surfaces: Wireless communication perspective.” Available: <https://doi.org/10.36227/techrxiv.19181693.v1>.

He, Jiguang, Henk Wymeersch, Tachporn Sanguanpuak, Olli Silvén, and Markku Juntti (2020), “Adaptive beamforming design for mmwave RIS-aided joint localization and communication.” *2020 IEEE Wireless Communications and Networking Conference Workshops (WCNCW)*, 1–6, IEEE.

He, Muxin, Wei Xu, Hong Shen, Guo Xie, Chunming Zhao, and Marco Di Renzo (2021), “Cooperative multi-RIS communications for wideband mmwave MISO-OFDM systems.” *IEEE Wireless Communications Letters*, 10, 2360–2364.

Heath, Robert W., Marios Kountouris, and Tianyang Bai (2013), “Modeling heterogeneous network interference using poisson point processes.” *IEEE Transactions on Signal Processing*, 61, 4114–4126.

Huang, C, A Zappone, G C Alexandropoulos, M Debbah, and C Yuen (2019), “Reconfigurable intelligent surfaces for energy efficiency in wireless communication.” *IEEE Transactions on wireless Communications*, 18, 4157–4170.

Hur, Sooyoung, Hyunkyu Yu, Jeongho Park, Wonil Roh, Celalettin U. Bas, Rui Wang, and Andreas F. Molisch (2018), “Feasibility of mobility for millimeter-wave systems based on channel measurements.” *IEEE Communications Magazine*, 56, 56–63.

Jo, Han-Shin, Young Jin Sang, Ping Xia, and Jeffrey G. Andrews (2012), “Heterogeneous cellular networks with flexible cell association: A comprehensive downlink SINR analysis.” *IEEE Transactions on Wireless Communications*, 11, 3484–3495.

Jung, Minchae, Walid Saad, Mérouane Debbah, and Choong Seon Hong (2020a), “Asymptotic optimality of reconfigurable intelligent surfaces: Passive beamforming and achievable rate.” *ICC 2020-2020 IEEE International Conference on Communications (ICC)*, 1–6, IEEE.

Jung, Minchae, Walid Saad, Youngrok Jang, Gyuyeol Kong, and Sooyong Choi (2020b), “Performance analysis of large intelligent surfaces LISs: Asymptotic data rate

and channel hardening effects.” *IEEE Transactions on Wireless Communications*, 19, 2052–2065.

Khaleel, Aymen and Ertugrul Basar (2020), “Reconfigurable intelligent surface-empowered MIMO systems.” *IEEE Systems Journal*, 15, 4358–4366.

Kodide, Alekhya, Thi My Chinh Chu, and Hans-Jurgen Zepernick (2016), “Outage probability of multiple relay networks over κ - μ shadowed fading.” *2016 10th International Conference on Signal Processing and Communication Systems (ICSPCS)*, 1–7, IEEE.

Kumar, Sikandar and Sonali Chouhan (2015), “Outage probability analysis of cognitive decode-and-forward relay networks over κ - μ shadowed channels.” *2015 21st Asia-Pacific Conference on Communications (APCC)*, 433–437, IEEE.

Lee, Chia-Han, Cheng-Yu Shih, and Yu-Sheng Chen (2013), “Stochastic geometry based models for modeling cellular networks in urban areas.” *Wireless networks*, 19, 1063–1072.

Lopez-Martinez, F. Javier, Jose F. Paris, and Juan M. Romero-Jerez (2017), “The κ - μ shadowed fading model with integer fading parameters.” *IEEE Transactions on Vehicular Technology*, 66, 7653–7662.

Lu, Xiao, Mohammad Salehi, Martin Haenggi, Ekram Hossain, and Hai Jiang (2021), “Stochastic geometry analysis of spatial-temporal performance in wireless networks: A tutorial.” *IEEE Communications Surveys & Tutorials*.

Lyu, Jiangbin and Rui Zhang (2020), “Spatial throughput characterization for intelligent reflecting surface aided multiuser system.” *IEEE Wireless Communications Letters*, 9, 834–838.

Mankar, Praful D., Goutam Das, and S. S. Pathak (2016), “Modeling and coverage analysis of BS-centric clustered users in a random wireless network.” *IEEE Wireless Communications Letters*, 5, 208–211.

Nguyen, Ba Cao, Tran Manh Haong, and Le The Dung (2019), “Performance analysis of vehicle-to-vehicle communication with full-duplex amplify-and-forward relay over double-rayleigh fading channels.” *Vehicular Communication*, 19, 1–9.

Özdoğan, Özgecan, Emil Björnson, and Erik G Larsson (2019), “Intelligent reflecting surfaces: Physics, propagation, and pathloss modeling.” *IEEE Wireless Communications Letters*, 9, 581–585.

Özdoğan, Özgecan, Emil Björnson, and Erik G Larsson (2020), “Using intelligent reflecting surfaces for rank improvement in MIMO communications.” *ICASSP 2020-2020 IEEE International Conference on Acoustics, Speech and Signal Processing (ICASSP)*, 9160–9164, IEEE.

Pan, C., H. Ren, K. Wang, W. Xu, M. ElKashlan, A. Nallanathan, and L. Hanzo (2020), “Multicell MIMO communications relying on intelligent reflecting surfaces.” *IEEE Transactions on Wireless Communications*, 19, 5218–5233.

Pan, Cunhua, Hong Ren, Kezhi Wang, Jonas Florentin Kolb, Maged ElKashlan, Ming Chen, Marco Di Renzo, Yang Hao, Jiangzhou Wang, A. Lee Swindlehurst, Xiaohu You, and Lajos Hanzo (2021), “Reconfigurable intelligent surfaces for 6G systems: Principles, applications, and research directions.” *IEEE Communications Magazine*, 59, 14–20.

Papazafeiropoulos, Anastasios, Cunhua Pan, Ahmet Elbir, Pandelis Kourtessis, Symeon Chatzinotas, and John M Senior (2021a), “Coverage probability of distributed IRS systems under spatially correlated channels.” *IEEE Wireless Communications Letters*, 10, 1722–1726.

Papazafeiropoulos, Anastasios, Cunhua Pan, Pandelis Kourtessis, Symeon Chatzinotas, and John M Senior (2021b), “Intelligent reflecting surface-assisted MU-MISO systems with imperfect hardware: Channel estimation and beamforming design.” *IEEE Transactions on Wireless Communications*.

Papoulis, Athanasios (1962), “The fourier integral and its applications.” *Polytechnic Institute of Brooklyn, McCraw-Hill Book Company Inc., USA, ISBN: 67-048447-3*.

PARIS, José F (2014), “Statistical characterization of κ — μ shadowed fading.” *IEEE transactions on vehicular technology*, 63, 518–526.

Pei, Xilong, Haifan Yin, Li Tan, Lin Cao, Zhanpeng Li, Kai Wang, Kun Zhang, and Emil Björnson (2021), “RIS-aided wireless communications: Prototyping, adaptive beamforming, and indoor/outdoor field trials.”

Pérez-Adán, Darian, Óscar Fresnedo, José P González-Coma, and Luis Castedo (2021), “Intelligent reflective surfaces for wireless networks: An overview of applications, approached issues, and open problems.” *Electronics*, 10, 2345.

pivotalcommware (2020). Available:<https://pivotalcommware.com/2019/11/04/pivotal-commware-achieves-gigabit-connectivity-in-live-5g-mmwave-demo-at-mobile-world-congress-los-angeles-2019/>.

Rajatheva, Nandana, Italo Atzeni, Emil Bjornson, Andre Bourdoux, Stefano Buzzi, Jean-Baptiste Dore, Serhat Erkucuk, Manuel Fuentes, Ke Guan, Yuzhou Hu, et al. (2020), “White paper on broadband connectivity in 6G.” *arXiv preprint arXiv:2004.14247*.

Rappaport, T S, Y Xing, G R MacCartney, A F Molisch, E Mellios, and J. Zhang (2017), “Overview of millimeter wave communications for fifth-generation (5G) wireless networks—with a focus on propagation models.” *IEEE Transactions on Antennas and Propagation*, 65, 6213–6230.

Saha, Chiranjib, Mehrnaz Afshang, and Harpreet S. Dhillon (2018), “3GPP-inspired hetnet model using poisson cluster process: Sum-product functionals and downlink coverage.” *IEEE Transactions on Communications*, 66, 2219–2234.

Saha, Chiranjib, Harpreet S. Dhillon, Naoto Miyoshi, and Jeffrey G. Andrews (2019), “Unified analysis of hetnets using poisson cluster processes under max-power association.” *IEEE Transactions on Wireless Communications*, 18, 3797–3812.

Samimi, Mathew K and Theodore S Rappaport (2014), “Characterization of the 28 GHz millimeter-wave dense urban channel for future 5G mobile cellular.” *NYU Wireless TR*, 1.

Samuh, Monjed H., Anas M. Salhab, and Ahmed H. Abd El-Malek (2021), “Performance analysis and optimization of RIS-assisted networks in Nakagami-m environment.”

Shafique, Taniya, Hina Tabassum, and Ekram Hossain (2022), “Stochastic geometry analysis of IRS-assisted downlink cellular networks.” *IEEE Transactions on Communications*, 70, 1442–1456.

Shi, Minwei, Kai Yang, Zhu Han, and Dusit Niyato (2019), “Coverage analysis of integrated sub-6GHz-mmwave cellular networks with hotspots.” *IEEE Transactions on Communications*, 67, 8151–8164.

Stoyan, Dietrich, Wilfrid S Kendall, Sung Nok Chiu, and Joseph Mecke (2013), *Stochastic geometry and its applications*. John Wiley & Sons.

Sun, S (2016), “Investigation of prediction accuracy, sensitivity, and parameter stability of large-scale propagation path loss models for 5G wireless communications.” *IEEE Transactions on Vehicular Technology*, 65, 2843–2860.

Sun, S, T A Thomas, T S Rappaport, H Nguyen, I Z Kovacs, and I Rodriguez (2015), “Path loss, shadow fading, and line-of-sight probability models for 5G urban macro-cellular scenarios.” *IEEE Globecom Workshops (GC Wkshps)*, 1–7.

Sun, Shu, Theodore S. Rappaport, Sundeep Rangan, Timothy A. Thomas, Amitava Ghosh, Istvan Z. Kovacs, Ignacio Rodriguez, Ozge Koymen, Andrzej Partyka, and Jan Jarvelainen (2016), “Propagation path loss models for 5G urban micro- and macro-cellular scenarios.” *2016 IEEE 83rd Vehicular Technology Conference (VTC Spring)*, 1–6.

Tang, Wankai, Xiang Li, Jun Yan Dai, Shi Jin, Yong Zeng, Qiang Cheng, and Tie Jun Cui (2019), “Wireless communications with programmable metasurface: Transceiver design and experimental results.” *China Communications*, 16, 46–61.

Tao, Qin, Junwei Wang, and Caijun Zhong (2020), “Performance analysis of intelligent reflecting surface aided communication systems.” *IEEE Communications Letters*, 24, 2464–2468.

Technical-report (2017), “Study on channel model for frequencies from 0.5 to 100 GHz.” *3GPP TR 38.901*, URL https://www.etsi.org/deliver/etsi_tr/138900_138999/138901/14.03.00_60/tr_138901v140300p.pdf.

Trampller, Michael E., Ricardo E. Lovato, and Xun Gong (2020), “Dual-resonance continuously beam-scanning x-band reflectarray antenna.” *IEEE Transactions on Antennas and Propagation*, 68, 6080–6087.

Trigui, Imène, Wessam Ajib, and Wei-Ping Zhu (2020), “A comprehensive study of reconfigurable intelligent surfaces in generalized fading.”

visorsurf (2020), “A hardware platform for software-driven functional metasurfaces.” Available:<http://www.visorsurf.eu/>.

Wang, Di, Li-Zheng Yin, Tie-Jun Huang, Feng-Yuan Han, Zi-Wen Zhang, Yun-Hua Tan, and Pu-Kun Liu (2020), “Design of a 1 bit broadband space-time-coding digital metasurface element.” *IEEE Antennas and Wireless Propagation Letters*, 19, 611–615.

Wang, Haiming, Peize Zhang, Jing Li, and Xiaohu You (2019), “Radio propagation and wireless coverage of LSAA-based 5G millimeter-wave mobile communication systems.” *China Communications*, 16, 1–18.

Wu, Q and R Zhang (2020), “Towards smart and reconfigurable environment: Intelligent reflecting surface aided wireless network.” *IEEE Communications Magazine*, 58, 106–112.

Wu, Qingqing (2019), “Intelligent reflecting surface enhanced wireless network via joint active and passive beamforming.” *IEEE Trans. Wireless Commun.*, 18, 5394–5409.

Wu, Qingqing, Shuowen Zhang, Beixiong Zheng, Changsheng You, and Rui Zhang (2021a), “Intelligent reflecting surface-aided wireless communications: A tutorial.” *IEEE Transactions on Communications*, 69, 3313–3351.

Wu, Wei, Zi Wang, Lu Yuan, Fuhui Zhou, Fei Lang, Baoyun Wang, and Qihui Wu (2021b), “IRS-enhanced energy detection for spectrum sensing in cognitive radio networks.” *IEEE Wireless Communications Letters*, 10, 2254–2258.

Xu, Peng, Wenqi Niu, Gaojie Chen, Yong Li, and Yonghui Li (2022), “Performance analysis of RIS-assisted systems with statistical channel state information.” *IEEE Transactions on Vehicular Technology*, 71, 1089–1094.

Yan, Wenjing, Xiaojun Yuan, and Xiaoyan Kuai (2020), “Passive beamforming and information transfer via large intelligent surface.” *IEEE Wireless Communications Letters*, 9, 533–537.

Yang, Liang, Fanxu Meng, Qingqing Wu, Daniel Benevides da Costa, and Mohamed-Slim Alouini (2020), “Accurate closed-form approximations to channel distributions of RIS-aided wireless systems.” *IEEE Wireless Communications Letters*, 9, 1985–1989.

Yang, Liang, Yin Yang, Daniel Benevides da Costa, and Imene Trigui (2021a), “Outage probability and capacity scaling law of multiple RIS-aided networks.” *IEEE Wireless Communications Letters*, 10, 256–260.

Yang, Lihua, Teng Joon Lim, Junhui Zhao, and Mehul Motani (2021b), “Modeling and analysis of hetnets with interference management using poisson cluster process.” *IEEE Transactions on Vehicular Technology*, 70, 12039–12054.

Yang, Zhixiang, Lei Feng, Fanqin Zhou, Xuesong Qiu, and Wenjing Li (2021c), “Analytical performance analysis of intelligent reflecting surface aided ambient backscatter communication network.” *IEEE Wireless Communications Letters*, 10, 2732–2736.

Yuan, Jide, Hien Quoc Ngo, and Michail Matthaiou (2020), “Towards large intelligent surface (lis)-based communications.” *IEEE Transactions on Communications*, 68, 6568–6582.

Yue, Xinwei and Yuanwei Liu (2021), “Performance analysis of intelligent reflecting surface assisted NOMA networks.” *IEEE Transactions on Wireless Communications*.

Zhang, Chao, Wenqiang Yi, Yuanwei Liu, Kun Yang, and Zhiguo Ding (2022), “Reconfigurable intelligent surfaces aided multi-cell NOMA networks: A stochastic geometry model.” *IEEE Transactions on Communications*, 70, 951–966.

Zhang, Hongliang, Boya Di, Lingyang Song, and Zhu Han (2020), “Reconfigurable intelligent surfaces assisted communications with limited phase shifts: How many phase shifts are enough?” *IEEE Transactions on Vehicular Technology*, 69, 4498–4502.

Zhang, Shuowen and Rui Zhang (2021), “Intelligent reflecting surface aided multi-user communication: Capacity region and deployment strategy.” *IEEE Transactions on Communications*, 69, 5790–5806.

Zhang, Yan, Jiayi Zhang, Marco Di Renzo, Huahua Xiao, and Bo Ai (2021), “Performance analysis of RIS-aided systems with practical phase shift and amplitude response.” *IEEE Transactions on Vehicular Technology*, 70, 4501–4511.

Zhang, Zijian and Linglong Dai (2021), “A joint precoding framework for wideband reconfigurable intelligent surface-aided cell-free network.” *IEEE Transactions on Signal Processing*, 69, 4085–4101.

Zhou, Gui, Cunhua Pan, Hong Ren, Kezhi Wang, Maged ElKashlan, and Marco Di Renzo (2021), “Stochastic learning-based robust beamforming design for RIS-aided millimeter-wave systems in the presence of random blockages.” *IEEE Transactions on Vehicular Technology*, 70, 1057–1061.

Zhu, Yongxu, Gan Zheng, and Kai-Kit Wong (2020), “Stochastic geometry analysis of large intelligent surface-assisted millimeter wave networks.” *IEEE Journal on Selected Areas in Communications*, 38, 1749–1762.

Zou, Y., S. Gong, J. Xu, W. Cheng, D. T. Hoang, and D. Niyato (2020), “Wireless powered intelligent reflecting surfaces for enhancing wireless communications.” *IEEE Transactions on Vehicular Technology*, 69, 12369–12373.

Zuo, Jiakuo, Yuanwei Liu, Ertugrul Basar, and Octavia A. Dobre (2020), “Intelligent reflecting surface enhanced millimeter-wave NOMA systems.” *IEEE Communications Letters*, 24, 2632–2636.